Sensor and Simulation Notes

Note 122

February 1971

Low-Frequency Magnetic Field Distribution of a Half Toroid Simulator Joined to a Finitely Conducting Ground: Simple Ground Connections

A. D. Varvatsis and M. I. Sancer
Northrop Corporate Laboratories
Pasadena, California

Abstract

In this note, we consider the low-frequency magnetic field distribution of a half toroid simulator joined to the ground in such a way that the current flows from the end point of the toroid directly into the ground and is collected likewise by the other end. Making the assumption that the contact areas with the ground are sufficiently small we find that the magnetic field on or above the ground due to these currents can be calculated by replacing the ground currents with two semi-infinite current elements oriented downward from the toroid end points to infinity. The magnitude of the current is the same as that in the toroid. For points below the ground the ground currents contribution is the same as that of two semi-infinite current elements carrying the same current as before, but oriented upward from the toroid end points to infinity. Plots are given of the field components at points on, above or below the ground surface. Additional plots are also presented that are related to the difference between the actual field and the low frequency component of the EMP magnetic field. Specifically we find the maximum value of the magnitude of the difference between these vector fields normalized to the magnitude of the EMP field. This maximum is found on the perimeter of a circle lying in the ground plane and centered at the origin, or the surface of a hemisphere resting on the ground and also centered at the origin and it is plotted against the corresponding radius normalized to the radius of the toroid.

I. Introduction

In a previous note[1] the low-frequency magnetic field of a half toroid simulator directly connected to an infinitely conducting ground has been analyzed. In the present note we consider the same situation except that the ground has a finite conductivity. It is known that the finitely conducting ground reflects the low-frequency content of the electromagnetic pulse due to a nuclear explosion as though it were infinitely conducting. This is no longer true for the case of a half toroid simulator joined to the ground through connections that allow the flow of currents into the ground. In this note we are primarily interested in the simulation of the low frequency magnetic field at or close to the origin of our coordinate system (see Fig. 1). We would like to study the deviation of this field from the field calculated in reference 1 and from the field in the actual situation. The actual situation refers to the low-frequency magnetic field of an electromagnetic pulse, due to a nuclear explosion, which impinges upon the ground. As we mentioned earlier the ground behaves as perfectly conducting for the low-frequency interaction and consequently the simulation would improve if the ground were infinitely conducting.

In the case of a finitely conducting ground one way to imitate an infinite conducting ground would be to change the geometry of the ground connections. This could be done in a manner which causes the currents flowing through them and into the ground to look like the image of the half toroid, at least for the calculation of the magnetic field at the origin of our coordinate system. This problem will be the subject of a future note. Returning to the subject of this note we would like to outline the method which we will employ to calculate the low frequency magnetic field. We assume that a steady current flows through the half toroid and that the pattern of the ground currents is independent of the inclination angle of the simulator with respect to the ground. This can be accomplished by making the contact areas with the ground sufficiently small. The last assumption allows us to concentrate on the effect of each feed point independently of the inclination angle. The magnetic field everywhere is the superposition of the magnetic field due to the half toroid and the magnetic field due to the ground currents. Using Ampere's law and symmetry arguments we prove that the field on and above the ground due to the ground

currents can be calculated by replacing the ground currents with two semi-infinite current elements oriented downward from the feed points to infinity. The field below the ground is calculated in a similar way except that the two semi-infinite current elements are oriented upward. We find that the ground currents produce no vertical component of the magnetic field; therefore, for an inclination angle $\xi_1 \neq 0$ (see Fig. 1) the half toroid produces a vertical component of the magnetic field at the origin. This is an undesirable feature and deteriorates the simulation of the EMP in a region at and close to the origin. We exhibit the results of our calculations as follows. For points on or above the ground we plot the total magnetic field normalized to $(I/2a)\cos \xi_1$, versus z/a with parameters x/a, y/a and ξ_1. $(I/2a)\cos \xi_1 \hat{a}_z$ is the EMP magnetic field to be simulated and it is also the field at the origin due to the half toroid for the infinite conductivity case. I is the current in the half toroid and a the radius of the half toroid. We denote the magnetic field normalized to I/2a as $\underline{h}$, i.e., $\underline{h} = (2a/I)\underline{H}$. To further compare the present situation with that of a perfectly conducting ground we compute $|\Delta \underline{h}|/\cos \xi_1$ where $\Delta \underline{h} = \underline{h} - \cos \xi_1 \hat{a}_z$ on the periphery of a circle situated on the ground and on the surface of a hemisphere resting on the ground. Both centers coincide with the origin. This quantity is a measure of how well a simulator simulates the EMP. It is zero at the origin for a perfectly conducting ground. We find the maximum deviations for the circle and the hemisphere and we plot them versus the appropriate radius normalized to the radius of the toroid, with ξ_1 as a parameter. For points in the ground we only plot the total magnetic field components, normalized to $(I/2a)\cos \xi_1$, versus z/a with x/a, y/a and ξ_1 as parameters.

II. Formulation

The analysis that follows is primarily based on the assumption that the flow pattern of the ground currents is independent of the manner that the half toroid or any arbitrary current loop is joined to the ground (Fig. 2). This will be the case if we make the contact areas with the ground sufficiently small. This flow pattern is the superposition of two independent flow patterns. Drawn independently they are depicted in Fig. 3. The flow lines are identical to the electrostatic lines converging or diverging from a point charge. Before we proceed with the calculation of the magnetic field we would like to examine the effect of the difference between the ground and air electric and magnetic permittivities. Notice that due to current continuity, $\nabla \cdot \underline{J} = 0$, the problem under consideration is purely magnetostatic governed by equations which do not involve the dielectric permittivity ε. Thus we can set $\varepsilon = \varepsilon_o$. The difference in the magnetic permittivity does not have a significant effect on the calculation of the magnetic field due to the fact that $\mu \approx \mu_o$.

We now concentrate on feed point 1 (Fig. 3), and we notice that the same ground flow configuration exists as in the situation depicted in Fig. 4. Due to current continuity, $(\partial \underline{D}/\partial t) = 0$ throughout all finite space and consequently we can apply Ampere's law $\oint \underline{H} \cdot \underline{d\ell} = I$ above or on the ground. Due to the aximuthal symmetry of the problem we find

$$\underline{H} = H_\phi a_\phi \quad , \quad H_\phi = \frac{I}{2\pi\rho} \quad . \tag{1}$$

where ρ is the distance from the observation point perpendicular to the wire carrying the current I. This $\underline{H}$ is the superposition of the field due to the semi-infinite current I and the field due to the ground currents. That is

$$\underline{H} = \underline{H}_{I(\text{upper})} + \underline{H}_G \tag{2}$$

Consider now the field due to a current flowing along an infinite straight wire in free space (Fig. 5). The field in the upper region, is given by

$$\underline{H}' = \frac{I}{2\pi\rho}\,\hat{a}_\phi = \underline{H}_{I(\text{upper})} + \underline{H}_{I(\text{lower})} \quad , \tag{3}$$

where upper and lower signify the contributions from the semi-infinite current elements above and below the mathematical surface that represents the surface of the ground. Comparing (3) to (2) and (1) we see that

$$\underline{H}_G = \underline{H}_{I(\text{lower})} \quad . \tag{4}$$

Thus the field above or on the ground due to the ground currents can be calculated by replacing the ground currents with a semi-infinite current I oriented downward in free space. Returning now to the original situation (Fig. 2) the fields on or above the ground can be calculated as the superposition of the fields from the currents depicted in Fig. 6.

Next we compute the field due to the ground currents at observation points below the ground. Again we concentrate on feed point 1 in Fig. 3. This field is the superposition of the field due to the semi-infinite wire above the ground plus the field due to the ground currents. In superimposing these two contributions we should be aware of the fact that current continuity is destroyed and charges have to be supplied at the breaking points to satisfy the continuity equation $\nabla \cdot \underline{J} + (\partial\rho/\partial t) = 0$ (Fig. 7). Considering the picture depicting the ground currents plus a charge $Q = It$ (Fig. 8) we use Maxwell's equation $\nabla \times \underline{H} = \underline{J} + (\partial \underline{D}/\partial t)$ and azimuthal symmetry to derive

$$2\pi\rho\, H_\phi = \int_S \underline{J} \cdot \underline{dS} + \int_S \frac{\partial \underline{D}}{\partial t} \cdot \underline{dS} \quad . \tag{5}$$

The properties of current elements with charges at the ends to satisfy the continuity equation have been studied in an another note[2]. Thus the magnetic field associated with the current element is given by the usual Biot-Savart law whereas the electric field has a static-like configuration, but varies, linearly with time. Thus, $\underline{D} = (It/4\pi r^2)\hat{a}_r$ whereas current continuity gives $\underline{J} = (-I/2\pi r^2)\hat{a}_r$. At this point we observe that the calculation of $\underline{D}$ does depend on ε and it would have been different from $(It/4\pi r^2)\hat{a}_r$ had we not set $\varepsilon = \varepsilon_o$. This point is discussed in the appendix. Using (5) and the above expressions for $\underline{J}$ and $\underline{D}$ we find

$$2\pi\rho\, H_\phi = \int_S -\frac{I}{4\pi r'^2}\,\hat{a}_{r'} \cdot \underline{dS} \quad . \tag{6}$$

The integral in (6) is equal to $\int_S (\partial \underline{D}'/\partial t) \cdot \underline{dS}$ where $\underline{D}'$ is due to a charge -It at the feed point. Thus H_ϕ due to the ground currents at observation points below the ground can be computed as the field due to a semi- infinite current element I oriented upward. This can easily be seen if we integrate equation $\nabla \times \underline{H}' = \underline{J}' + (\partial \underline{D}'/\partial t)$ over a contour the plane of which does not cross the semi-infinite current. Returning to the original situation (Fig. 2) the fields below the ground can be calculated as the superposition of the fields due to currents as depicted in Fig. 9.

So far we have considered a particular ground connection which assumes the same ground flow pattern independently of the manner that the current loop joins the ground. An alternative connection would be to insert metallic rods of length L perpendicular into the ground. If this is the case then we can prove that for the calculation of the field on or above the ground the length L is immaterial. The proof goes along the same lines as for the calculation of the field on or above the ground which we gave before. The field, however, below the ground does depend on L. This alternative ground connection will not be further considered.

III. Total Magnetic Field at a Given Observation Point

The total magnetic field at a given point on or above the ground is the superposition of the field due to the half toroid and the field due to ground currents. The field due to the half toroid has been calculated in reference 1. The ground currents as we showed in section II can be replaced by two semi-infinite current elements oriented downward from the feed points to infinity. The field due to a semi-infinite current element can be calculated as follows. At the finite point we consider a charge -It to satisfy the continuity equation $(dQ/dt) + I = 0$. Let us choose an observation point with $z' \geq 0$ (see Fig. 12). The magnetic field will only have an H_ϕ component, which due to symmetry will not depend on ϕ. From Maxwell's equation $\nabla \times \underline{H} = \underline{J} + (\partial \underline{D}/\partial t)$ we find

$$2\pi\rho H_\phi = I + \int_S \frac{\partial \underline{D}}{\partial t} \cdot \underline{dS} \quad . \tag{7}$$

In reference 2 it has been shown that $\underline{D} = (-It/4\pi r^2)\hat{a}_r$. Substituting this value into (7) we obtain

$$2\pi\rho H_\phi = I + \frac{-I}{4\pi} \int_S \frac{\hat{a}_{r'}}{r'^2} \cdot \underline{dS} \quad . \tag{8}$$

The surface integral $\int_S (\hat{a}_r/r'^2) \cdot \underline{dS}$ is the solid angle corresponding to the half angle α and it is equal to $2\pi(1 - \cos\alpha)$. Equation (8) then gives

$$H_\phi = \frac{I}{4\pi\rho} (1 + \cos\alpha) \quad . \tag{9}$$

Consider now an observation point with $z' < 0$ (see Fig. 11 provided we set $\varepsilon = \varepsilon_o$). From $\nabla \times \underline{H} = \underline{J} + (\partial \underline{D}/\partial t)$ we obtain

$$2\pi\rho H_\phi = \int_S \frac{\partial \underline{D}}{\partial t} \cdot \underline{dS}$$

and $-\int_S (\hat{a}_{r'}/r'^2) \cdot \underline{dS}$ is the solid angle corresponding to the half angle β. Noting that $\cos\beta = -\cos\alpha$ we obtain equation (9). Thus (9) holds for any observation point. Consider now the half toroid situation and an observation

point P(x,y,z) with $x \geq 0$ (Fig. 13). The field at P due to a semi-infinite current at 1 is parallel to $(\underline{R}_1 \times \hat{a}_x)/R_1 \sin \alpha_1$ where α_1 is the angle between $-\hat{a}_x$ and $\underline{R}_1$. The magnitude of the field is given by (9) where ρ is equal to $R_1 \sin \alpha_1$. Simple algebraic manipulations yield

$$
\begin{aligned}
H_{1x} &= 0 \\
H_{1y} &= -\frac{IR_{1z}}{4\pi R_1^2(1 - \cos \alpha_1)} \\
H_{1z} &= \frac{IR_{1y}}{4\pi R_1^2(1 - \cos \alpha_1)}
\end{aligned}
\tag{10}
$$

where

$$
\begin{aligned}
\cos \alpha_1 &= -\frac{x}{R_1} \\
R_{1y} &= y + a \\
R_{1z} &= z \\
R_1 &= \left[x^2 + (y + a)^2 + z^2\right]^{\frac{1}{2}}
\end{aligned}
\tag{11}
$$

Similar calculations for the field due to the semi-infinite current at 2 yield

$$
\begin{aligned}
H_{2x} &= 0 \\
H_{2y} &= \frac{IR_{2z}}{4\pi R_2^2(1 - \cos \alpha_2)} \\
H_{2z} &= \frac{-IR_{2y}}{4\pi R_2^2(1 - \cos \alpha_2)}
\end{aligned}
\tag{12}
$$

where

$$\cos \alpha_2 = -\frac{x}{R_2}$$

$$R_{2y} = y - a$$

$$R_{2z} = z \qquad (13)$$

$$R_2 = [x^2 + (y - a)^2 + z^2]^{\frac{1}{2}}$$

Next we consider the magnetic field in the ground due to the ground currents. The contribution due to the half toroid can be calculated with the aid of reference 1. As we showed in section II for calculation of the field at points in the ground the ground currents can be replaced by two semi-infinite current elements oriented upward from the feed points to infinity. We then understand that for points with $x < 0$ we can use formulas (10) and (12) provided we set

$$\cos \alpha_1 = \frac{x}{R_1}$$

$$\cos \alpha_2 = \frac{x}{R_2} \quad .$$

Finally we present the formulas for the magnetic field due to the half toroid. They are valid for any observation point above, on or below the ground and their derivation is given in reference 1.

$$H_{tx} = (H_\lambda \sin \beta + H_\beta \cos \beta)\cos \xi_1 - H_3 \sin \xi_1$$

$$H_{ty} = H_\beta \sin \beta - H_\lambda \cos \beta$$

$$H_{tz} = H_3 \sin \xi_1 - (H_\lambda \sin \beta + H_\beta \cos \beta)\cos \xi_1$$

where the subscript t indicates the toroid field, and

$$H_\lambda = \frac{I}{16\pi a}\frac{B}{A}\left(\frac{m}{A}\right)^{\frac{1}{2}}\left\{\frac{2-m}{1-m}\left[E\left(\frac{\pi+\beta}{2}\middle|m\right)-E\left(\frac{\beta}{2}\middle|m\right)\right]-2\left[F\left(\frac{\pi+\beta}{2}\middle|m\right)-F\left(\frac{\beta}{2}\middle|m\right)\right]\right.$$
$$\left.+\frac{m(2-m)}{1-m}\sin\frac{\beta}{2}\cos\frac{\beta}{2}\left\{\left[1-m\sin^2\left(\frac{\beta}{2}\right)\right]^{-\frac{1}{2}}+\left[1-m\cos^2\left(\frac{\beta}{2}\right)\right]^{-\frac{1}{2}}\right\}\right\}$$

$$H_\beta = \frac{I}{8\pi a}\frac{B}{A}\left(\frac{m}{A}\right)^{\frac{1}{2}}\left\{\left[1-m\cos^2\left(\frac{\beta}{2}\right)\right]^{-\frac{1}{2}}-\left[1-m\sin^2\left(\frac{\beta}{2}\right)\right]^{-\frac{1}{2}}\right\}$$

$$H_3 = \frac{I}{4\pi a}A^{-3/2}m^{\frac{1}{2}}\left\{\frac{1}{4(1-m)}\left[(1+A)m-2A\right]\left[E\left(\frac{\pi+\beta}{2}\middle|m\right)-E\left(\frac{\beta}{2}\middle|m\right)\right]+\frac{A}{2}\left[F\left(\frac{\pi+\beta}{2}\middle|m\right)-F\left(\frac{\beta}{2}\middle|m\right)\right]\right.$$
$$\left.+\frac{m}{4(1-m)}\left[(1+A)m-2A\right]\sin\frac{\beta}{2}\cos\frac{\beta}{2}\left\{\left[1-m\sin^2\left(\frac{\beta}{2}\right)\right]^{-\frac{1}{2}}+\left[1-m\cos^2\left(\frac{\beta}{2}\right)\right]^{-\frac{1}{2}}\right\}\right\}$$

$$A = \left\{x^2\cos^2\xi_1 + y^2 + z^2\sin^2\xi_1 + xz\sin 2\xi_1\right\}^{\frac{1}{2}}/a$$

$$B = \frac{-x\sin\xi_1 + z\cos\xi_1}{a}$$

$$m = \frac{4A}{(1+A)^2 + B^2}$$

$$\beta = \arctan\frac{x\cos\xi_1 + z\sin\xi_1}{-y}$$

$$E(p+s|q) - E(p|q) = \int_p^{p+s}(1 - q\sin^2 t)^{\frac{1}{2}}dt$$

$$F(p+s|q) - F(p|q) = \int_p^{p+s}(1 - q\sin^2 t)^{-\frac{1}{2}}dt$$

Discussion of Results

The results of this work will be discussed as falling into two categories, above and below the ground. In the region above and on the ground we can compare our results with those that consider the ground to be perfectly conducting[1]. In the perfectly conducting case ($\sigma = \infty$) the region near the origin is where the best simulation of the EMP occurs and at the origin the simulation is exact. In the finitely conducting case ($\sigma \neq \infty$) considered in this note, the simulation suffers even at the origin. The major effect of the finite conductivity of the ground on the simulation is the presence of a nonzero x-component of the field on the ground surface;whereas, in the perfectly conducting case this component is zero. The value of this component on the ground is plotted in figures 17A, 25A, 33A, 41A and 49A and it is seen to increase with increasing ξ_1. The y and z components of the magnetic field are also affected by the finite conductivity of the ground, but to a lesser extent than the x component.

The combined effect on the EMP simulation can be observed in figures 54 through 57. These figures contain plots of $|\Delta \underline{h}|/\cos \xi_1$ maximized on the perimeter of a circle or the surface of a hemisphere, each centered at the origin. Specifically the figures contain these maxima plotted against the appropriate radius normalized to the radius of the toroid, r/a, and they have ξ_1 as a parameter. From these plots we can see that in the important region near the origin the finite conductivity deteriorates the simulation of the EMP. For larger values of r/a the maximum deviation for the $\sigma \neq \infty$ case tends to stay below the $\sigma = \infty$ case. For the hemispherical region this occurs beyond the range of our plot (r/a = .6). For the circular region in the ground plane the transition occurs at r/a $\approx$ .25 for $2\xi_1/\pi$ = .2, at r/a $\approx$ .55 for $2\xi_1/\pi$ = .5, and beyond the range of our plot for $2\xi_1/\pi$ = 0, .7 and .9. This behavior can be understood if we recall that in the $\sigma \neq \infty$ case we have ground currents that are replaced by two semi-infinite current elements, while for $\sigma = \infty$, we have an image half loop. For any given ξ_1, as r/a increases the field and consequently the maximum deviation change more rapidly due to two current half loops rather than to one half loop and two semi-infinite current elements.

In discussing the fields that penetrate into the ground we note a difference in the behavior of the x component of the magnetic field from the y and z components. For all three components the rate of decay increases with increasing ξ_1; however, the decay rate of h_x has the most sensitive ξ_1 dependence. This is the case because it is only the half toroid that produces the h_x component while the other components are due to both the half toroid and ground currents. We also observe that the decay rate for all three components increases with increasing y for ξ_1 fixed. The reason for this is that an increasing y corresponds to a closer proximity to the currents primarily causing the underground fields, i.e. the half toroid and one of the two semi-infinite equivalent current elements. (This current element corresponds to ground contact number 2.) In general the rate of change of a magnetic field is larger when it is near its current source than when it is further away from its source.

In conclusion we would like to summarize the main undesirable features caused by the finite conductivity of the ground relative to a perfectly conducting ground. a) The magnetic field in the symmetry plane xz and especially close to the origin deviates considerably from the magnetic field that would exist if the ground were perfectly conducting. b) Increasing the inclination angle ξ_1 of the toroid increases the field distortion relative to the infinite conductivity case. c) The maximum normalized field deviation $|\underline{\Delta h}|/\cos \xi_1$ over the surface of a hemisphere, or the perimeter of a circle both centered at the origin, assumes large values close to the origin, thus deteriorating the simulation.

Table of Plots

Fixed Parameter	$h_x/\cos\xi_1$ vs. z/a					$h_y/\cos\xi_1$ vs. z/a					$h_z/\cos\xi_1$ vs. z/a				
$2\xi_1/\pi$	0	.2	.5	.7	.9	0	.2	.5	.7	.9	0	.2	.5	.7	.9
y/a = 0	14A	22A	30A	38A	46A						14C	22C	30C	38C	46C
y/a = .5	15A	23A	31A	39A	47A	15B	23B	31B	39B	47B	15C	23C	31C	39C	47C
y/a = .8	16A	24A	32A	40A	48A	16B	24B	32B	40B	48B	16C	24C	32C	40C	48C
x/a = 0	17A	25A	33A	41A	49A	17B	25B	33B	41B	49B	17C	25C	33C	41C	49C
x/a = -.2	18A	26A	34A	42A	50A	18B	26B	34B	42B	50B	18C	26C	34C	42C	50C
x/a = -.5	19A	27A	35A	43A	51A	19B	27B	35B	43B	51B	19C	27C	35C	43C	51C
x/a = -.8	20A	28A	36A	44A	52A	20B	28B	36B	44B	52B	20C	28C	36C	44C	52C
x/a = -1	21A	29A	37A	45A	53A	21B	29B	37B	45B	53B	21C	29C	37C	45C	53C

Maximum Deviation Plots

$\frac{|\underline{h} - \hat{a}_z \cos\xi_1|}{\cos\xi_1}$ maximized over a circle versus $\frac{r}{a}$, Figure No. 54

Figure No. 54 with expanded ordinate scale, Figure No. 55

$\frac{|\underline{h} - \hat{a}_z \cos\xi_1|}{\cos\xi_1}$ maximized over a hemisphere versus $\frac{r}{a}$, Figure No. 56

Figure No. 56 with expanded ordinate scale, Figure No. 57

Appendix

Consider the situation depicted in Fig. 10. The magnetic field at any point is the superposition of the field due to the semi-infinite current I going straight up and the field due to the ground currents. As we mentioned before charges -It and It have to be supplied at the breaking point to satisfy the continuity equation $\nabla \cdot \underline{J} + (\partial\rho/\partial t) = 0$. In free space the magnetic field due to a current element has been computed in a previous note[2] and is given by the Biot-Savart law. In the presence of two different dielectrics this is no longer true. Consider for example Fig. 11. For observation points say below the tip of the current

$$2\pi\rho\, H_\phi = \int_S \frac{\partial \underline{D}_{II}}{\partial t} \cdot \underline{dS} \quad . \tag{A-1}$$

The displacement vector $\underline{D}$ due to -It does depend on ε. $\underline{D}$ can be calculated as follows. Consider a charge Q at the interface of two dielectrics as in Fig. 10. To calculate $\underline{D}$ in region I we assume that the entire space has a permittivity ε_o but the charge has a value equal to Q_I. For fields in region II we assume that the entire space has a permittivity ε and the charge has a value Q_{II}. Thus in region I, $\underline{D}_I = (Q_I/4\pi r^2)\hat{a}_r$ and in region II, $\underline{D}_{II} = (Q_{II}/4\pi r^2)\hat{a}_r$. Applying Gauss's law for the original situation we find

$$\frac{Q_I}{2} + \frac{Q_{II}}{2} = Q \quad . \tag{A-2}$$

Continuity of the tangential electric field along the interface gives

$$\frac{1}{\varepsilon_o}\frac{Q_I}{4\pi r^2} = \frac{1}{\varepsilon}\frac{Q_{II}}{4\pi r^2} \quad ,$$

or

$$\frac{Q_I}{\varepsilon_o} = \frac{Q_{II}}{\varepsilon} \tag{A-3}$$

From (A-2) and (A-3) we find

$$Q_I = \frac{2\varepsilon_o}{\varepsilon+\varepsilon_o} Q$$

$$Q_{II} = \frac{2\varepsilon}{\varepsilon+\varepsilon_o} Q \quad . \tag{A-4}$$

Returning to (A-1) we obtain

$$2\pi\rho\ H_\phi = \frac{2\varepsilon I}{\varepsilon+\varepsilon_o} \int_S \frac{\hat{a}_{r'}}{4\pi r'^2} \cdot \underline{dS} \quad . \tag{A-5}$$

and H_ϕ can be computed easily since $-\int (\hat{a}_{r'}/r'^2) \cdot \underline{dS}$ represents the solid angle corresponding to the half angle β (Fig. 11). If we compute the field due to the ground currents and add this to the field computed by (A-5) we will find that the total field is independent of ε which is true for the original situation (Fig. 10).

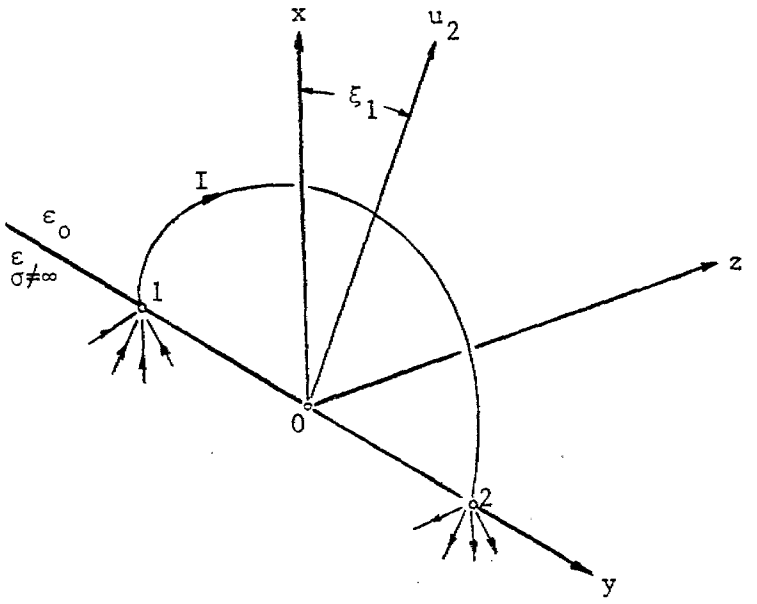

Figure 1. The half toroid simulator directly joined to a finitely conducting ground. The u_2 axis lies in the plane of the toroid.

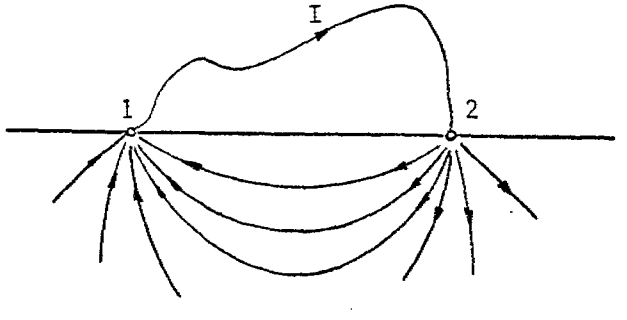

Figure 2. Flow pattern of ground currents for any arbitrary loop directly joined to the ground.

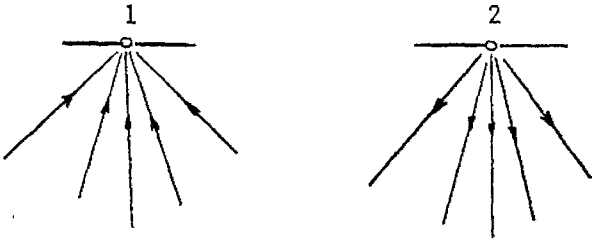

Figure 3. Flow patterns for ground currents independently drawn.

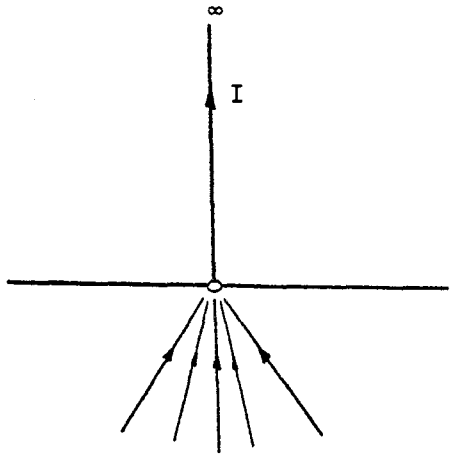

Figure 4. Semi-infinite current directly feeding into the ground.

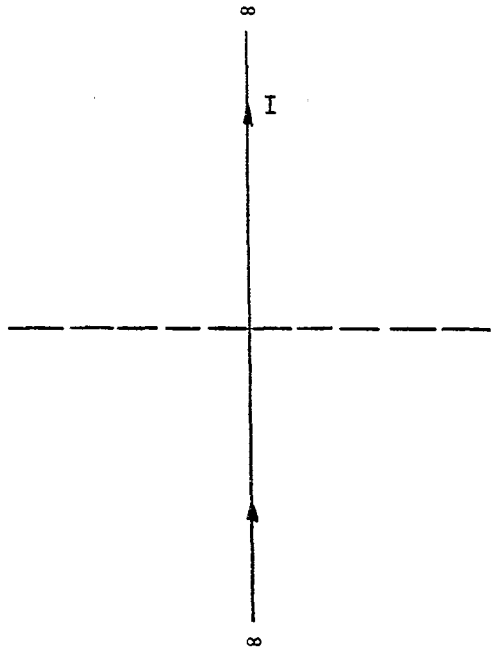

Figure 5. Infinite current bisected by an imaginary plane representing the ground interface.

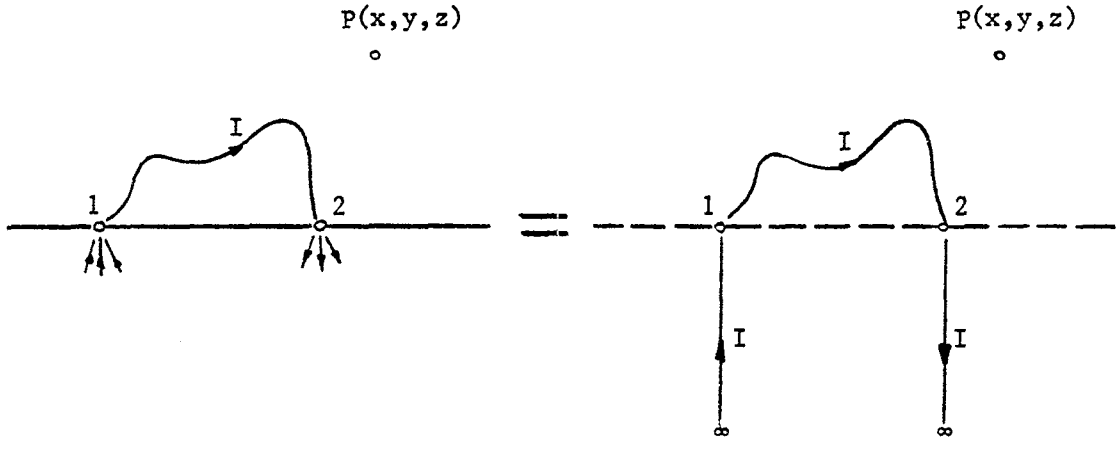

Figure 6. Equivalent currents for the calculation of the field at a point on or above the ground.

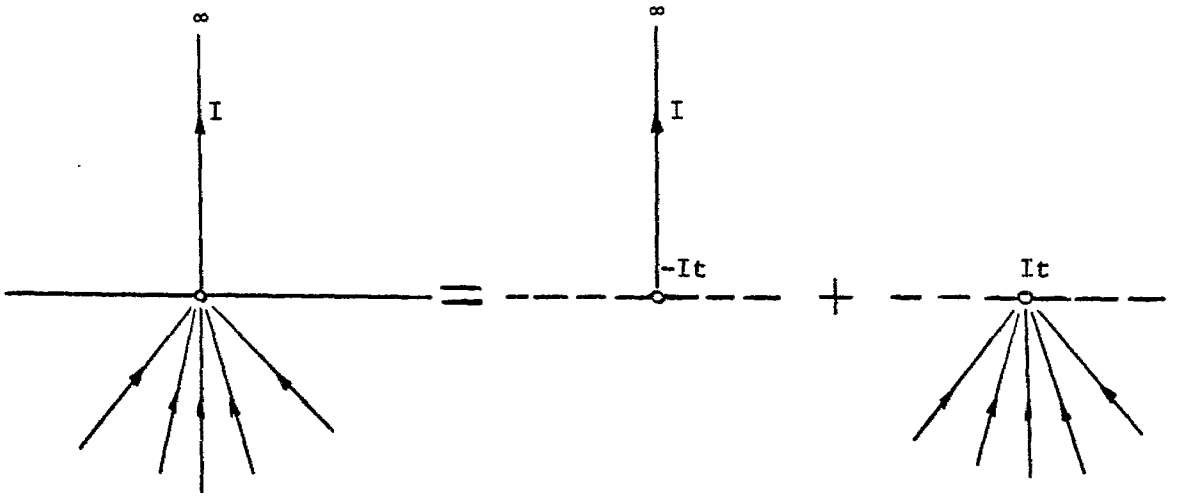

Figure 7. The charges -It and It are supplied at the breaking points to satisfy the continuity equation.

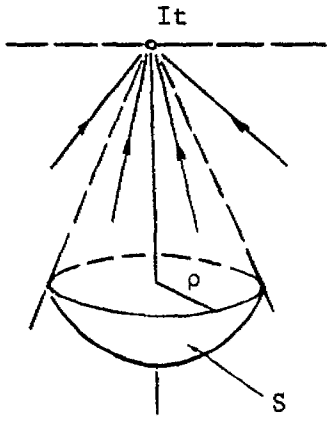

Figure 8. Geometry for the calculation of the field in the ground due to ground currents.

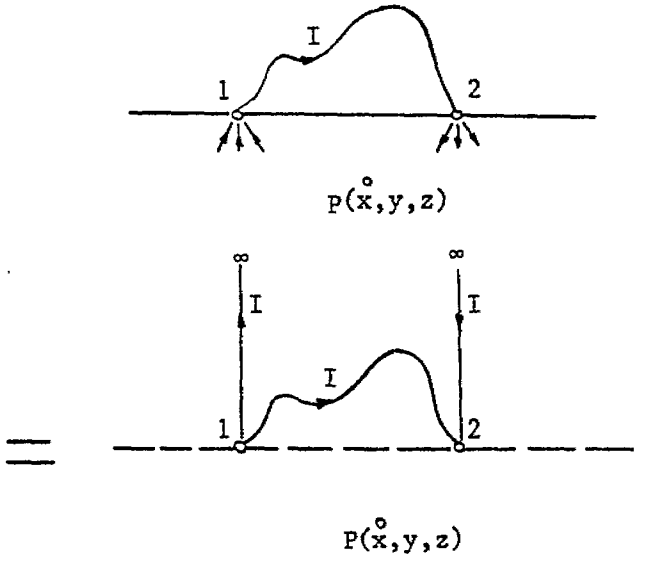

Figure 9. Equivalent currents for the calculation of the field at a point in the ground

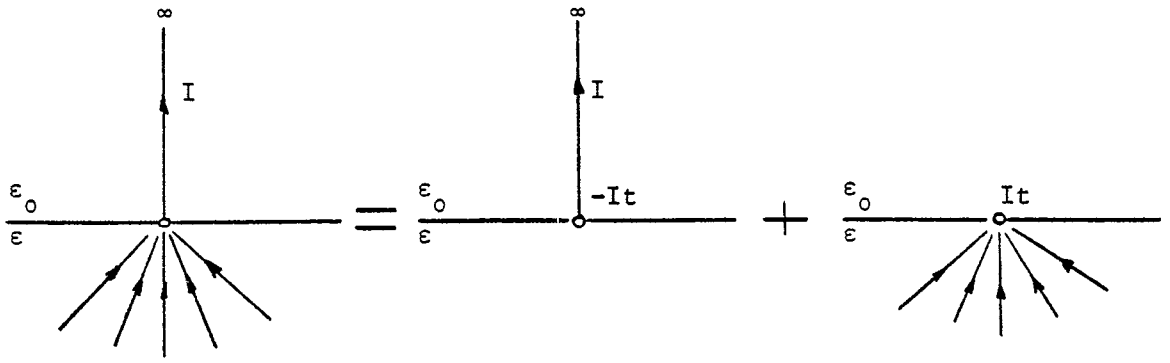

Figure 10. Semi-infinite current feeding into the ground the permittivity ε of which is different from that of the air.

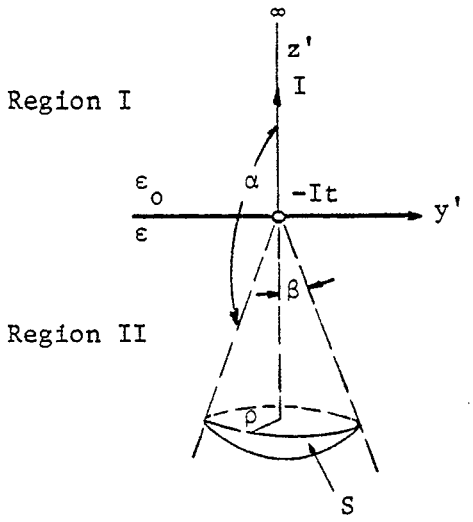

Figure 11. Geometry for the calculation of the field due to a semi-infinite current at a point with $z' < 0$.

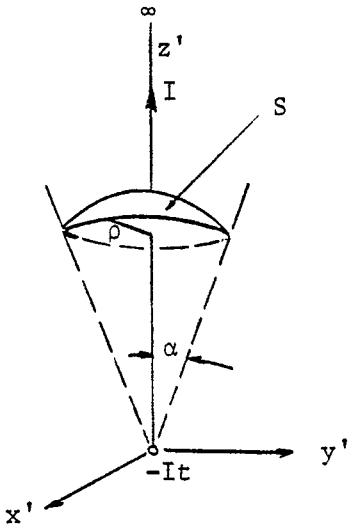

Figure 12. Geometry for the calculation of the field due to a semi-infinite current at a point with $z' > 0$.

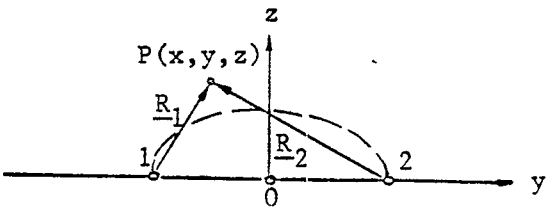

Figure 13. Calculation of the total field at P(x,y,z) with $x \geq 0$. The dotted line is the projection of the half toroid on the ground interface yz.

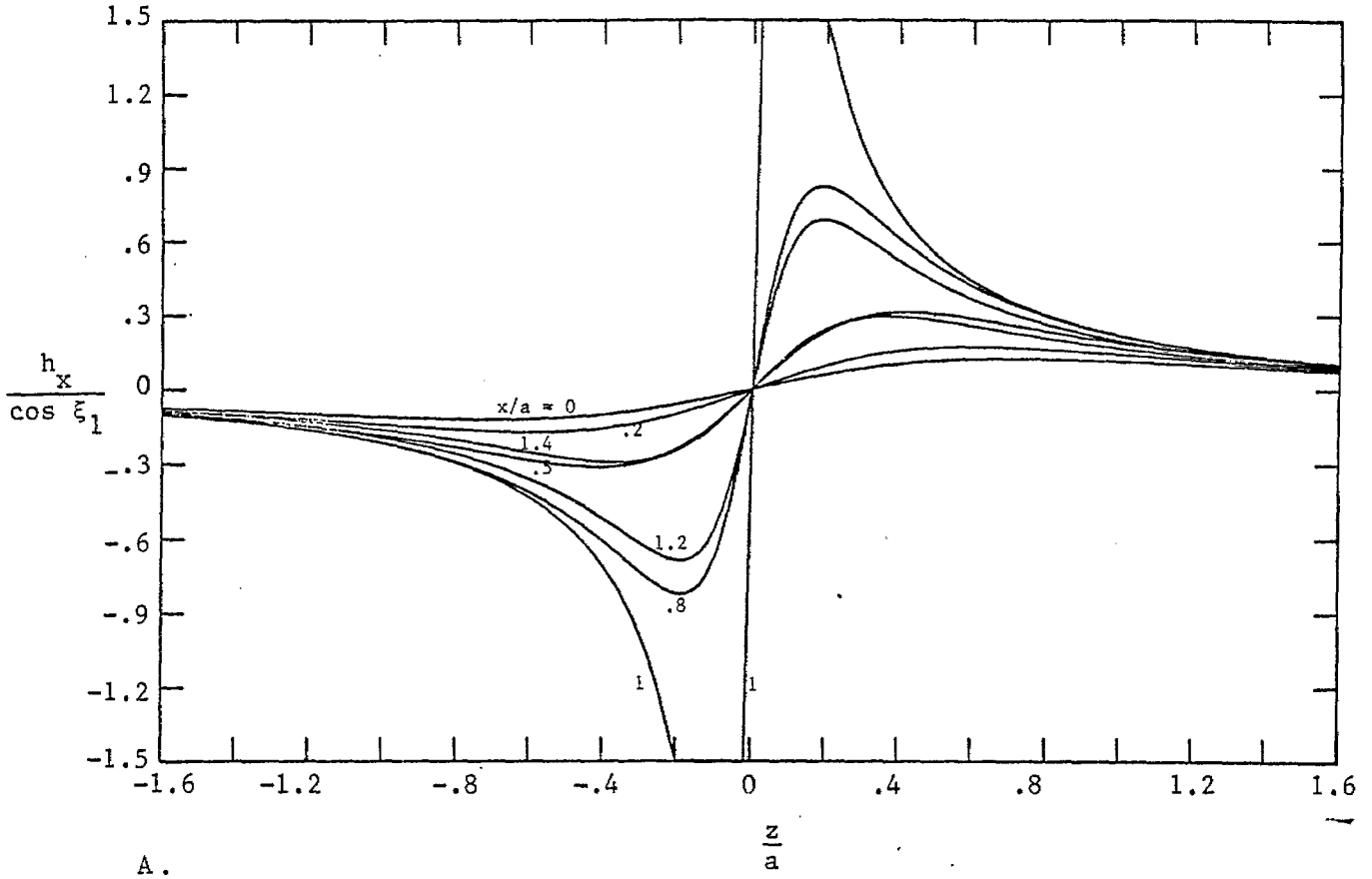

A.

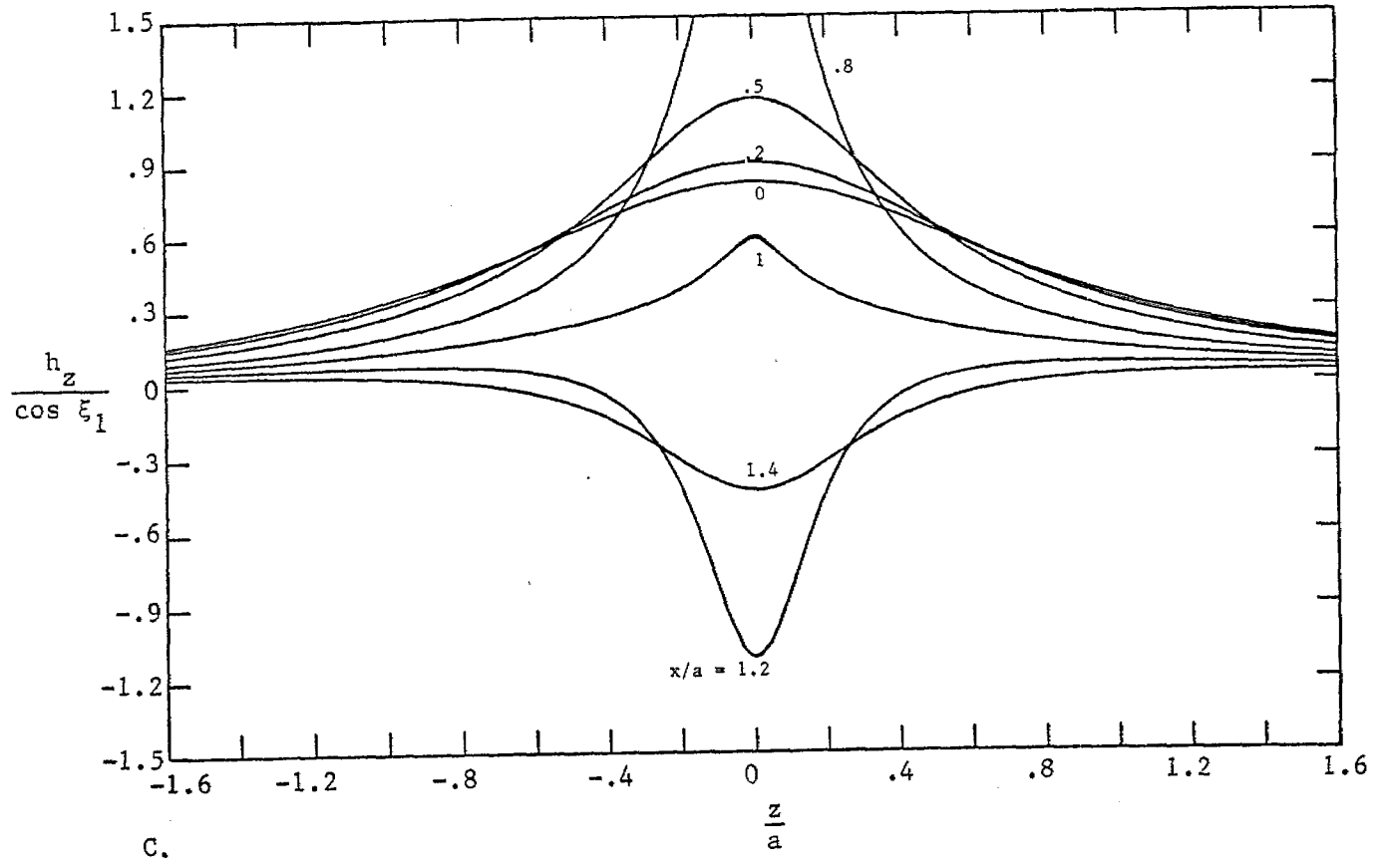

C.

Figure 14. Magnetic Field Components as a Function of z; $\frac{2\xi_1}{\pi} = 0$; $\frac{y}{a} = 0$.

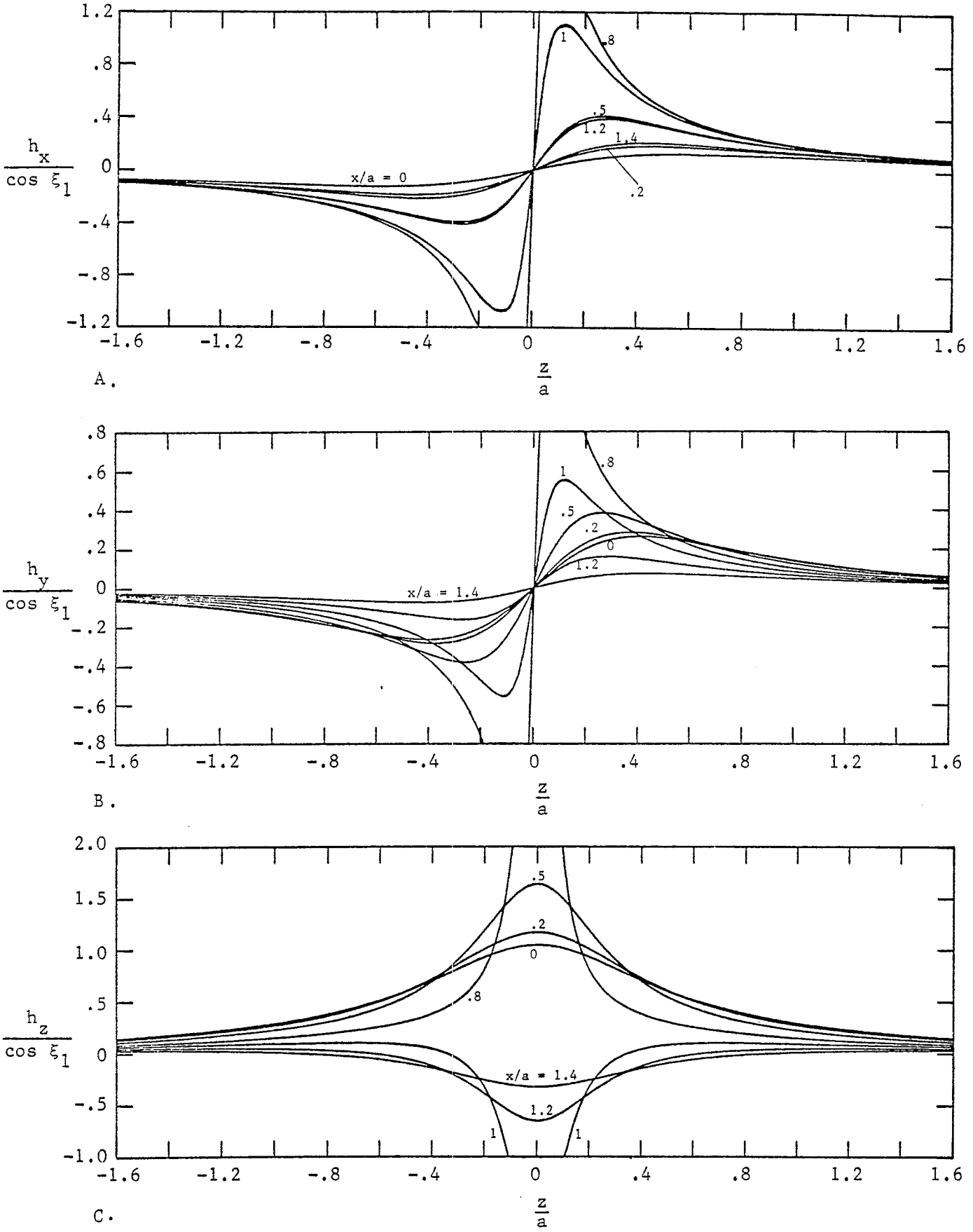

Figure 15. Magnetic Field Components as a Function of z: $\frac{2\xi_1}{\pi} = 0$; $\frac{y}{a} = .5$.

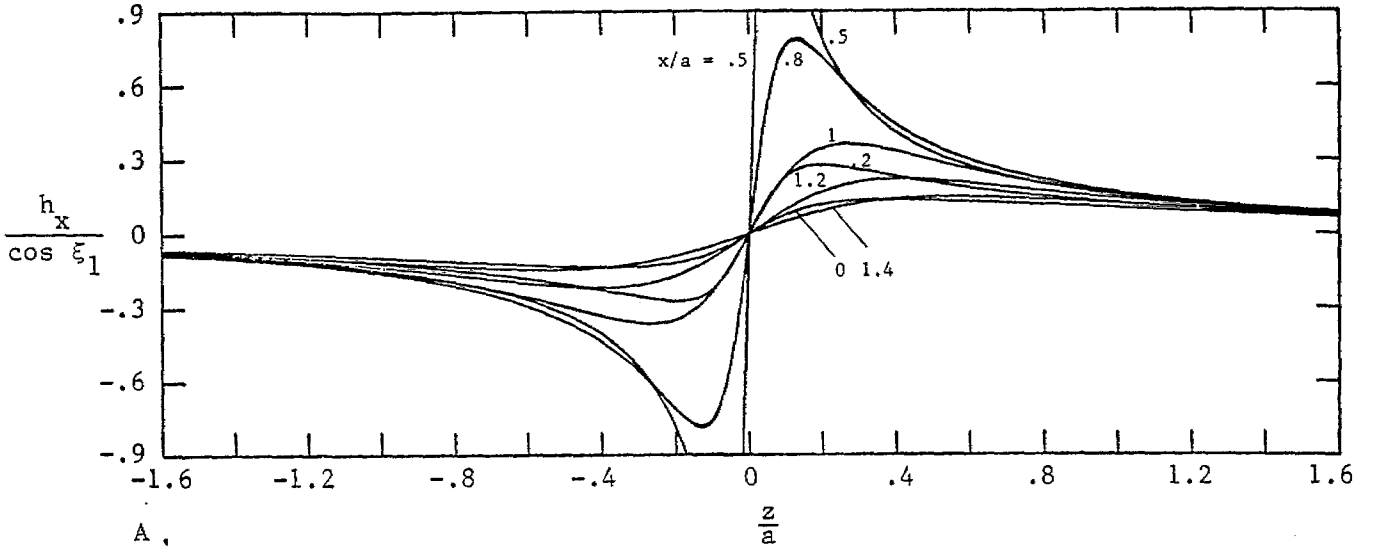

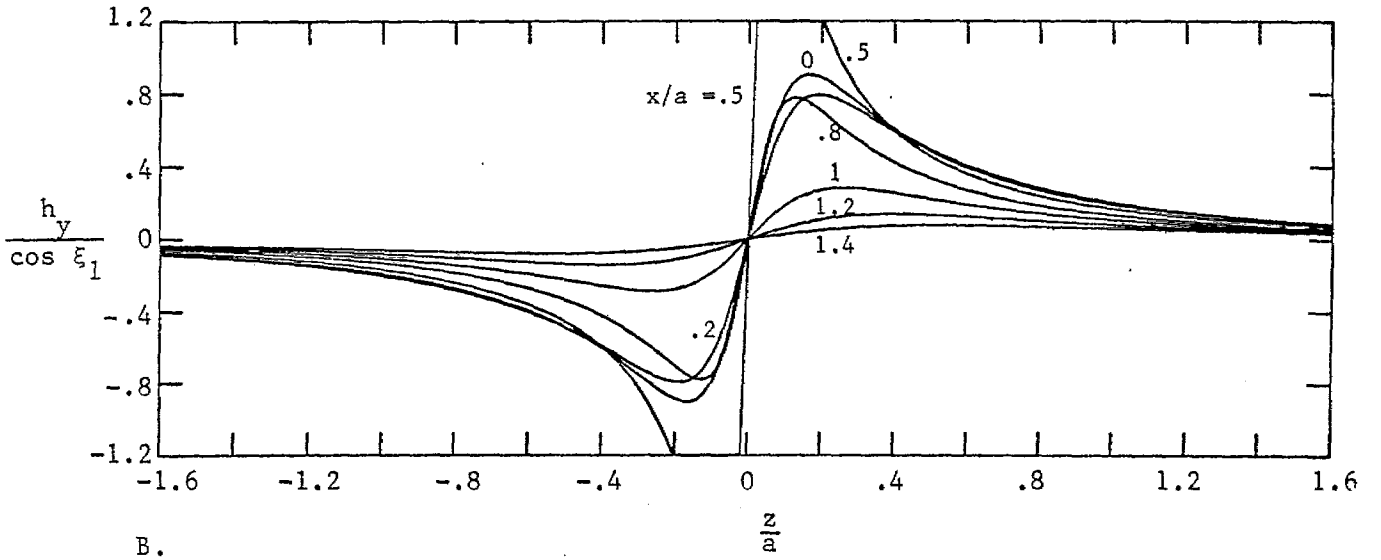

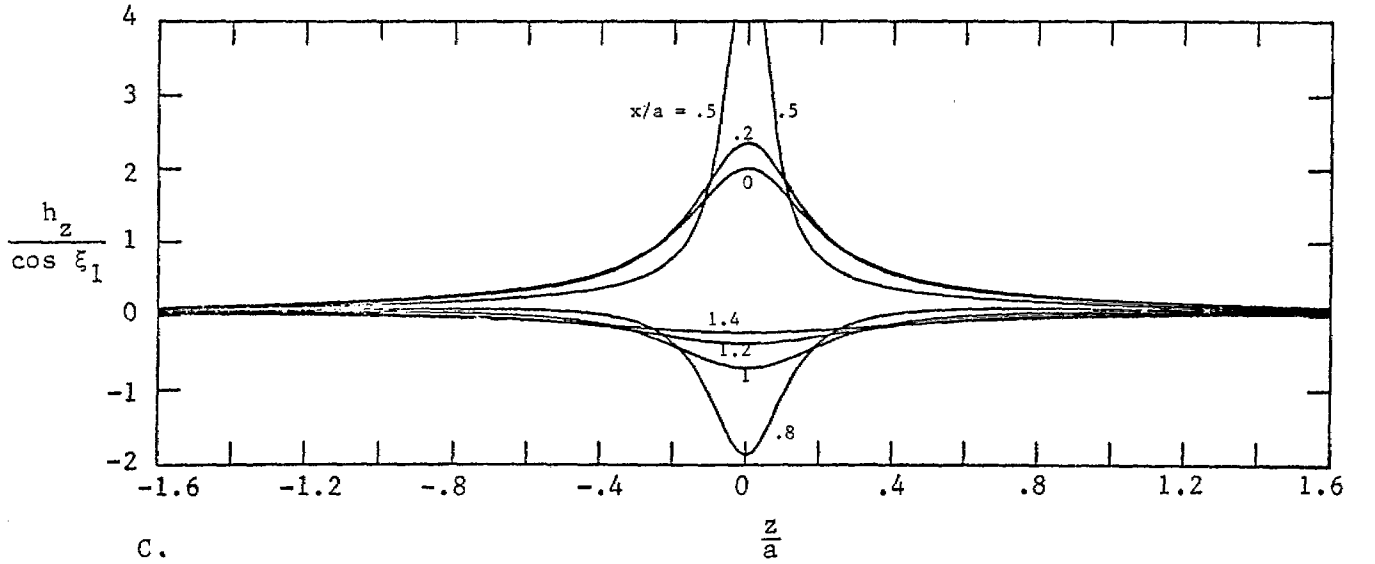

Figure 16. Magnetic Field Components as a Function of z: $\frac{2\xi_1}{\pi} = 0$; $\frac{y}{a} = .8$.

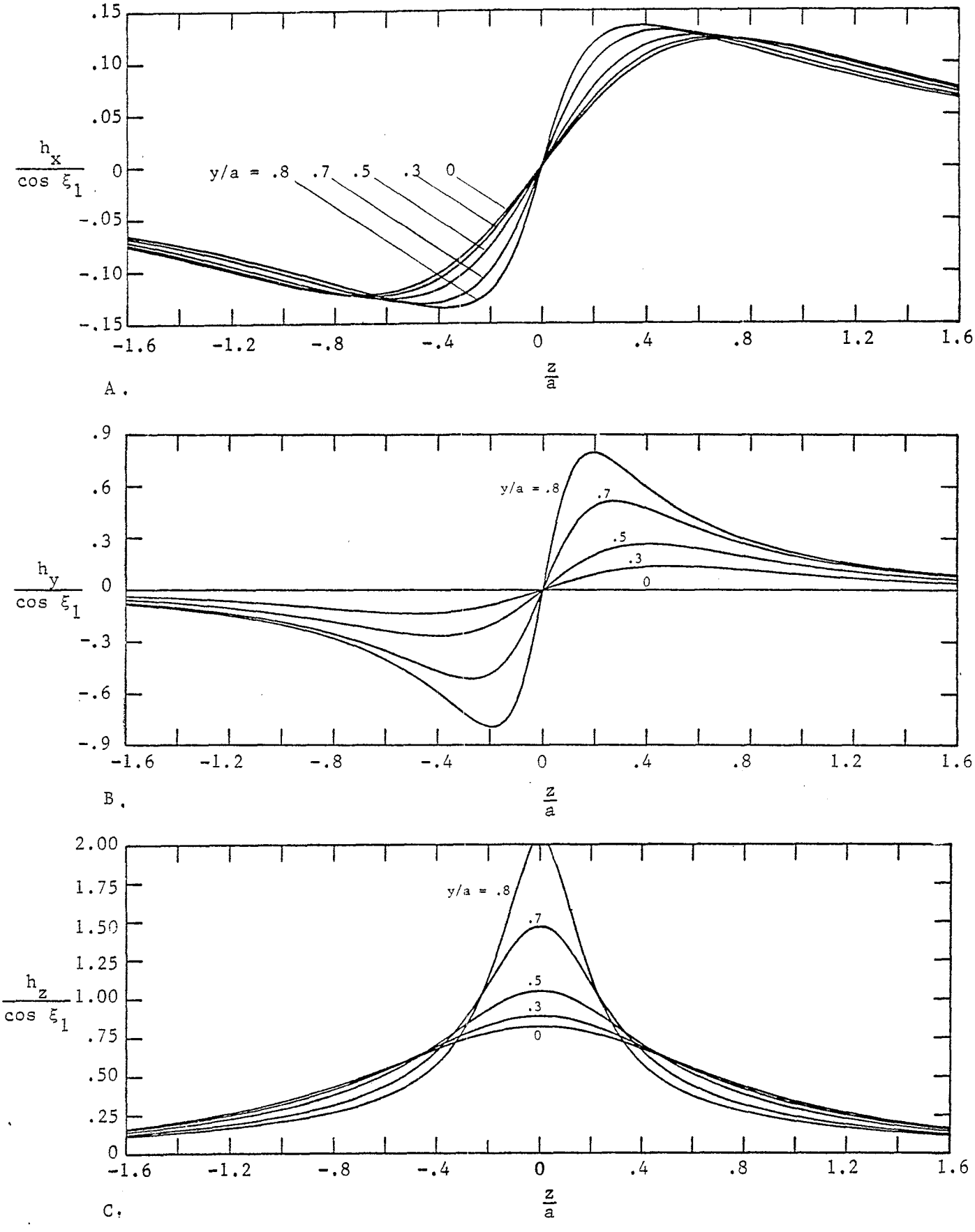

Figure 17. Magnetic Field Components as a Function of z: $\frac{2\xi_1}{\pi} = 0$; $\frac{x}{a} = 0$.

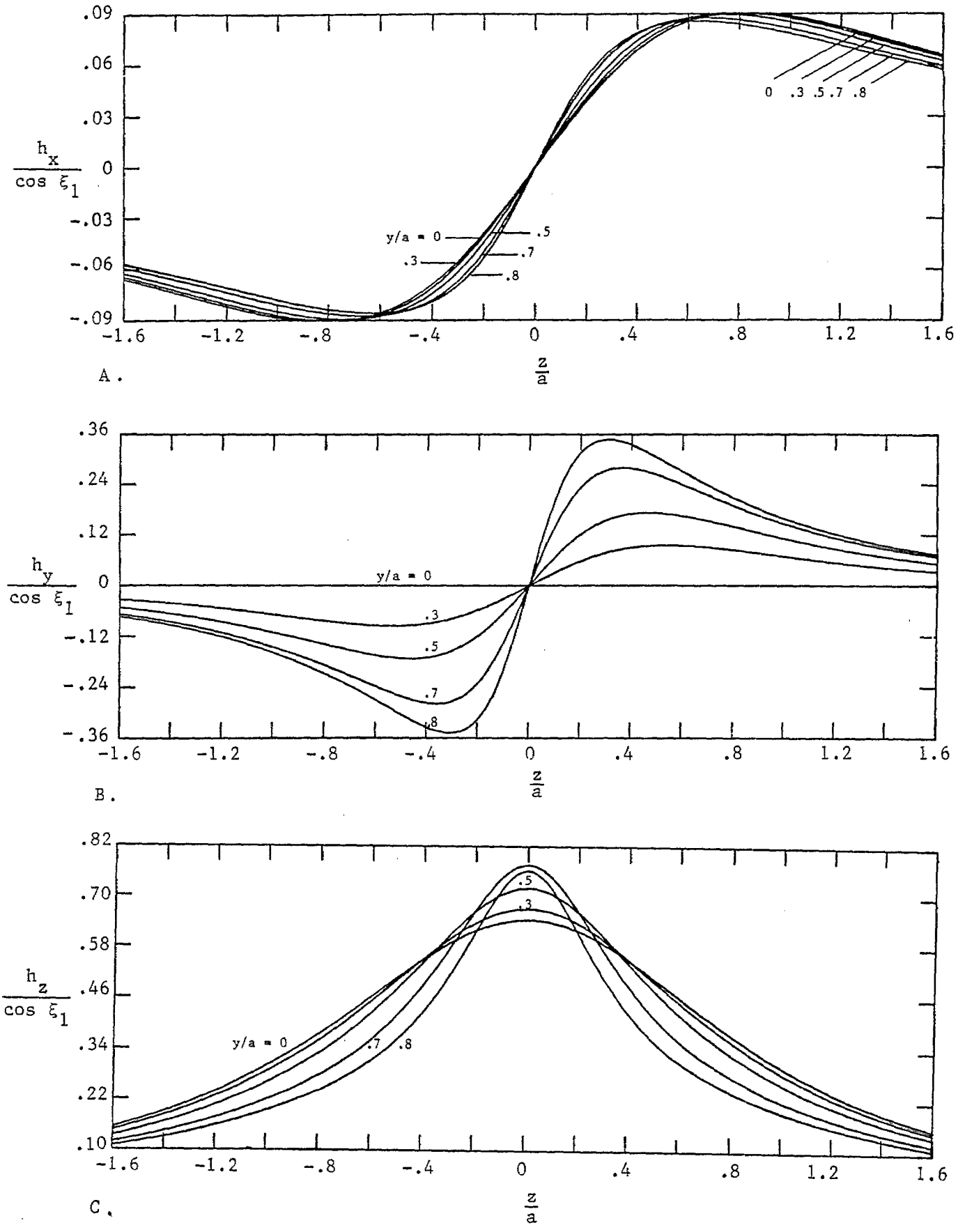

Figure 18. Magnetic Field Components as a Function of z: $\frac{2\xi_1}{\pi} = 0$; $\frac{x}{a} = -.2$.

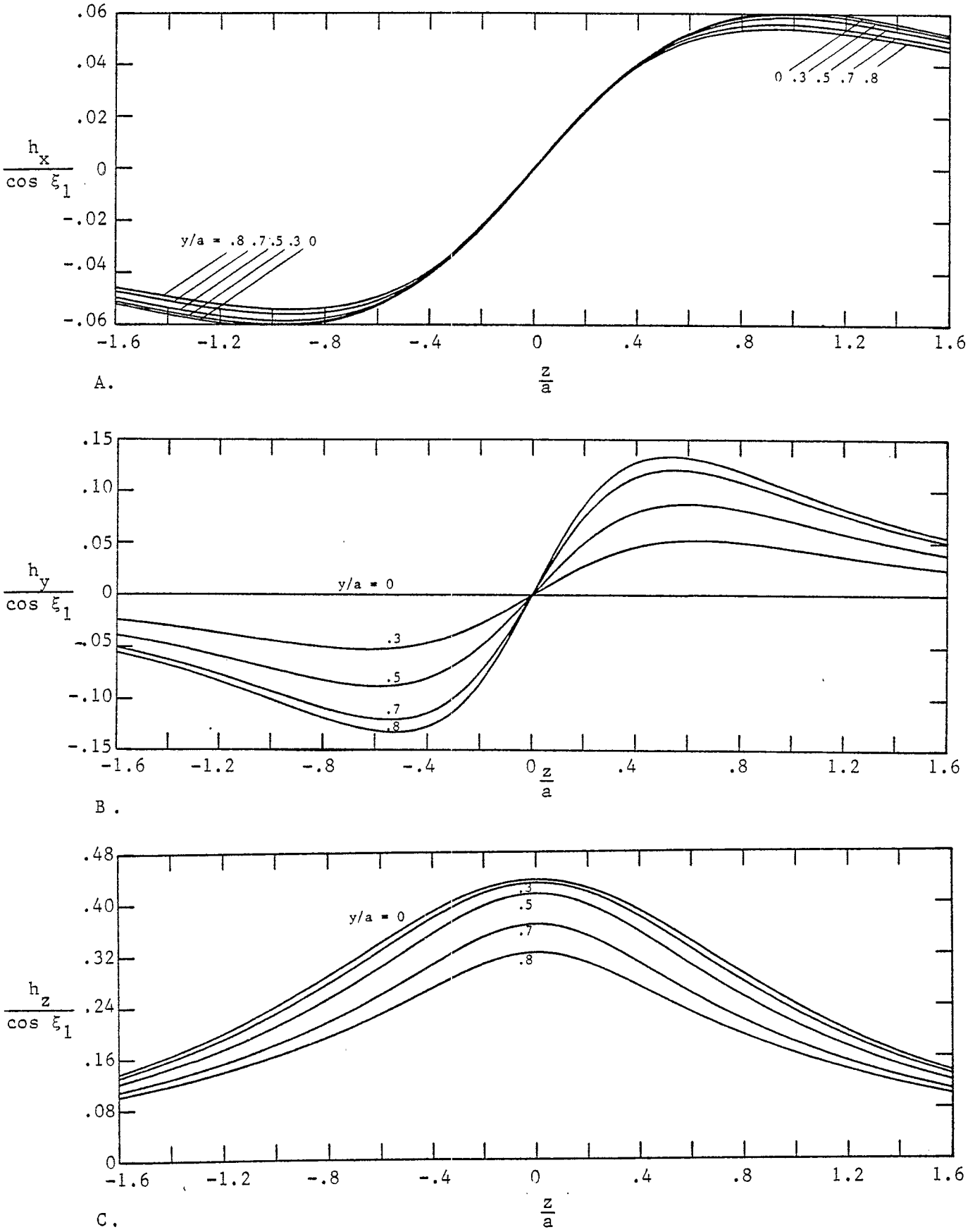

Figure 19. Magnetic Field Components as a Function of z: $\frac{2\xi_1}{\pi} = 0$; $\frac{x}{a} = -.5$.

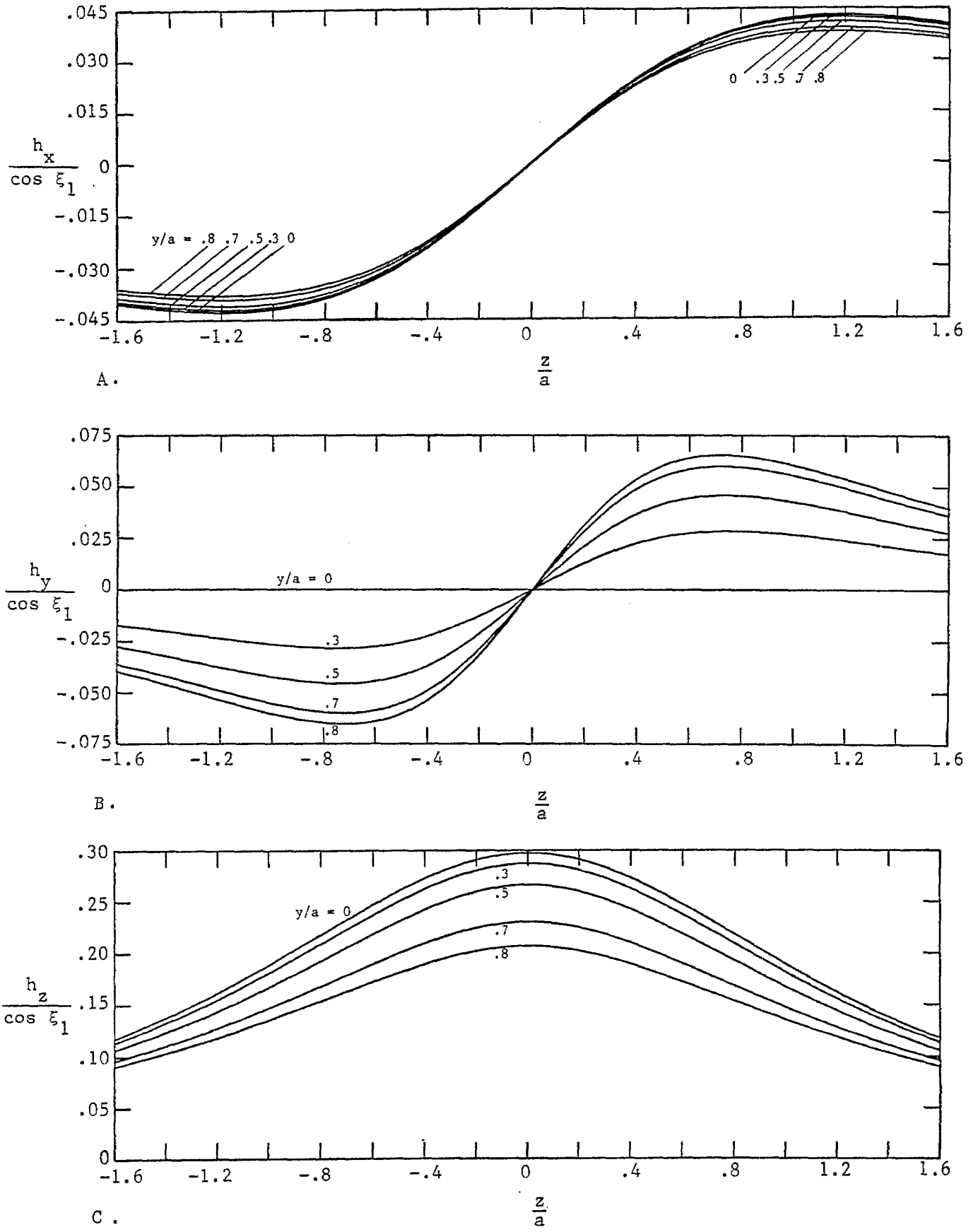

Figure 20. Magnetic Field Components as a Function of z; $\frac{2\xi_1}{\pi} = 0$; $\frac{x}{a} = .8$.

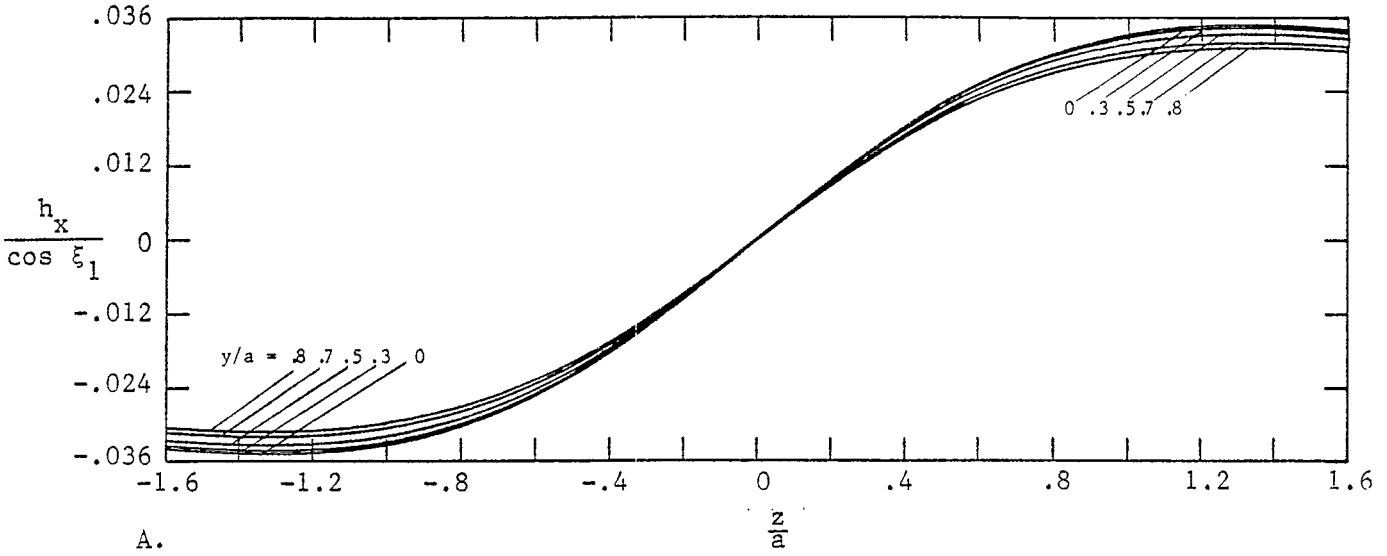

A.

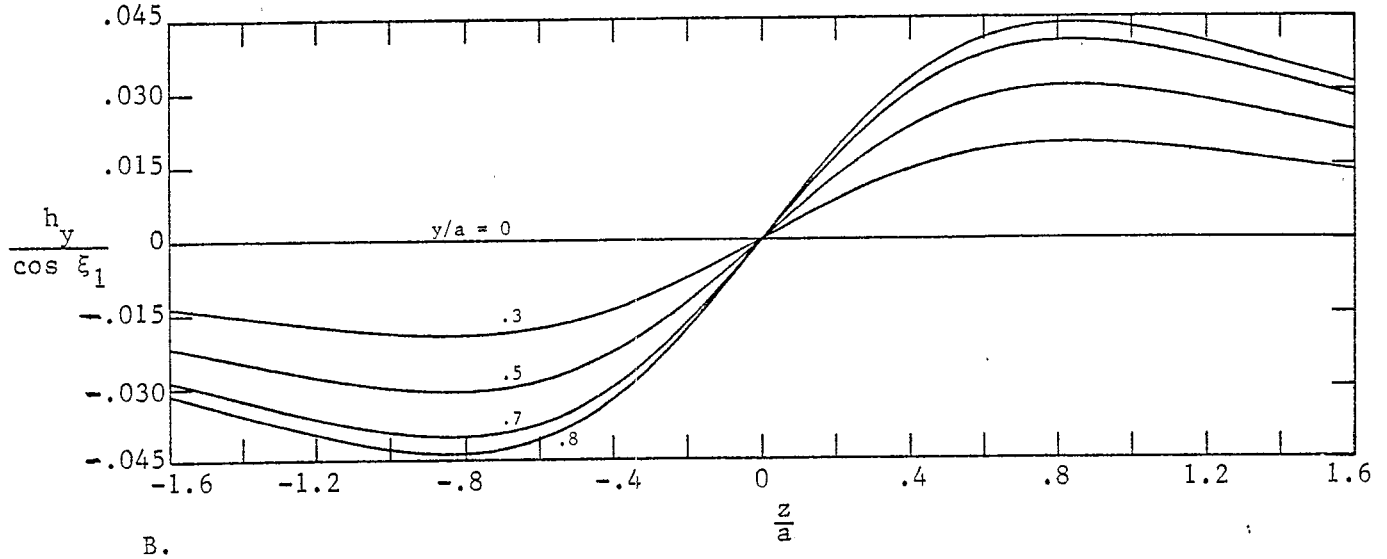

B.

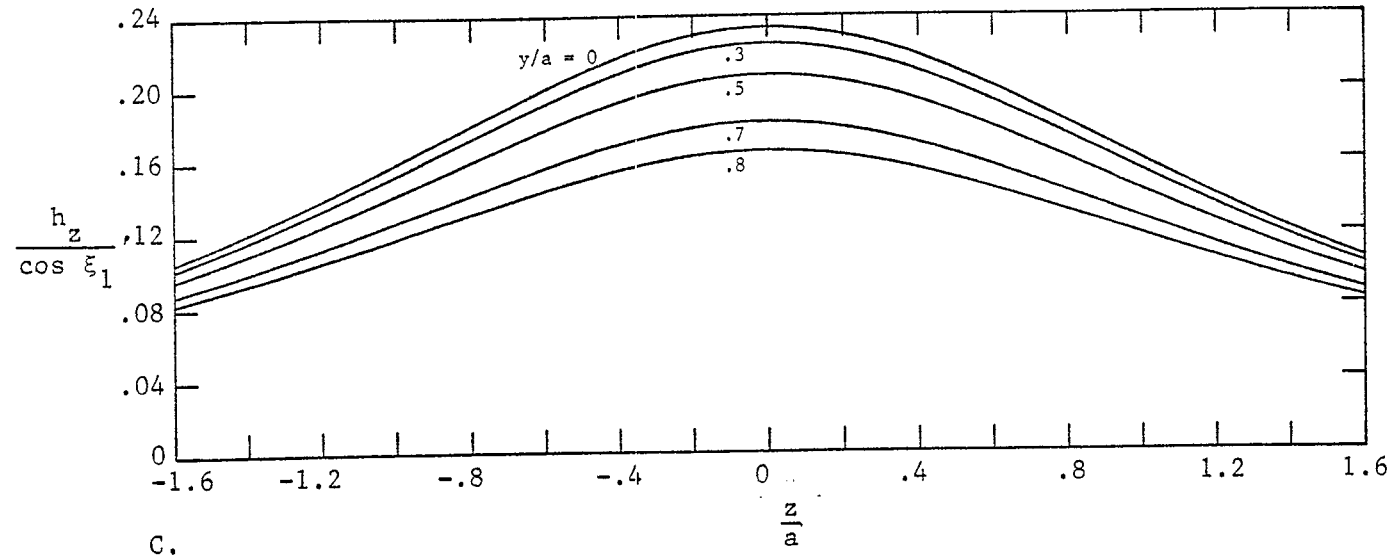

C.

Figure 21. Magnetic Field Components as a Function of z: $\frac{2\xi_1}{\pi} = 0$; $\frac{x}{a} = -1$.

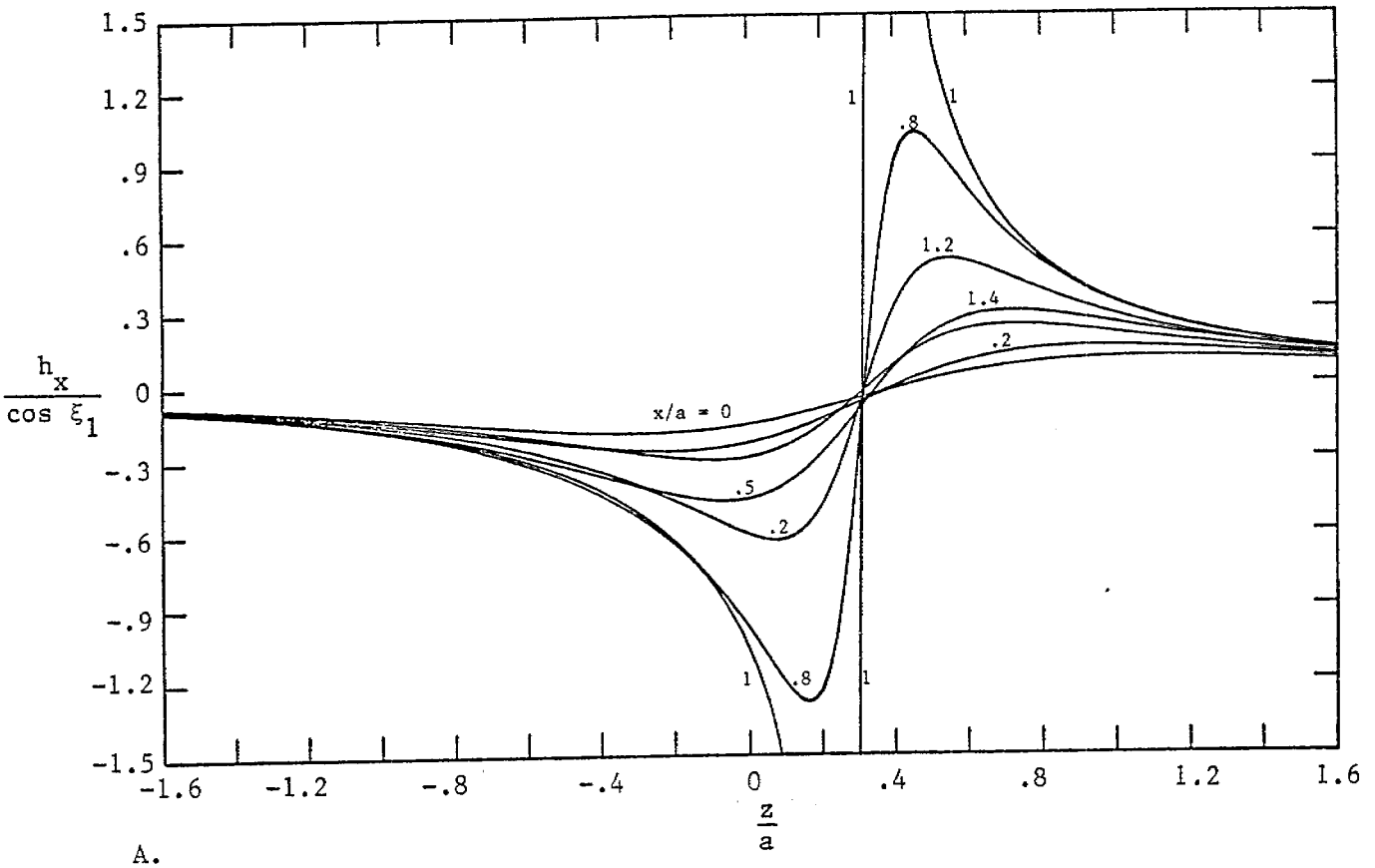

A.

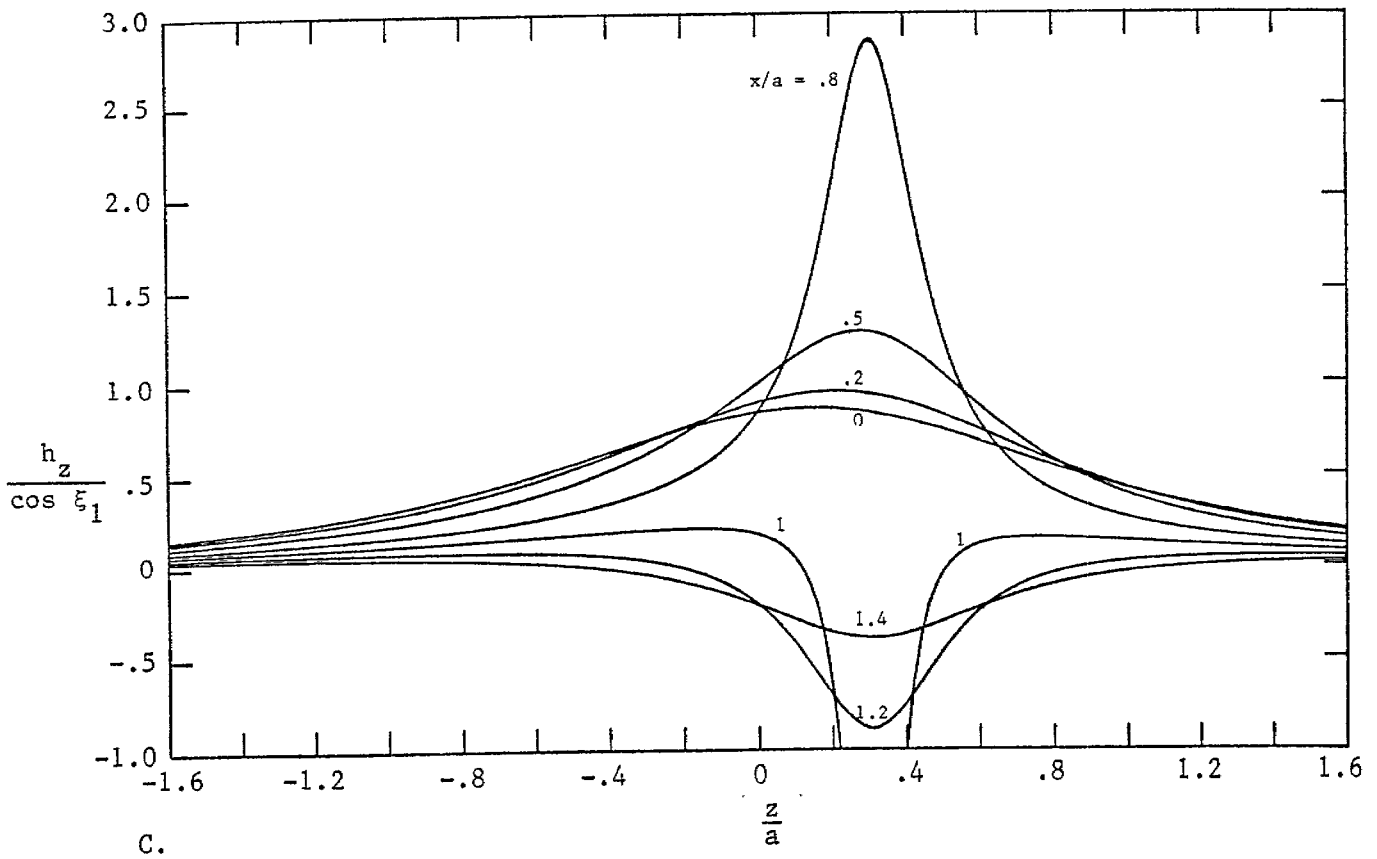

C.

Figure 22. Magnetic Field Components as a Function of z: $\frac{2\xi_1}{\pi} = .2$; $\frac{y}{a} = 0$.

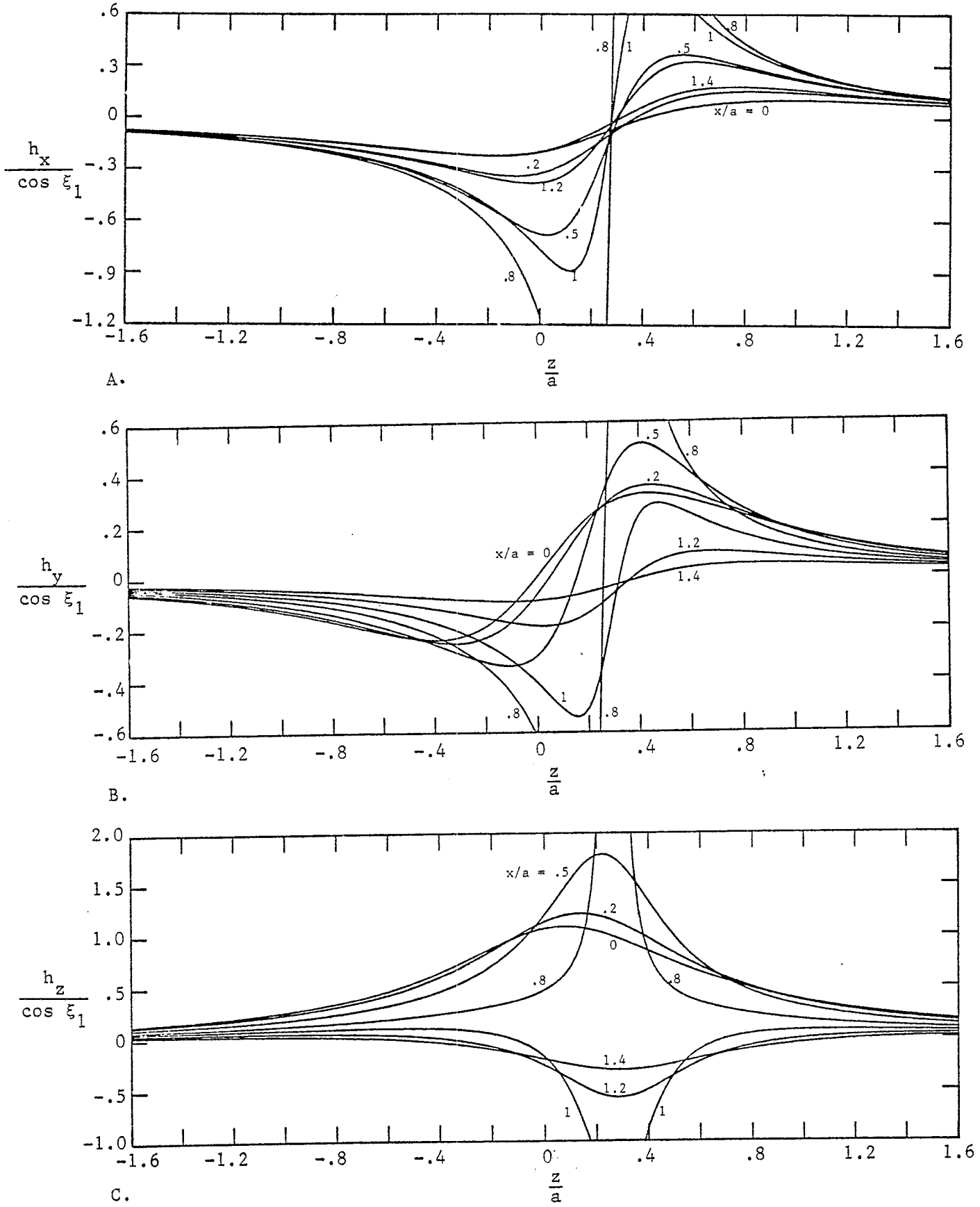

Figure 23. Magnetic Field Components as a Function of z: $\frac{2\xi_1}{\pi} = .2$; $\frac{y}{a} = .5$.

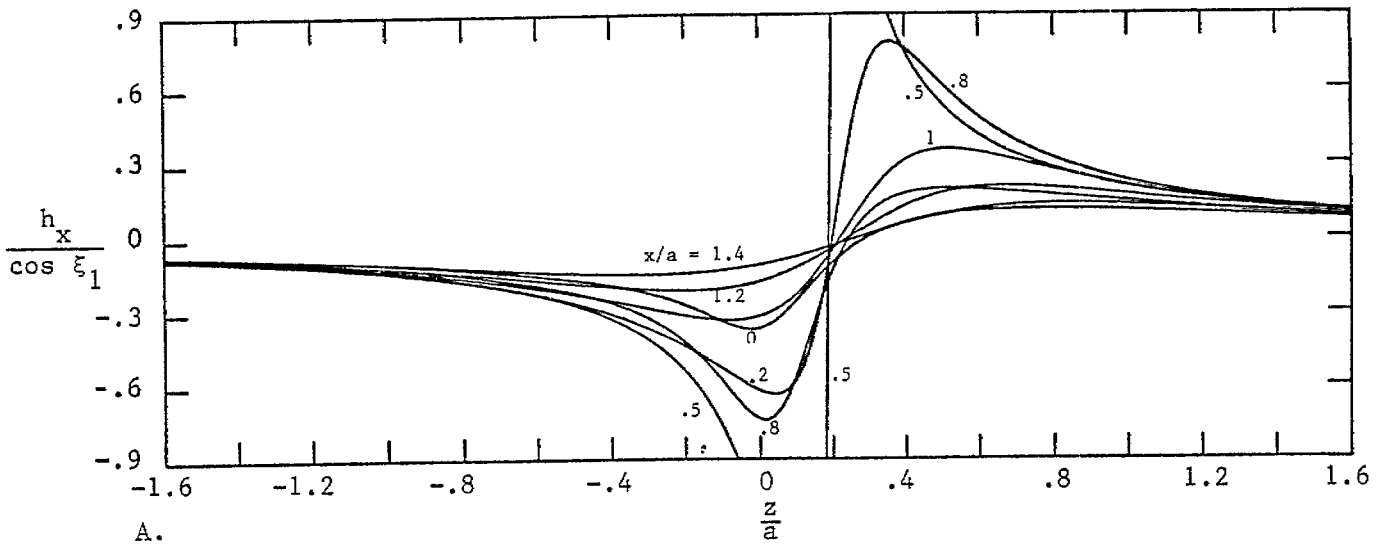

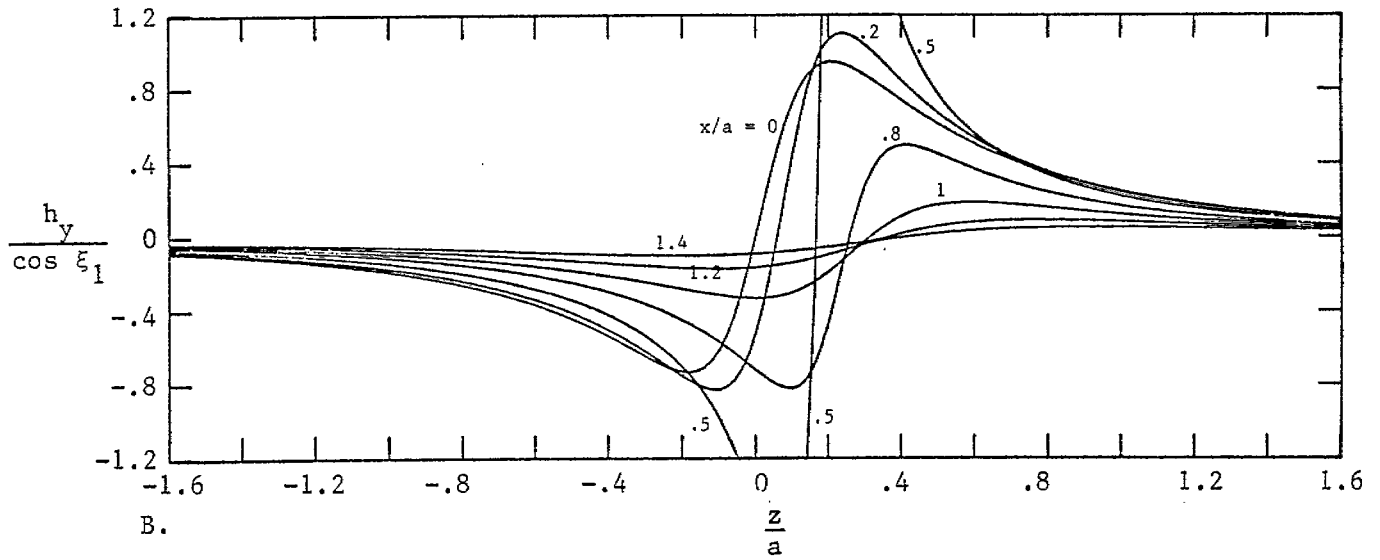

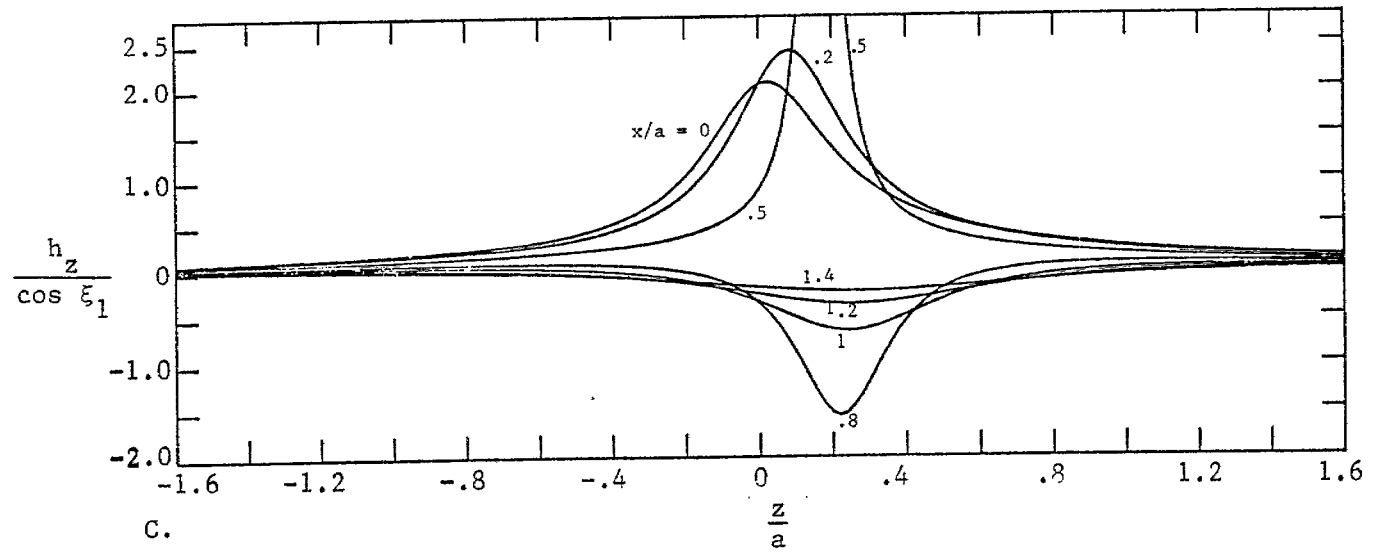

Figure 24. Magnetic Field Components as a Function of z: $\frac{2\xi_1}{\pi} = .2$; $\frac{y}{a} = .8$.

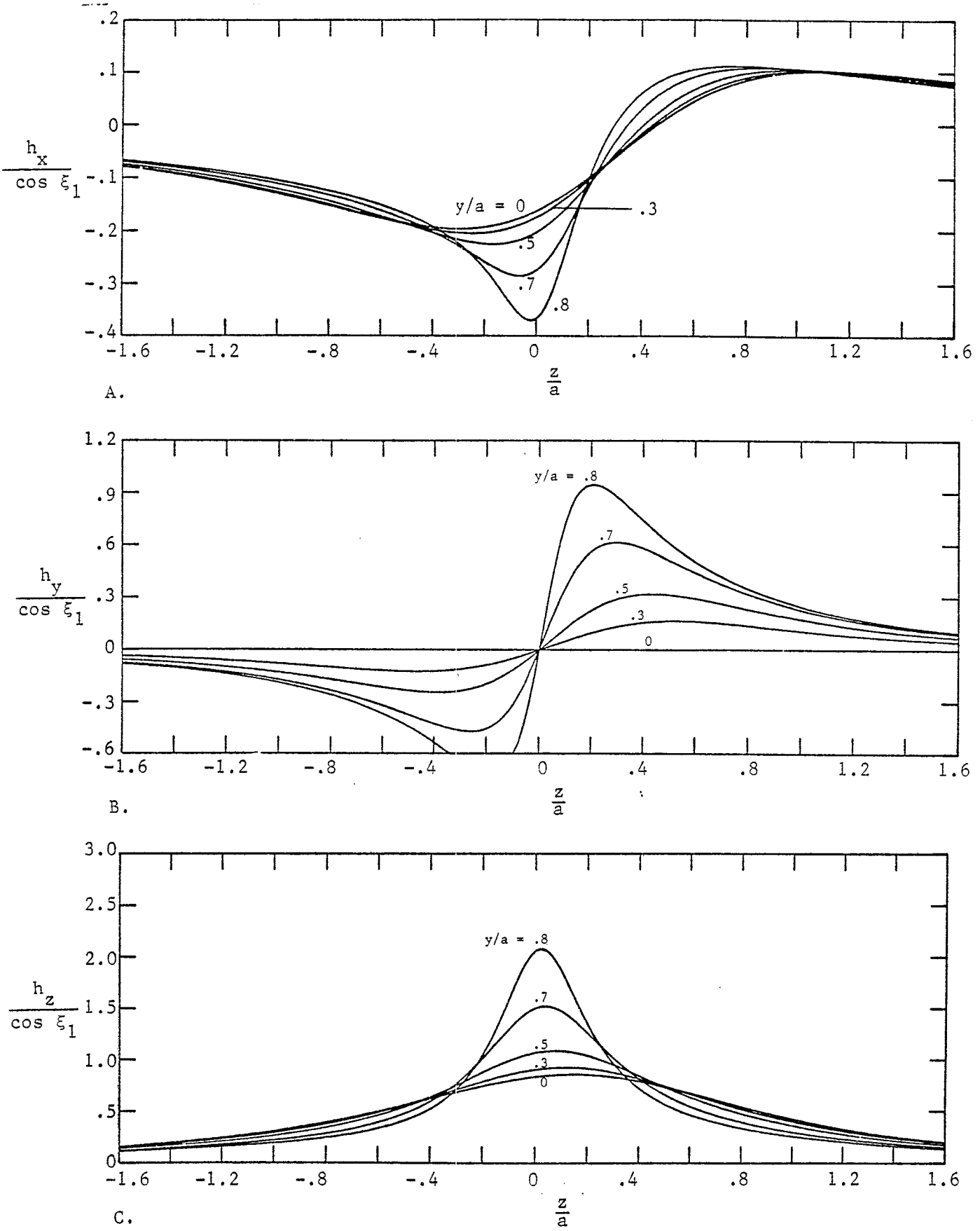

Figure 25. Magnetic Field Components as a Function of z: $\frac{2\xi_1}{\pi} = .2$; $\frac{x}{a} = 0$.

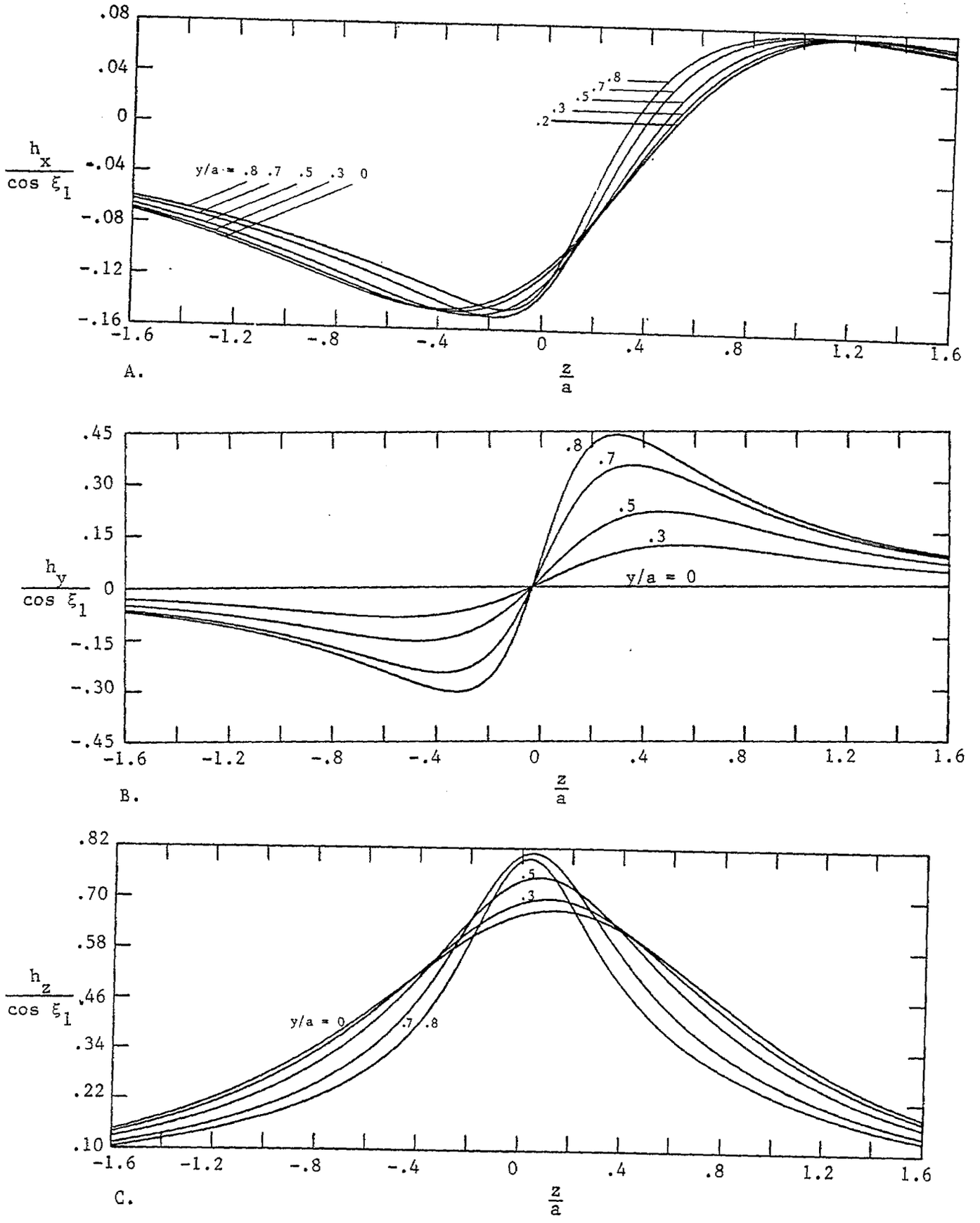

Figure 26. Magnetic Field Components as a Function of z: $\frac{2\xi_1}{\pi} = .2$; $\frac{x}{a} = -.2$.

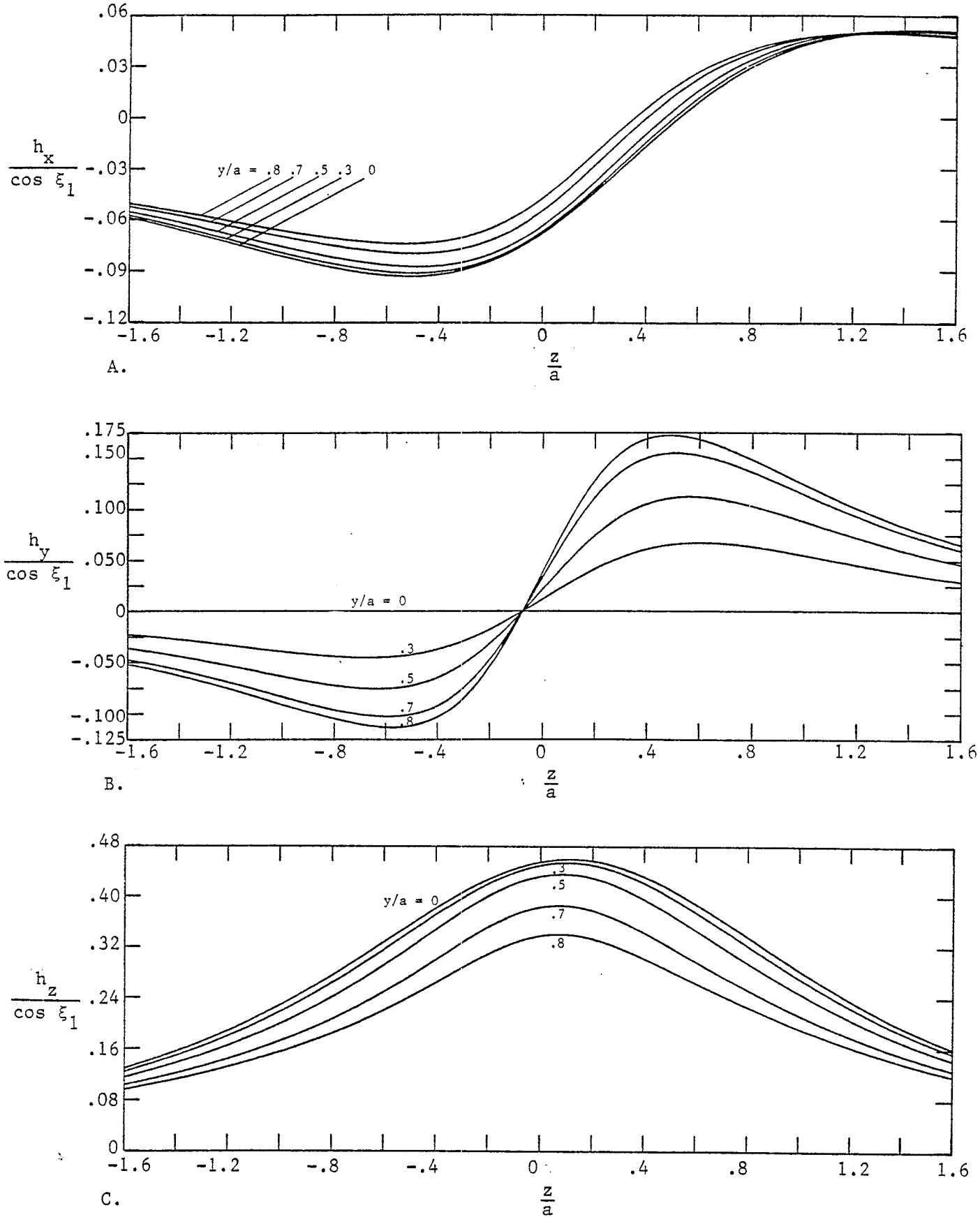

Figure 27. Magnetic Field Components as a Function of z: $\frac{2\xi_1}{\pi} = .2$; $\frac{x}{a} = -.5$.

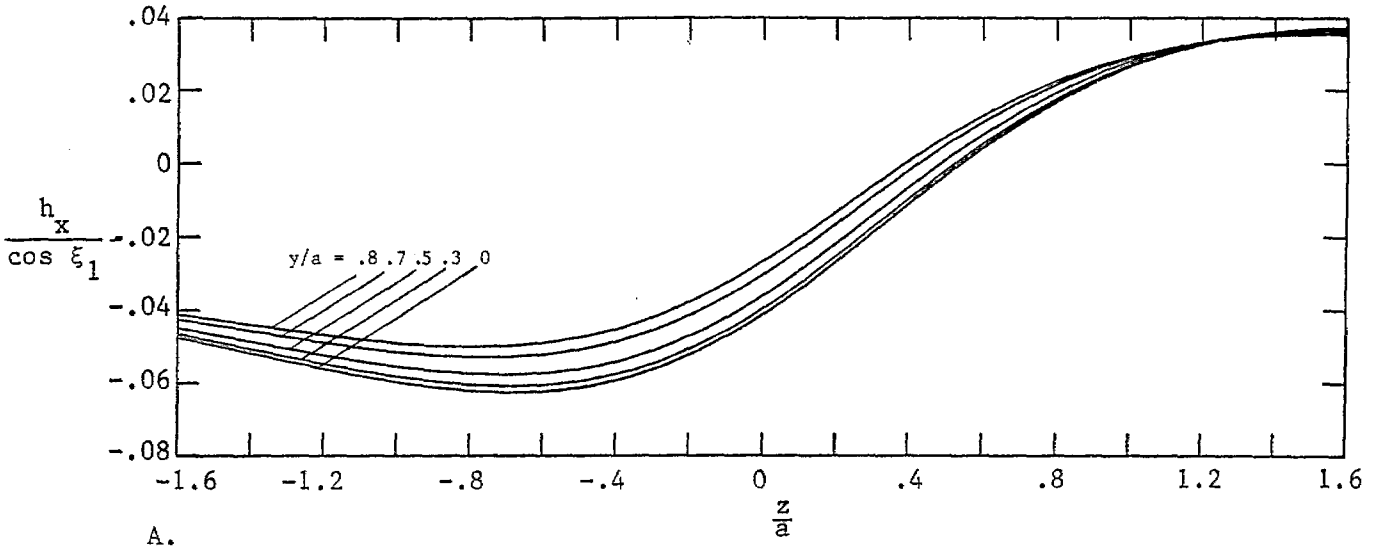

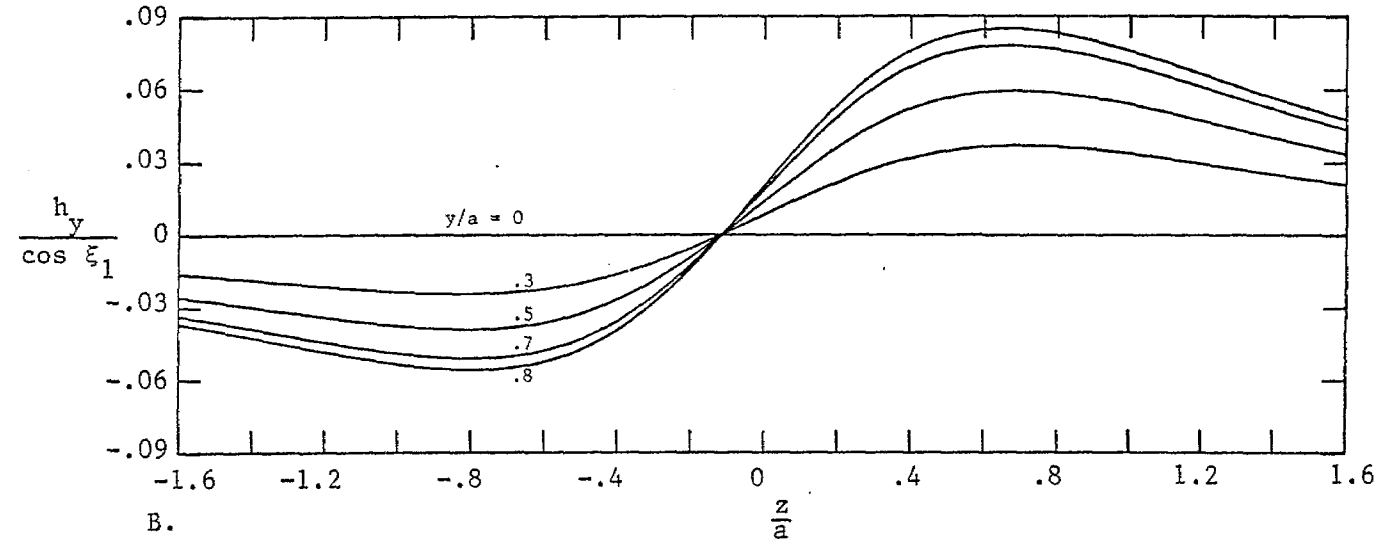

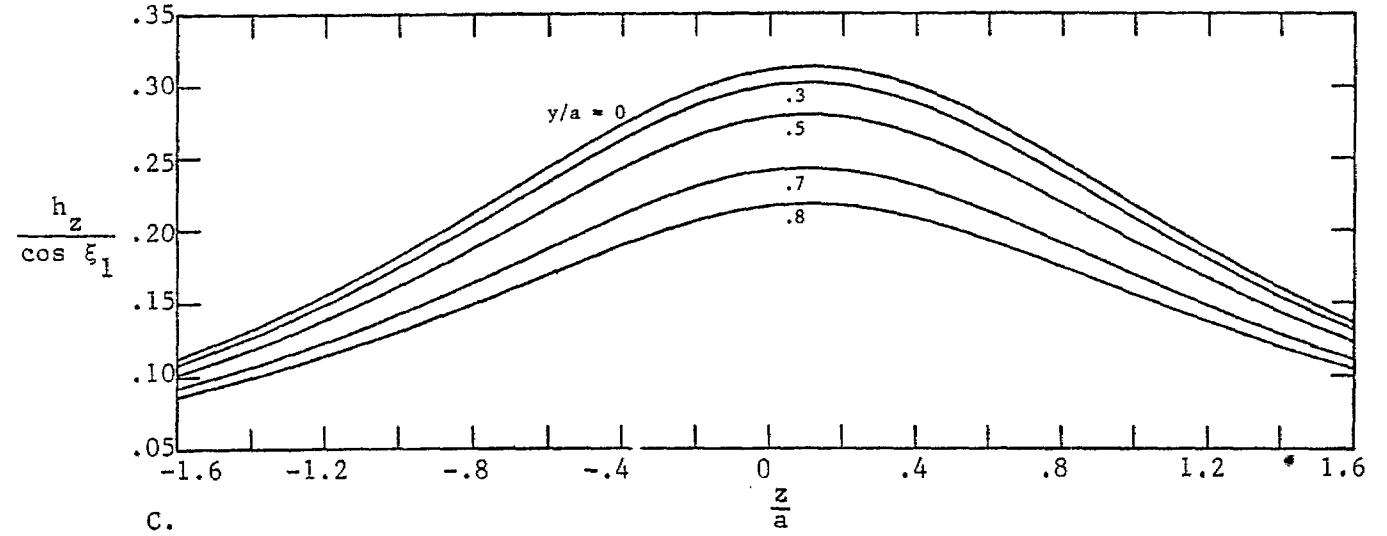

Figure 28. Magnetic Field Components as a Function of z: $\frac{2\xi_1}{\pi} = .2$; $\frac{x}{a} = -.8$.

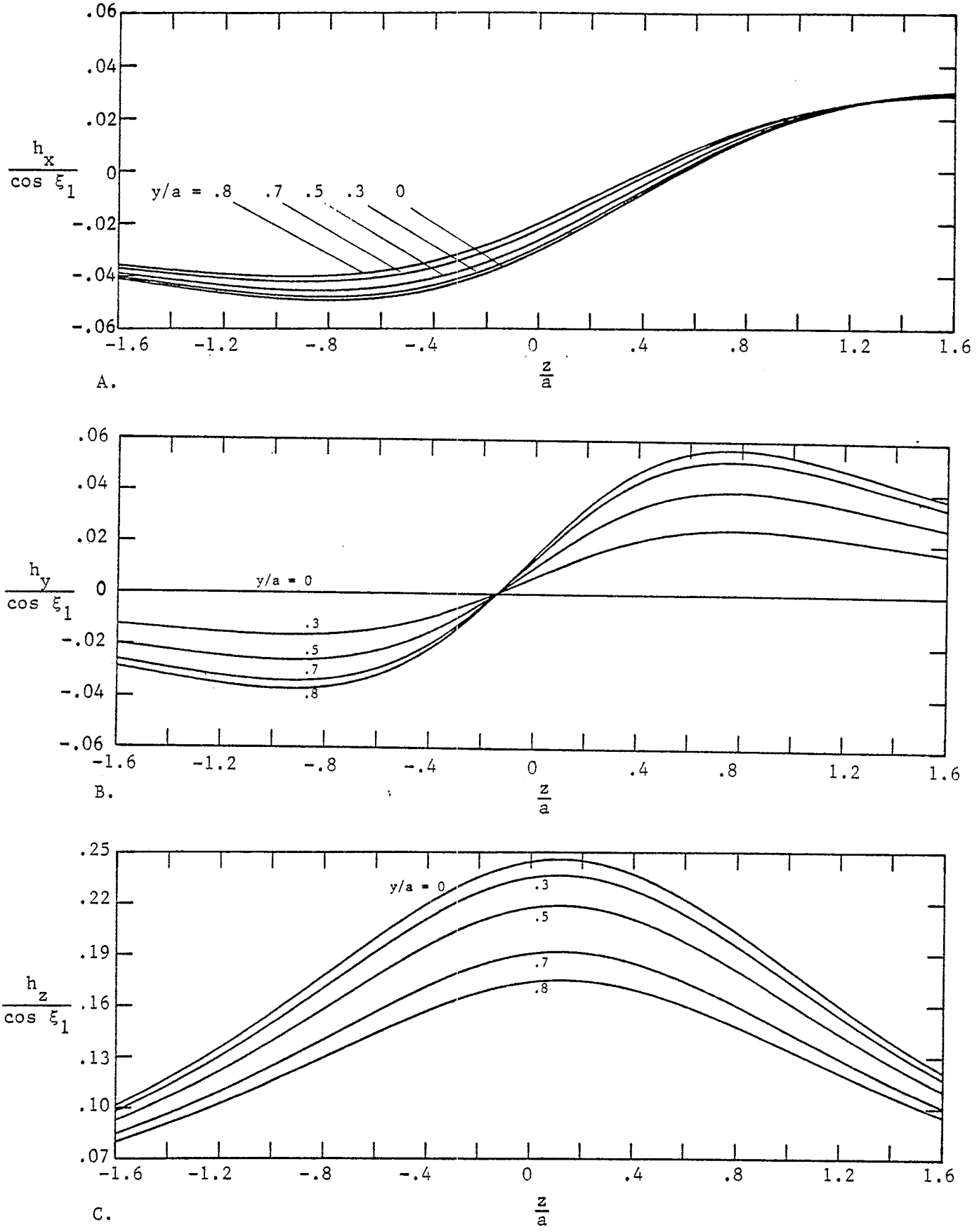

Figure 29. Magnetic Field Components as a Function of z: $\frac{2\xi_1}{\pi} = .2$; $\frac{x}{a} = -1$.

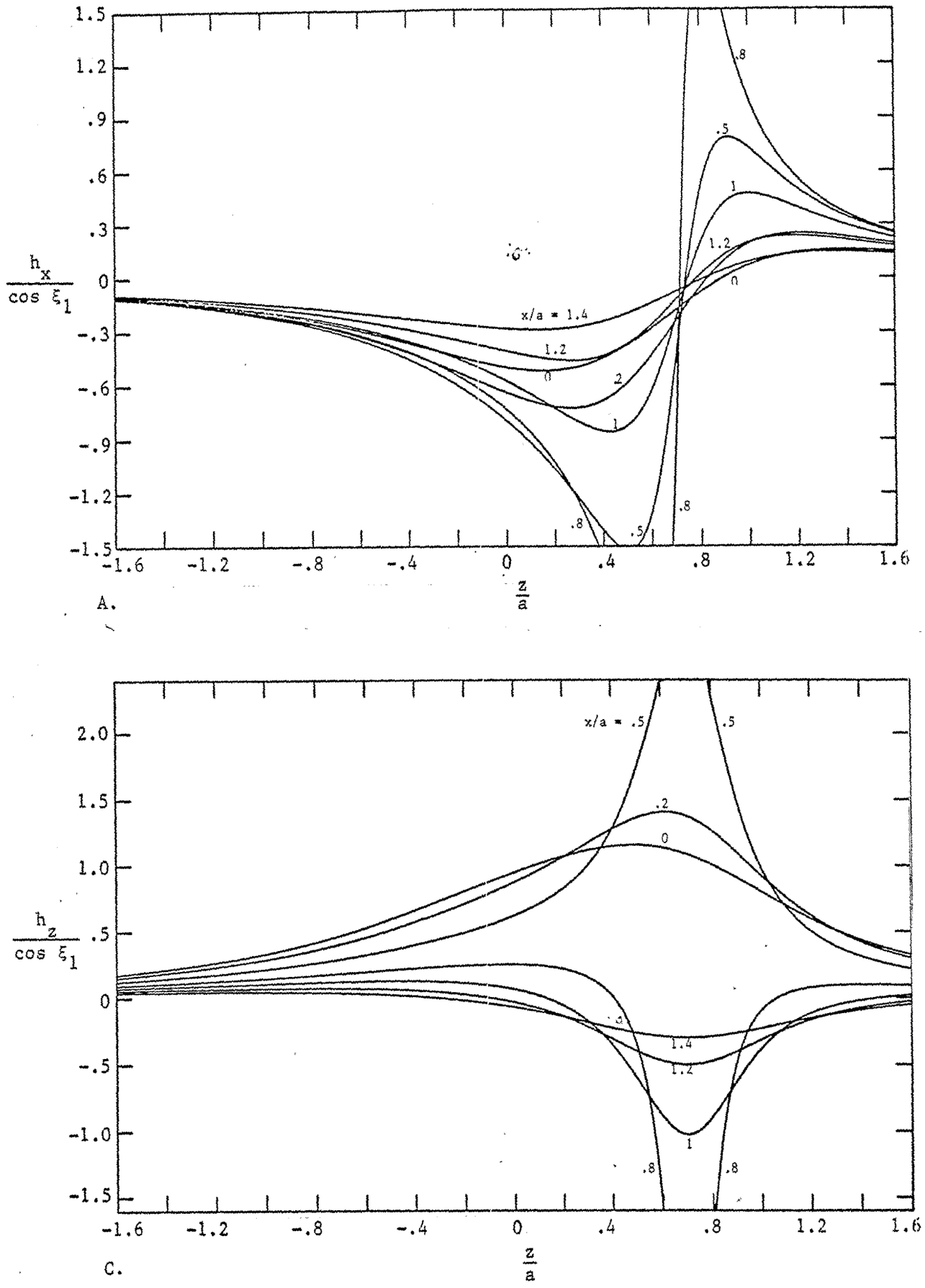

Figure 30. Magnetic Field Components as a Function of z: $\frac{2\xi_1}{\pi} = .5$; $\frac{Y}{a} = 0$.

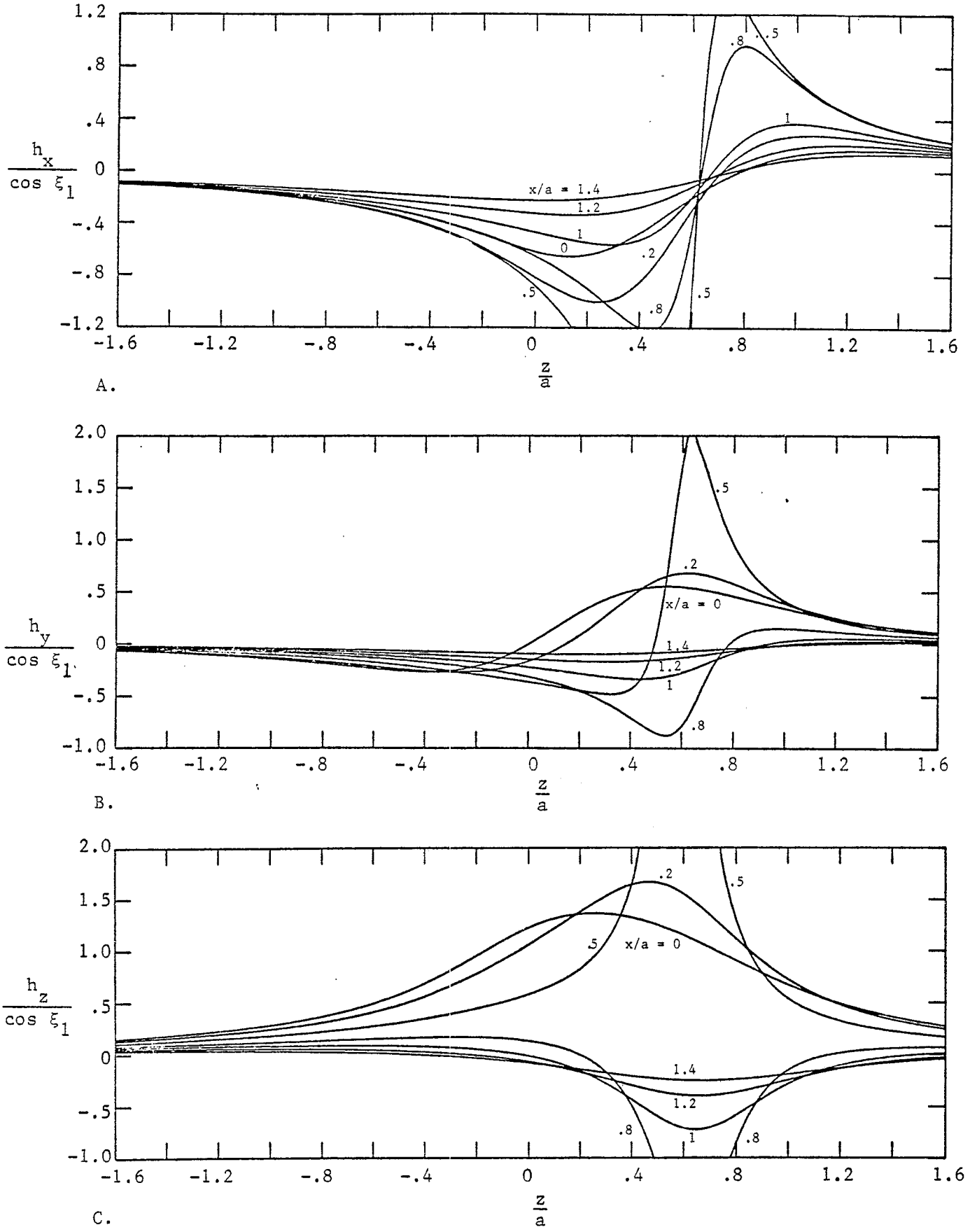

Figure 31. Magnetic Field Components as a Function of z: $\frac{2\xi_1}{\pi} = .5$; $\frac{y}{a} = .5$.

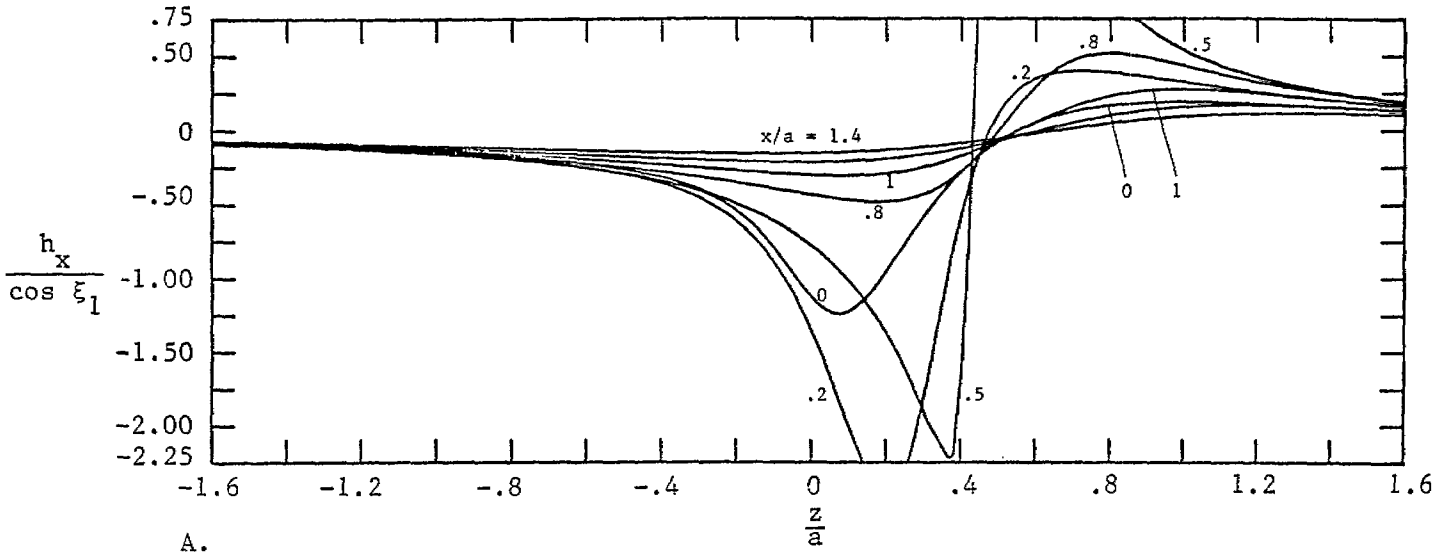

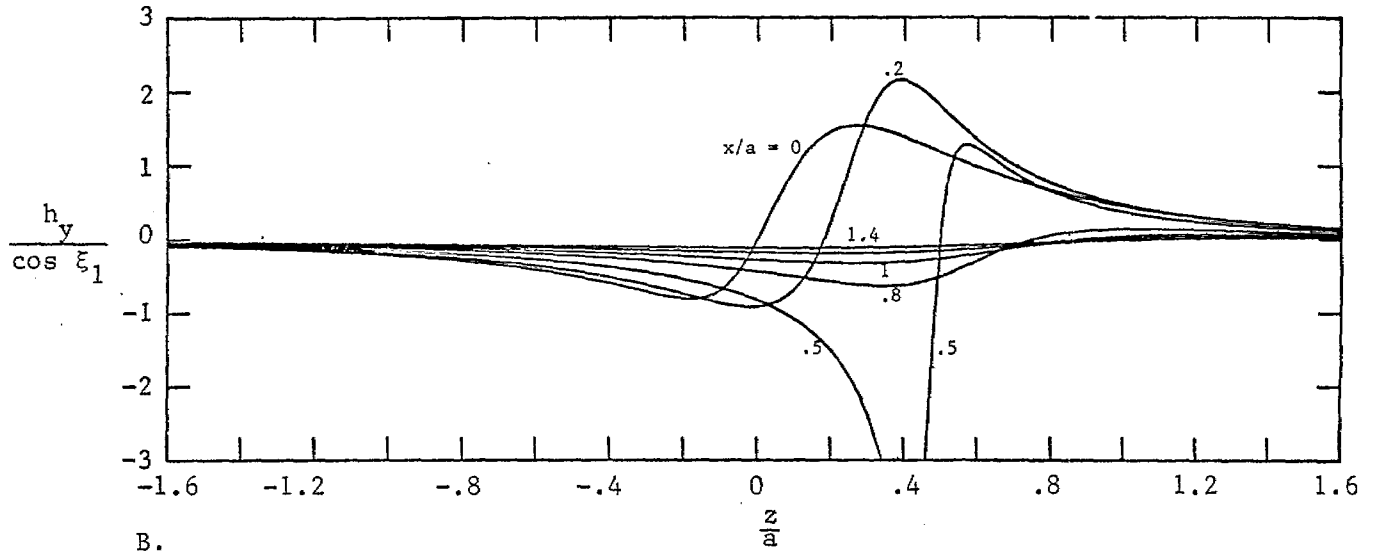

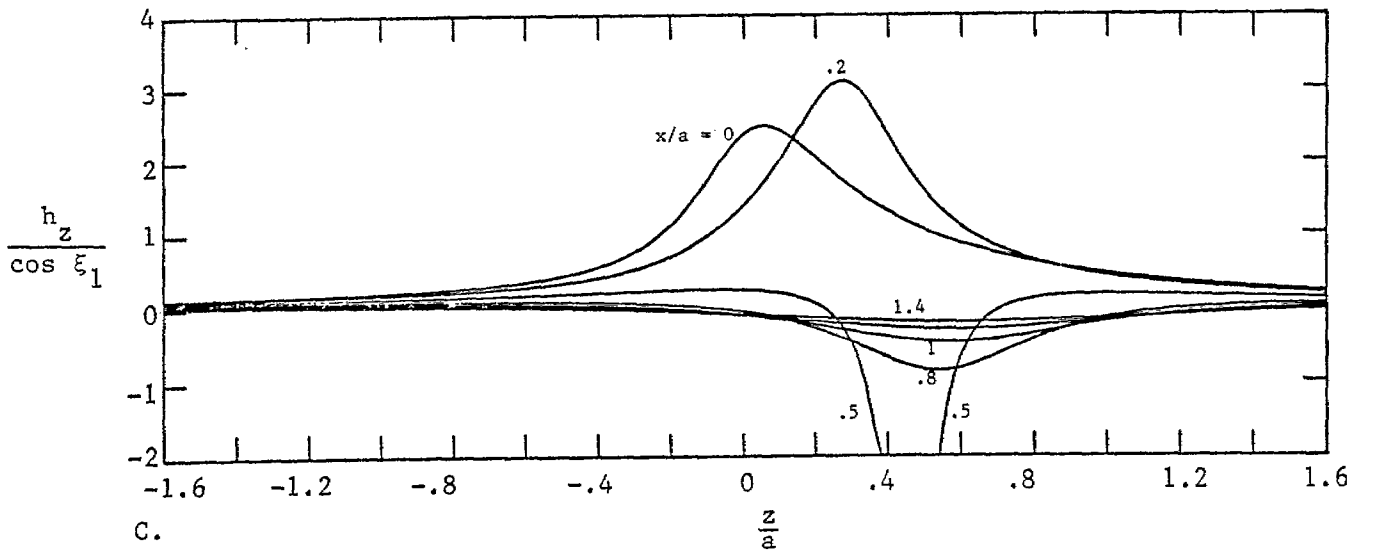

Figure 32. Magnetic Field Components as a Function of z; $\frac{2\xi_1}{\pi} = .5$; $\frac{y}{a} = .8$.

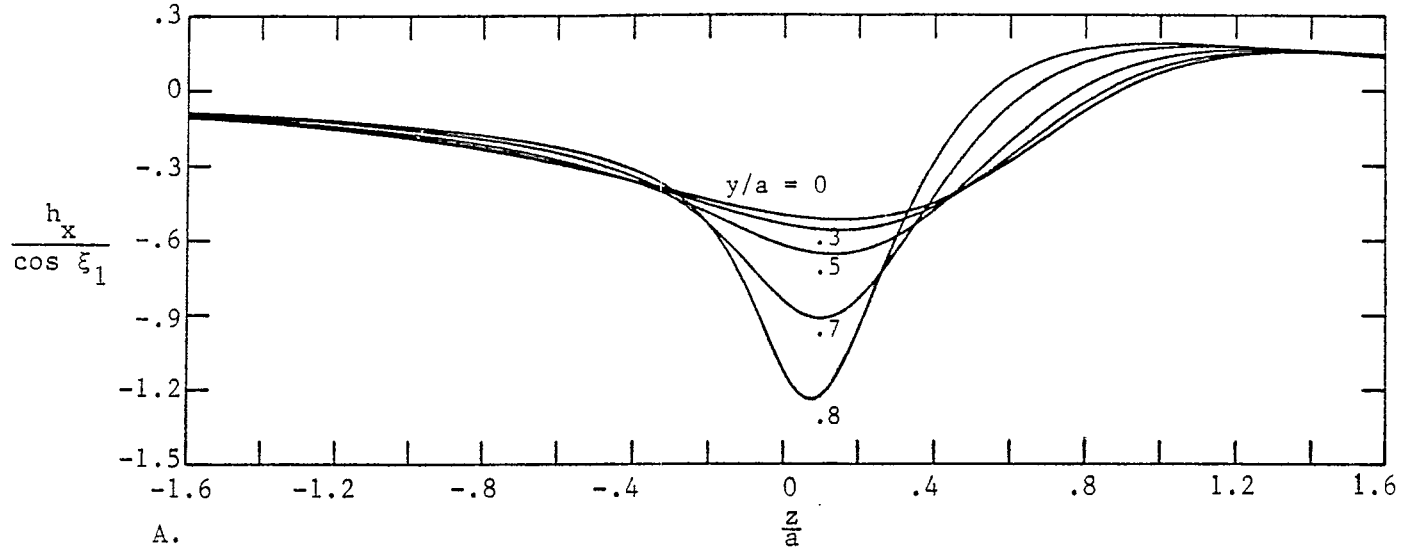

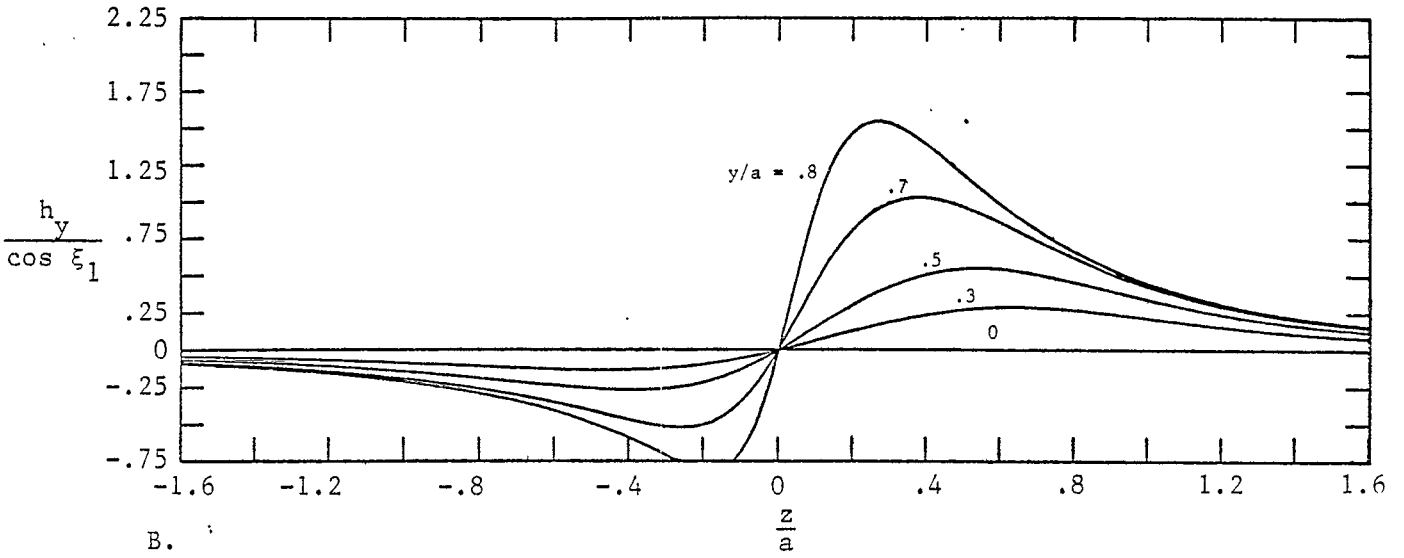

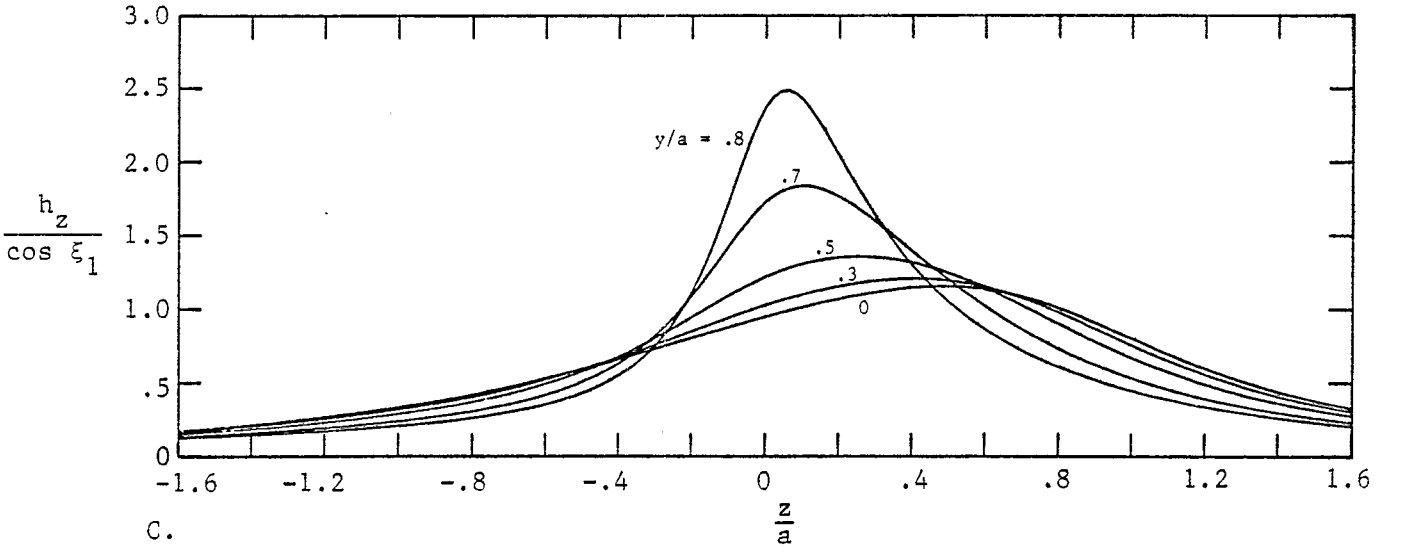

Figure 33. Magnetic Field Components as a Function of z: $\frac{2\xi_1}{\pi} = .5$; $\frac{x}{a} = 0$.

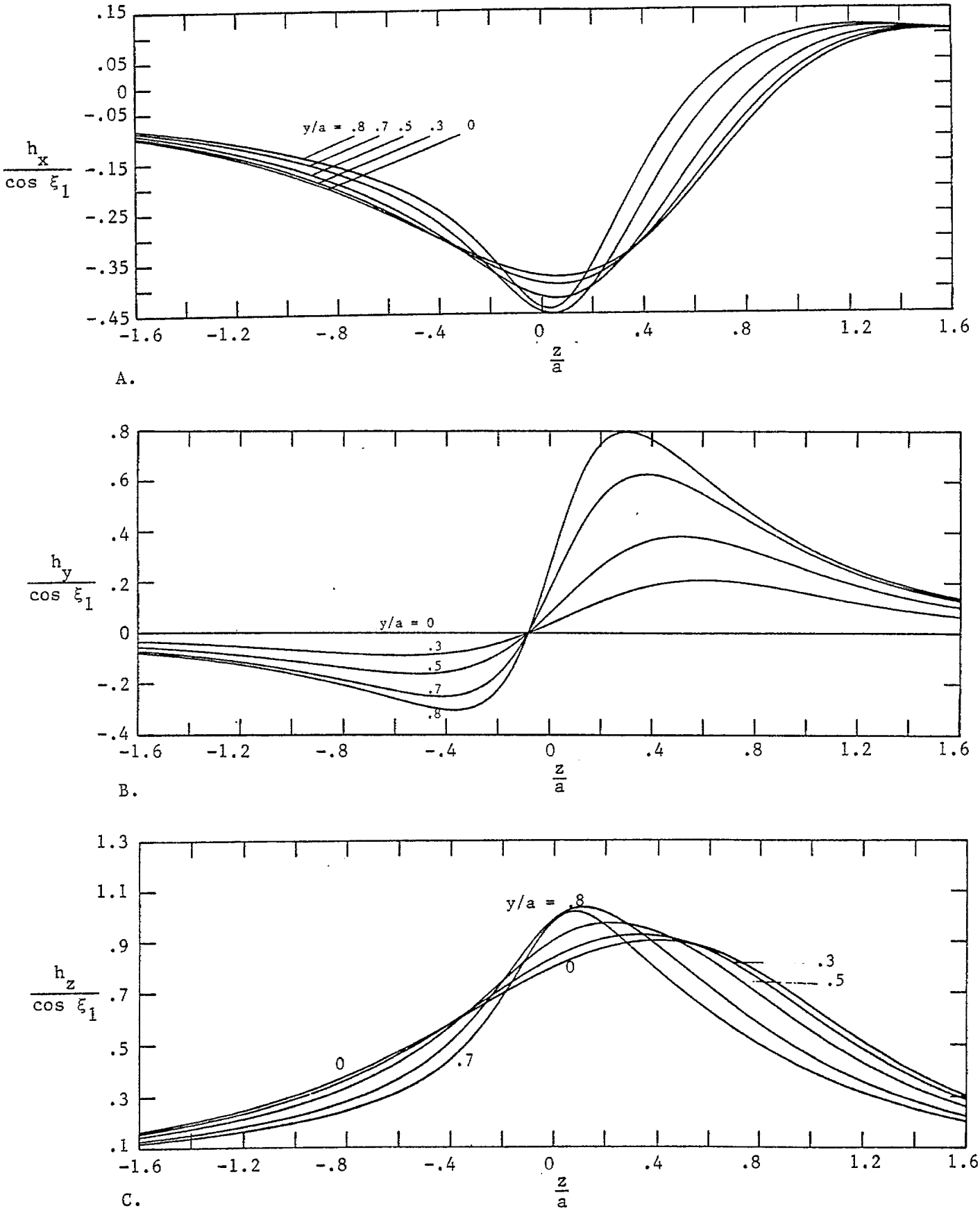

Figure 34. Magnetic Field Components as a Function of z: $\frac{2\xi_1}{\pi} = .5$; $\frac{x}{a} = -.2$.

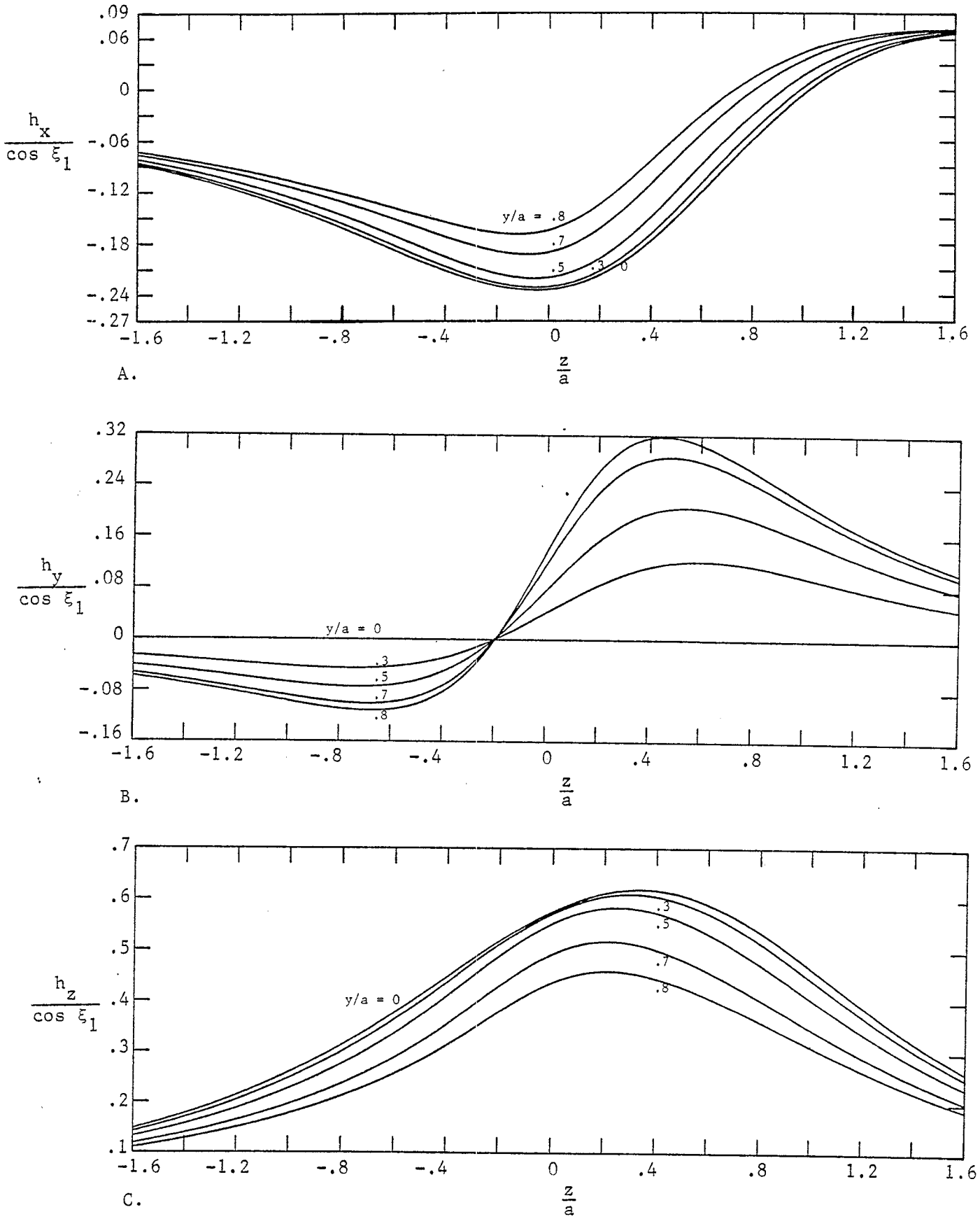

Figure 35. Magnetic Field Components as a Function of z: $\frac{2\xi_1}{\pi} = .5$; $\frac{x}{a} = -.5$.

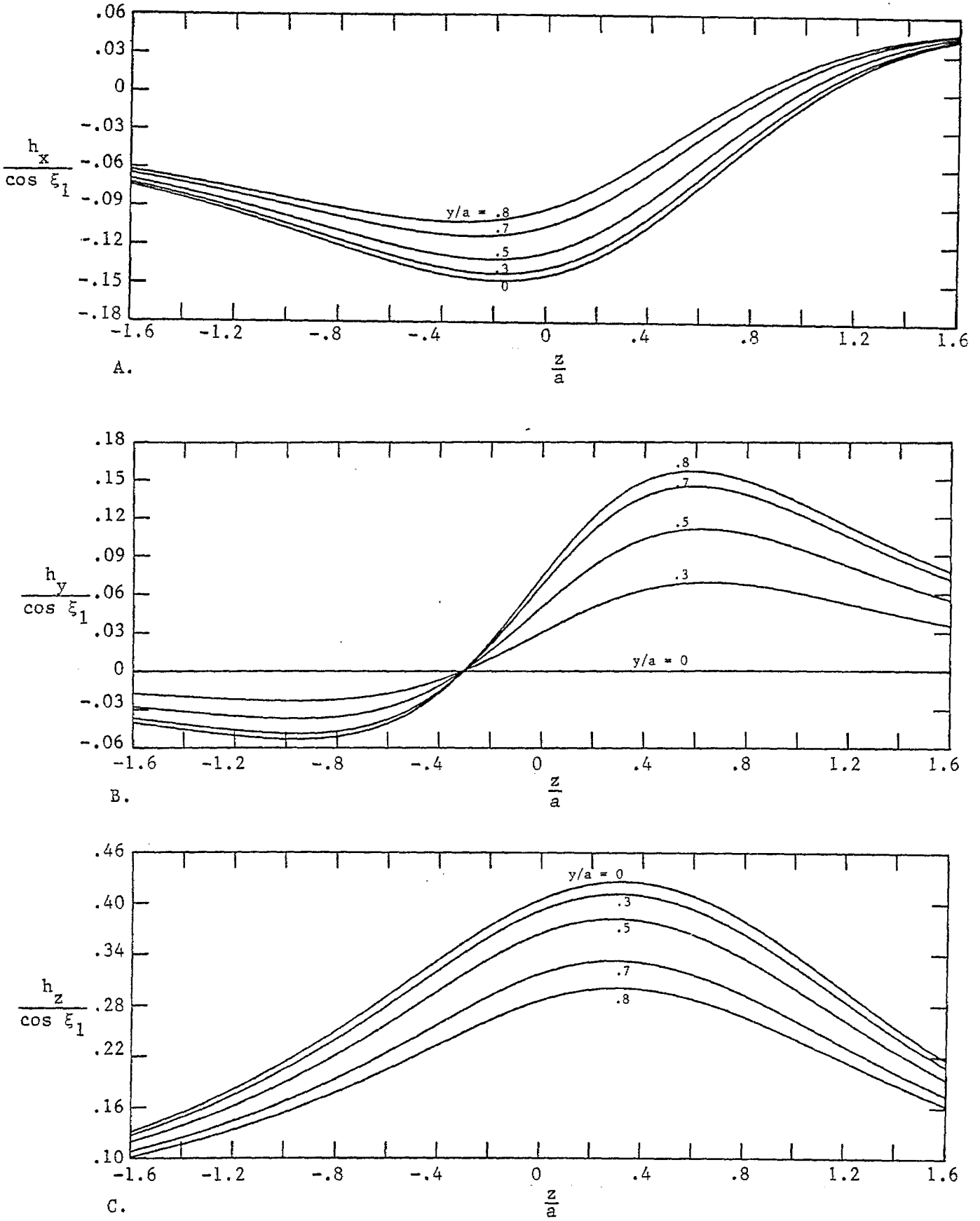

Figure 36. Magnetic Field Components as a Function of z: $\frac{2\xi_1}{\pi} = .5$; $\frac{x}{a} = -.8$.

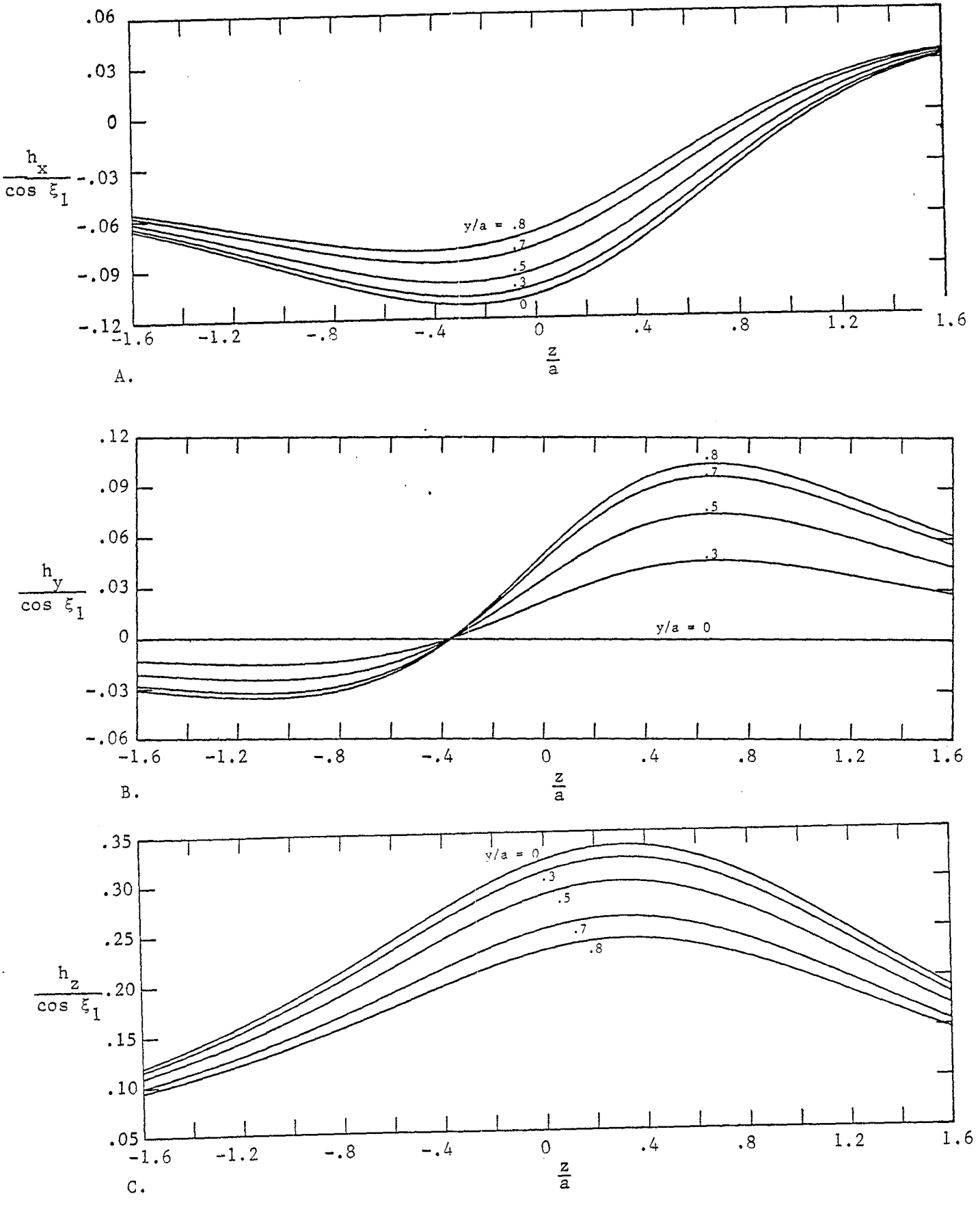

Figure 37. Magnetic Field Components as a Function of z: $\frac{2\xi_1}{\pi} = .5$; $\frac{x}{a} = -1.$

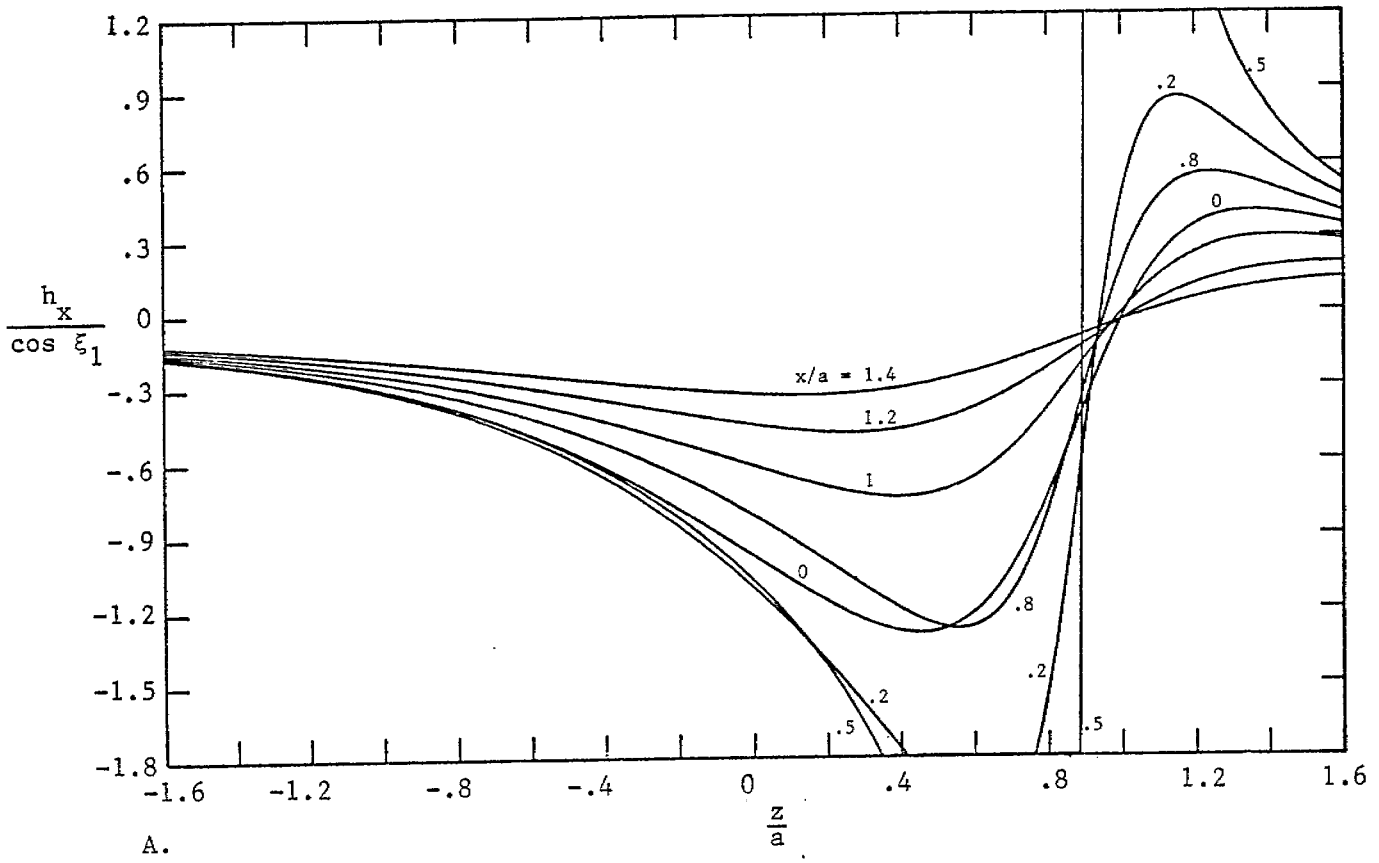

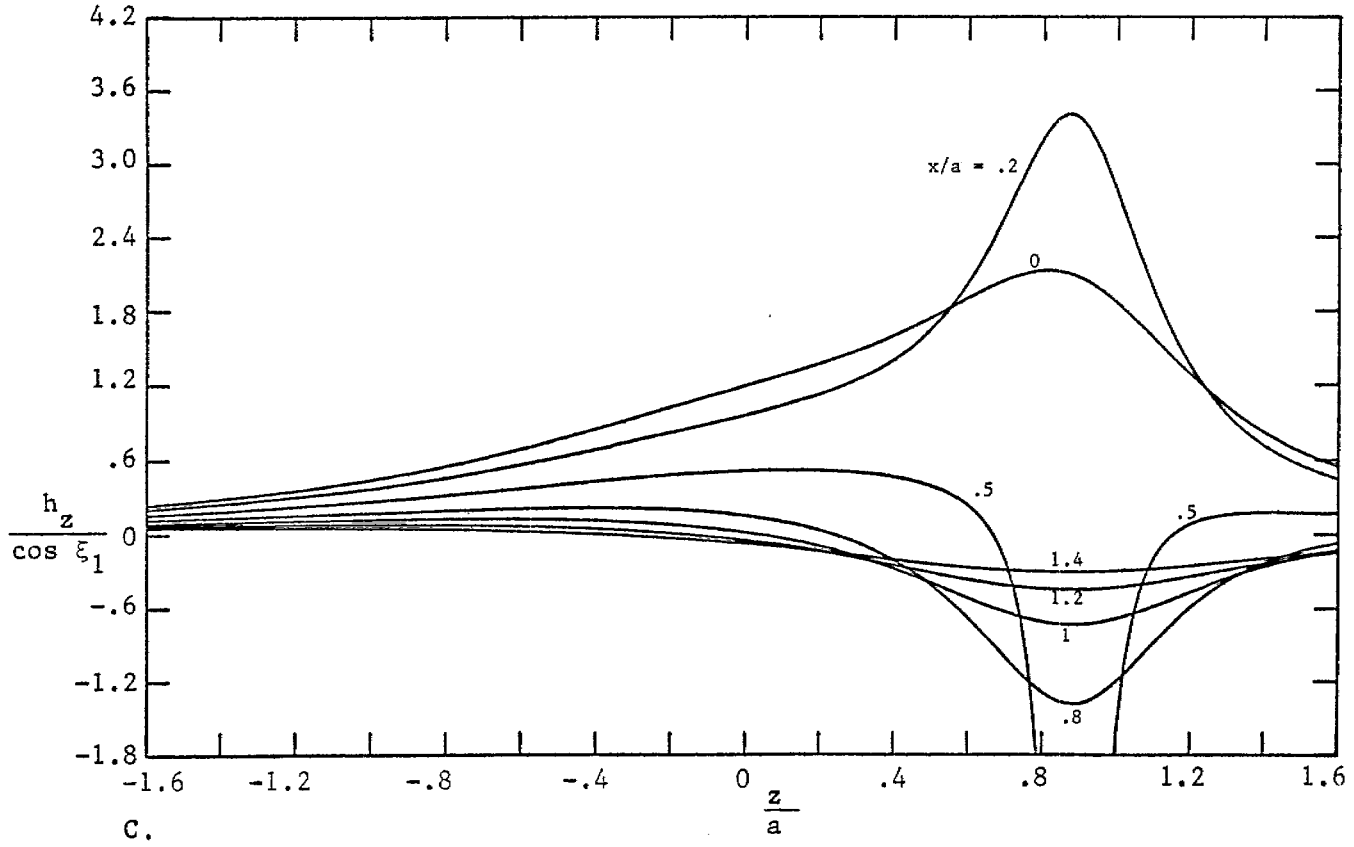

Figure 38. Magnetic Field Components as a Function of z; $\frac{2\xi_1}{\pi} = .7$; $\frac{Y}{a} = 0$.

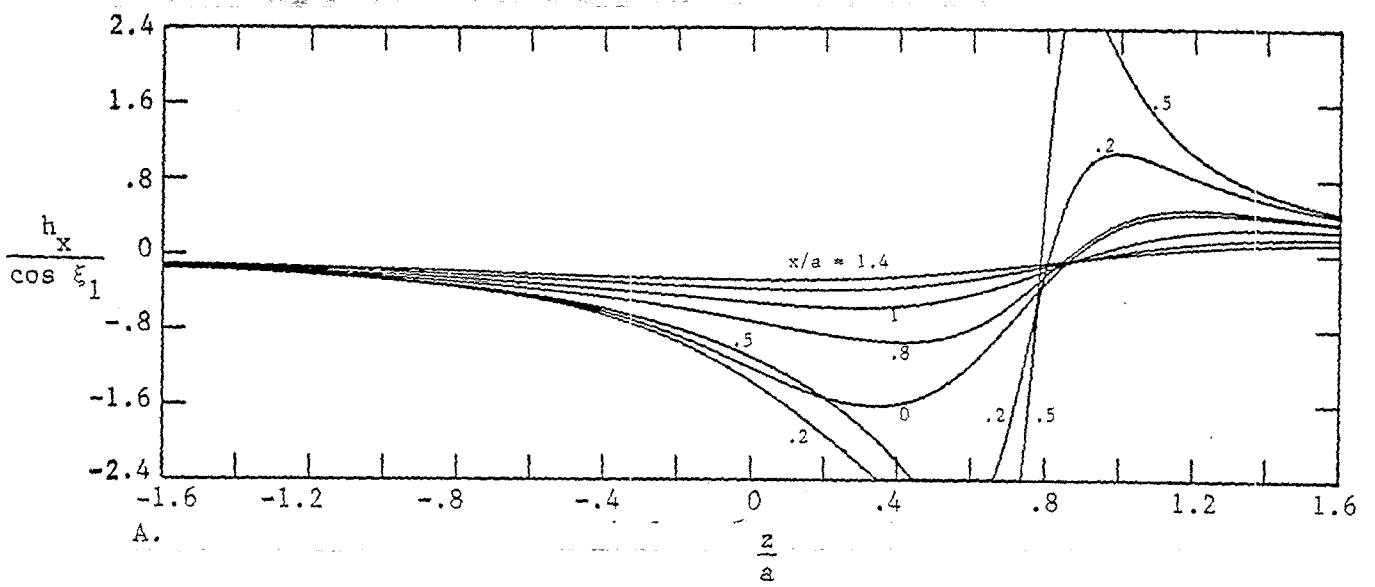

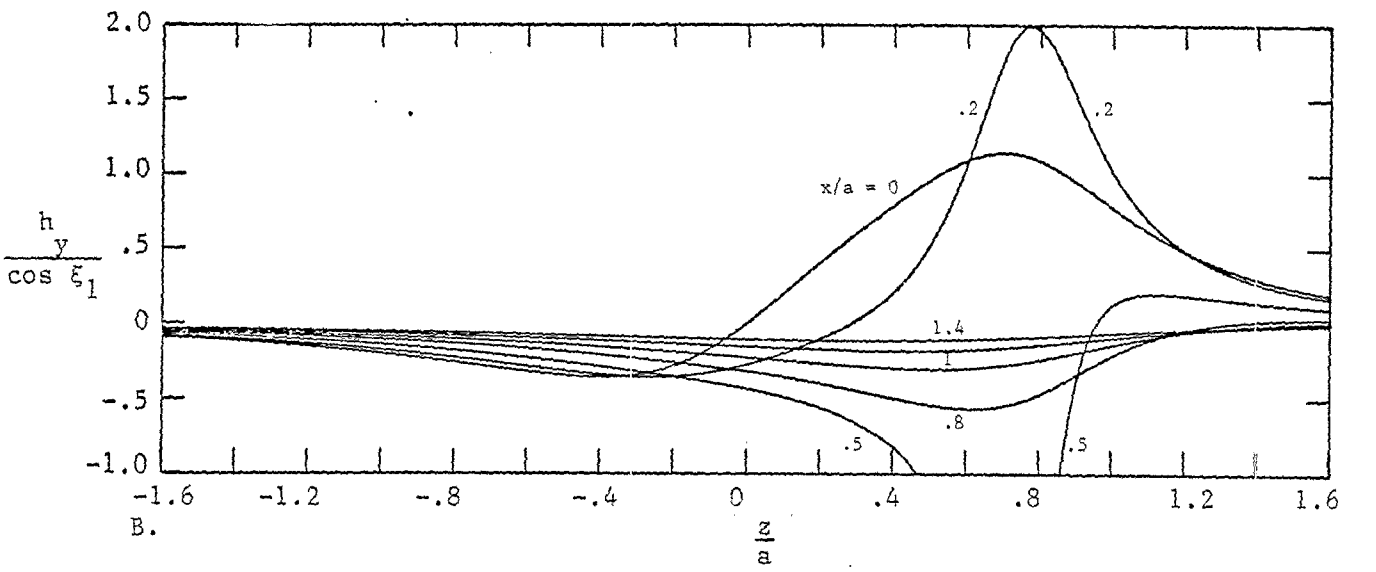

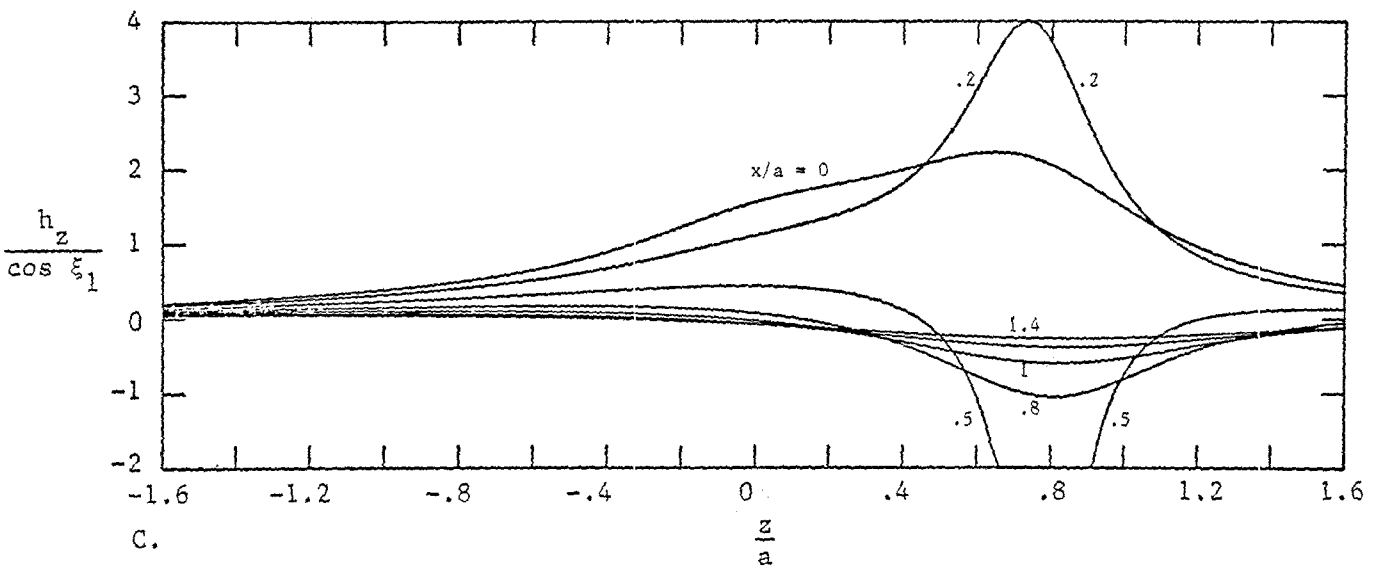

Figure 39. Magnetic Field Components as a Function of z: $\frac{2\xi_1}{\pi} = .7$; $\frac{y}{a} = .5$.

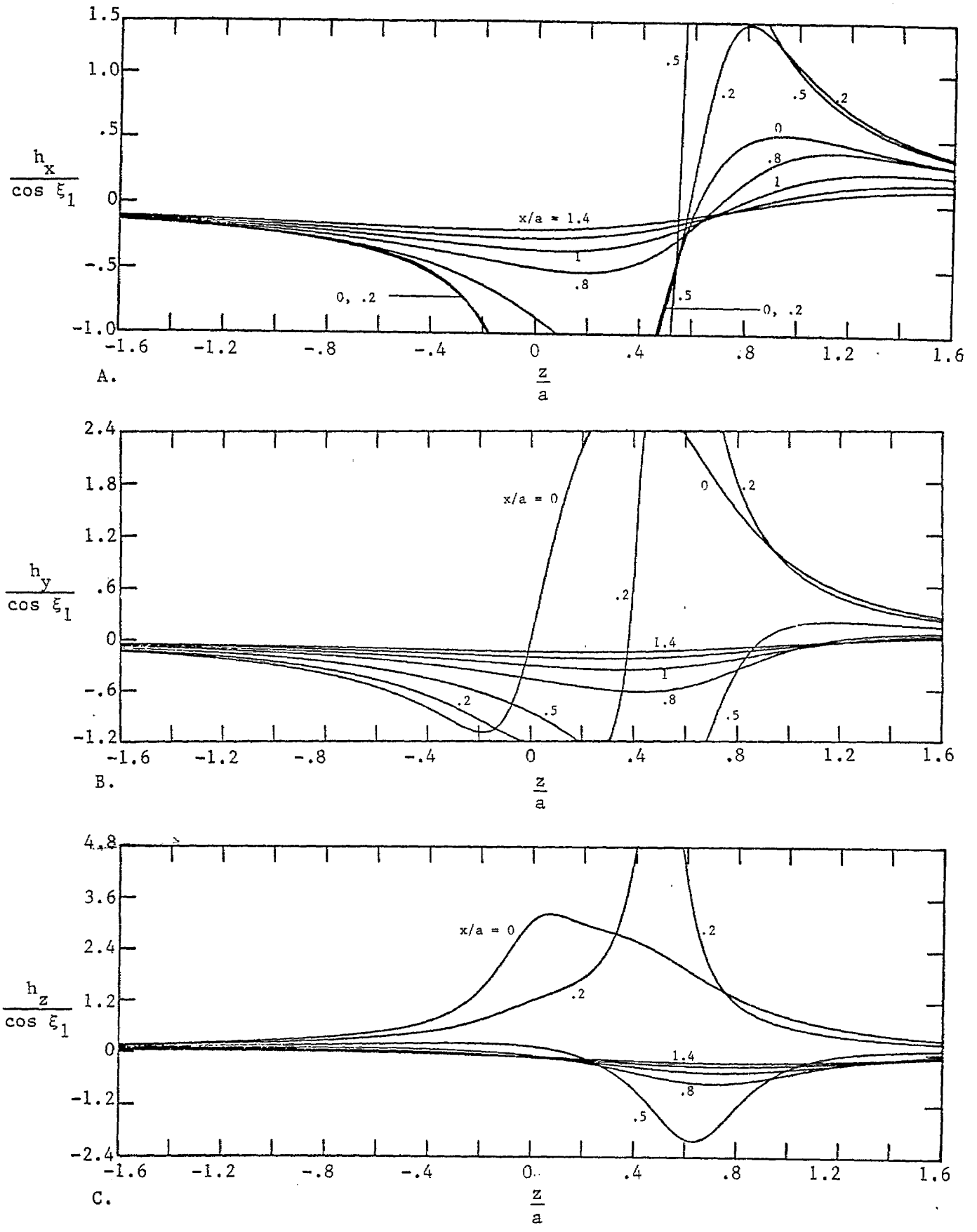

Figure 40. Magnetic Field Components as a Function of z: $\frac{2\xi_1}{\pi} = .7$; $\frac{y}{a} = .8$.

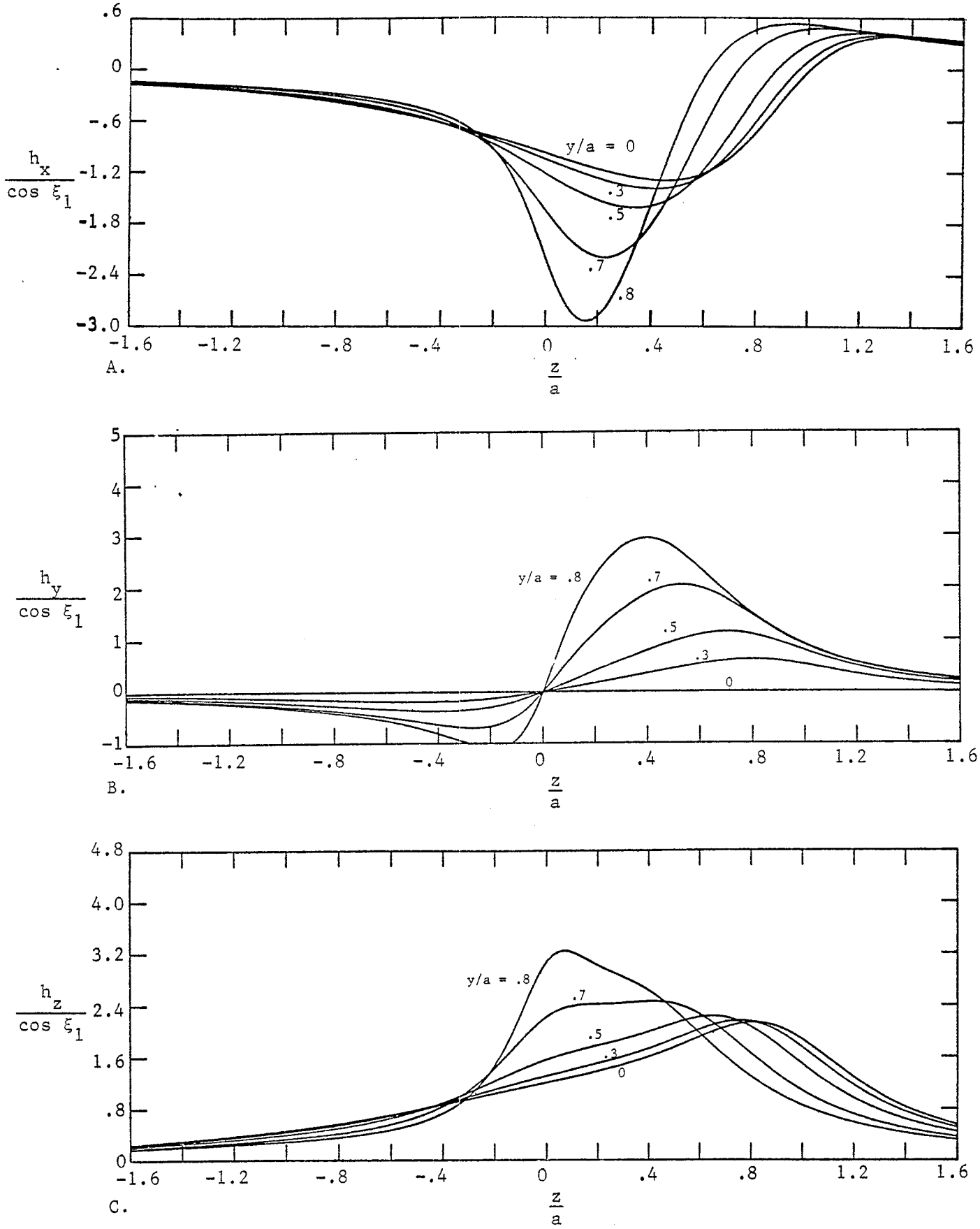

Figure 41. Magnetic Field Components as a Function of z: $\frac{2\xi_1}{\pi} = .7$; $\frac{x}{a} = 0$.

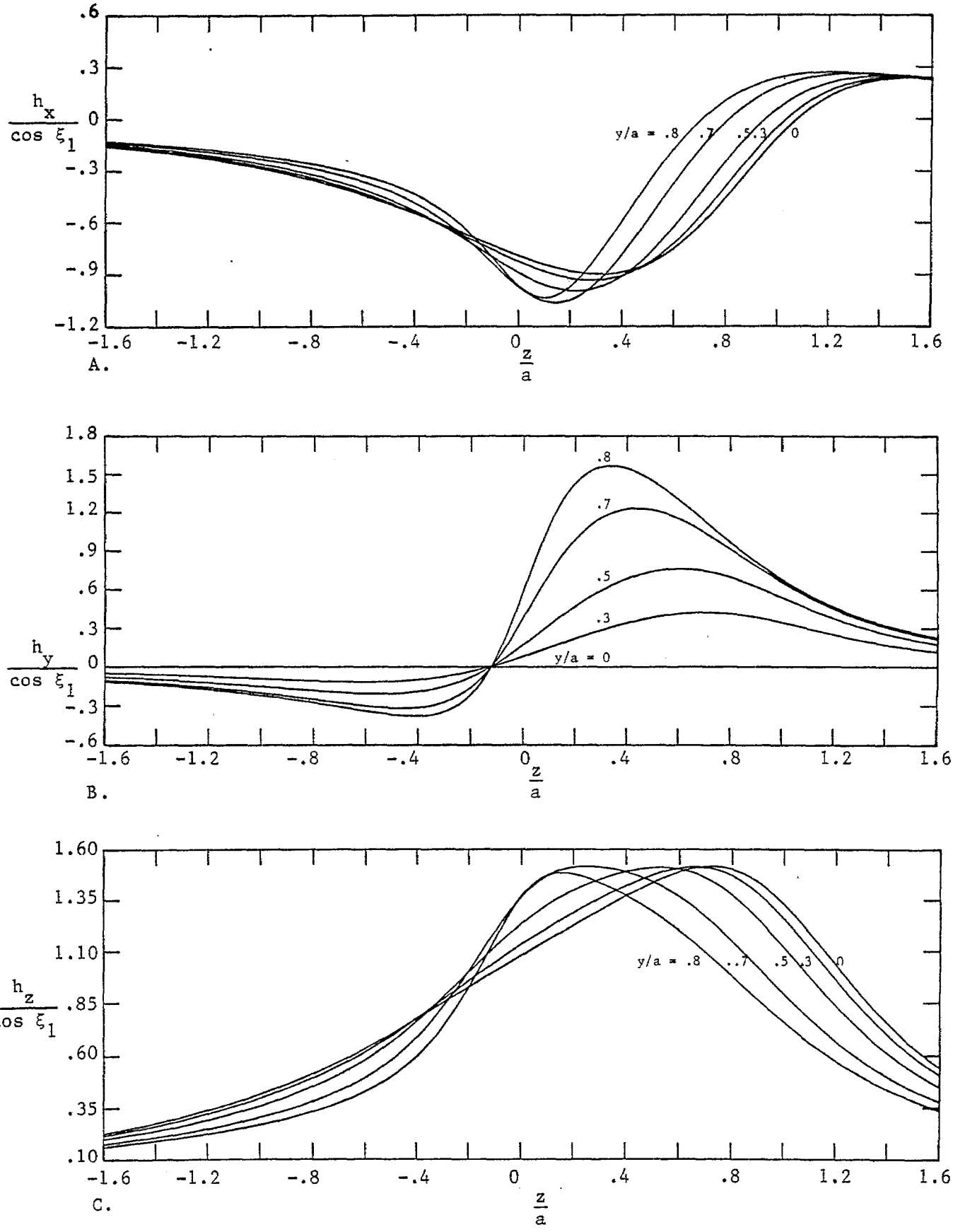

Figure 42. Magnetic Field Components as a Function of z; $\frac{2\xi_1}{\pi} = .7$; $\frac{x}{a} = -.2$.

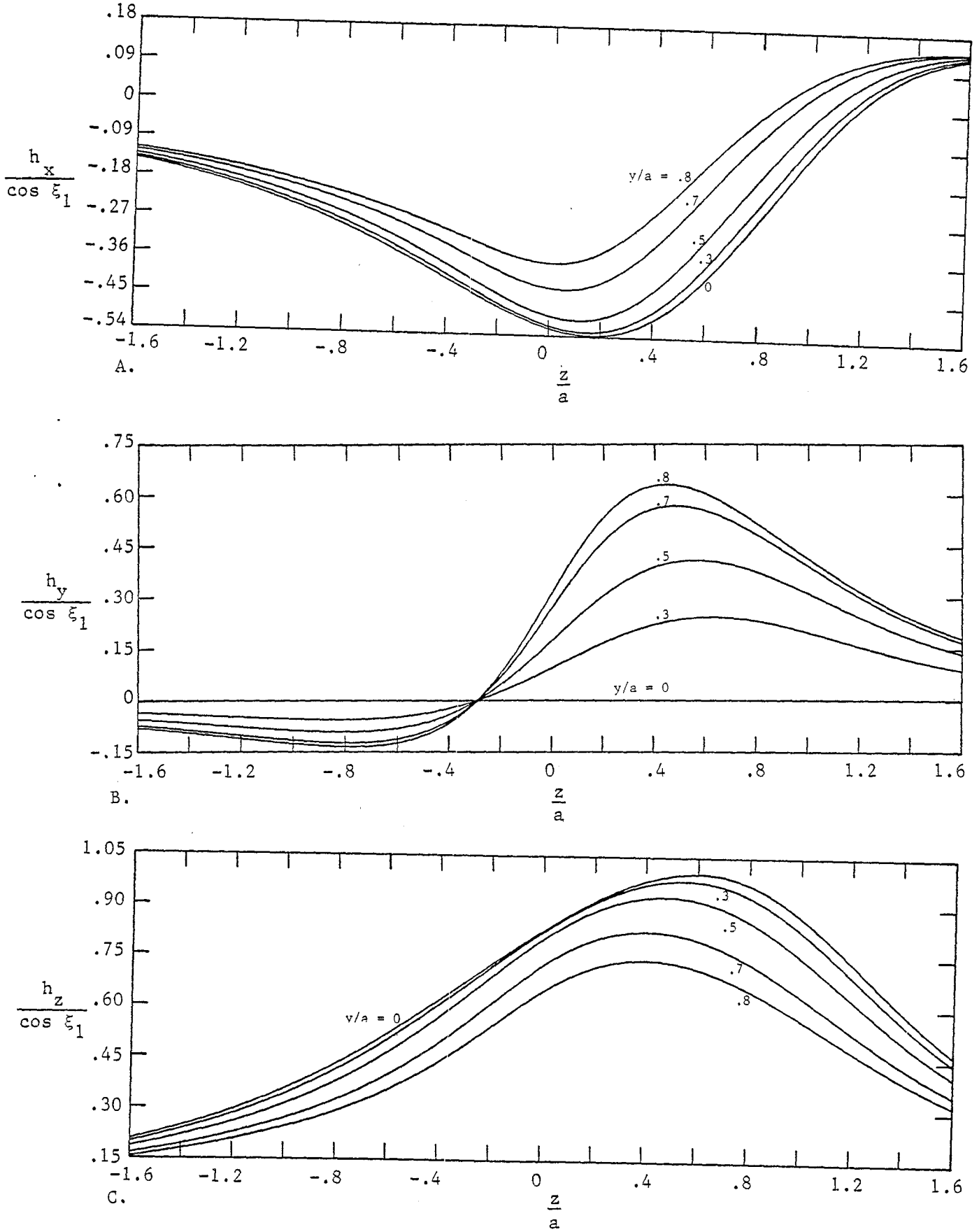

Figure 43. Magnetic Field Components as a Function of z: $\frac{2\xi_1}{\pi} = .7$; $\frac{x}{a} = -.5$.

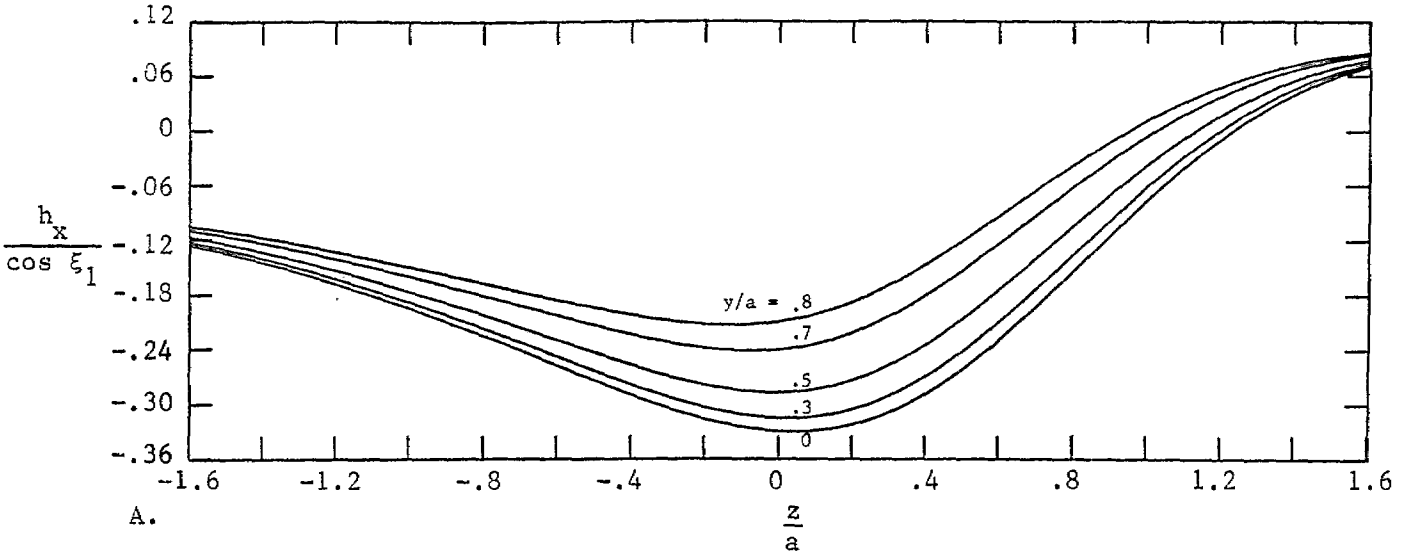

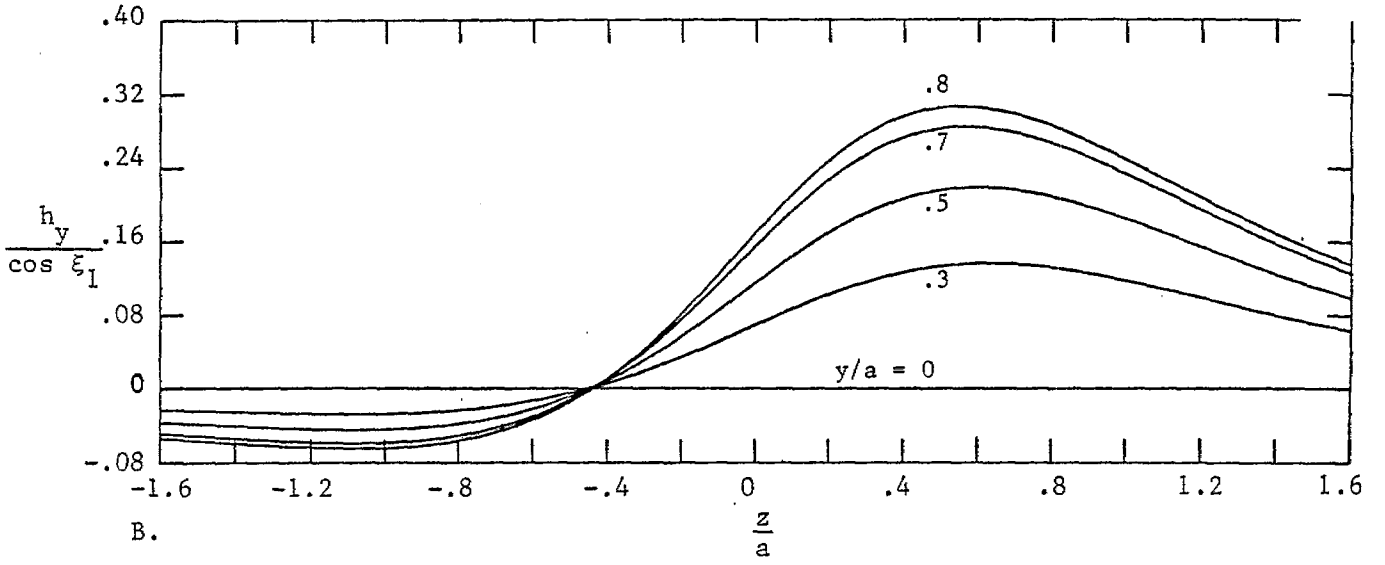

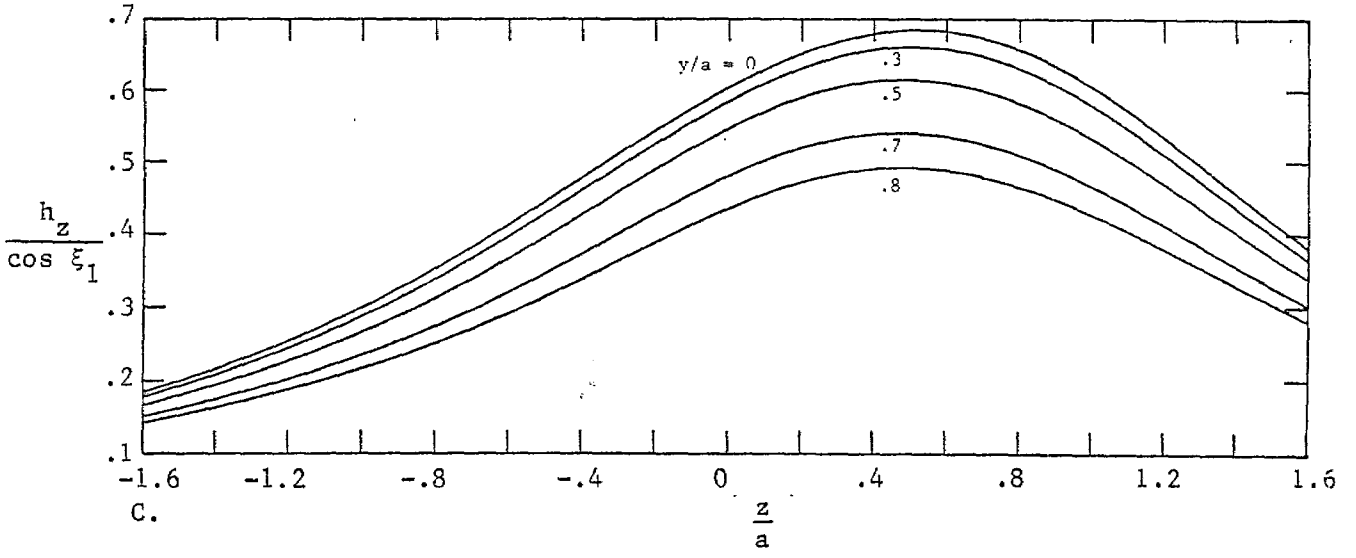

Figure 44. Magnetic Field Components as a Function of z: $\frac{2\xi_1}{\pi} = .7$; $\frac{x}{a} = -.8$.

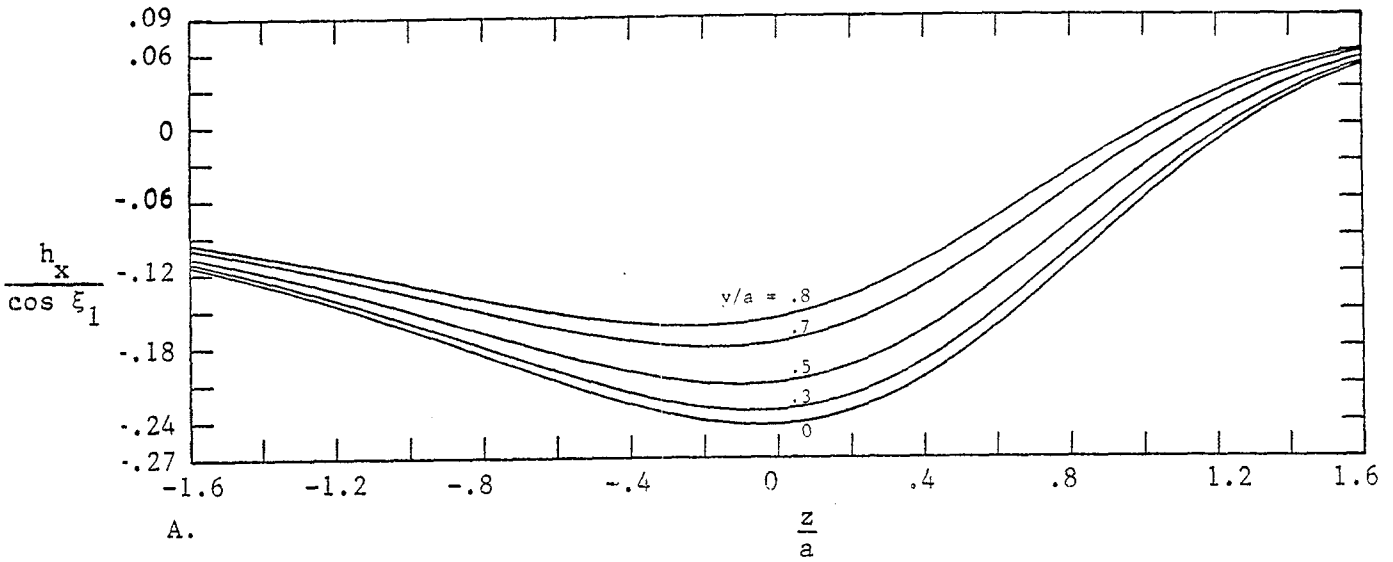

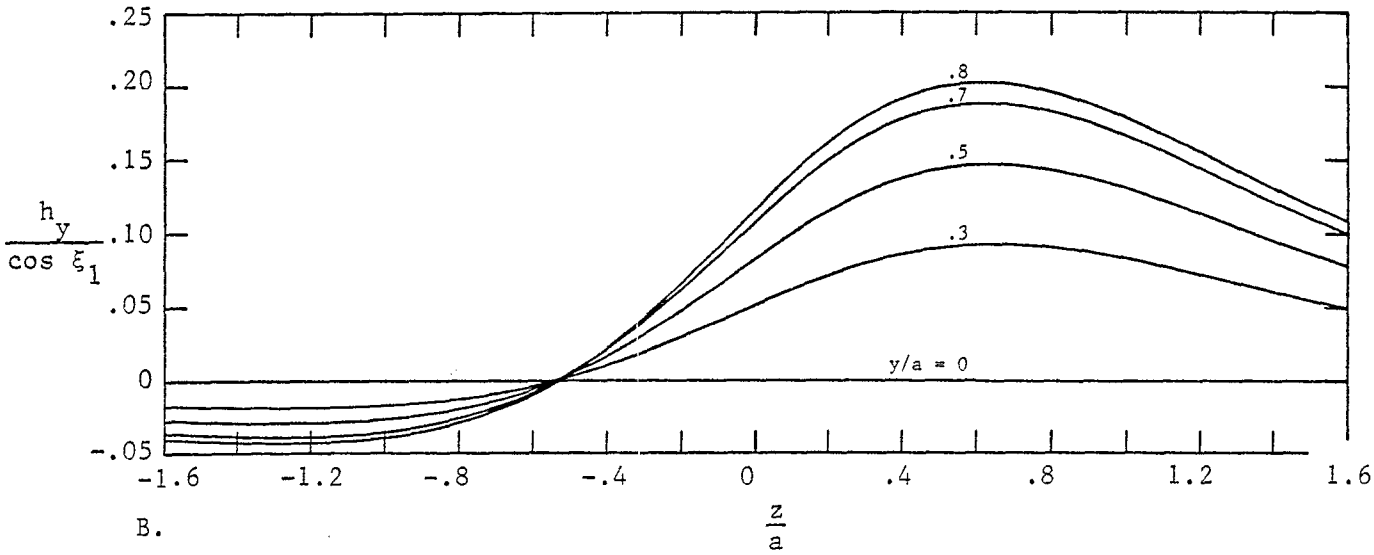

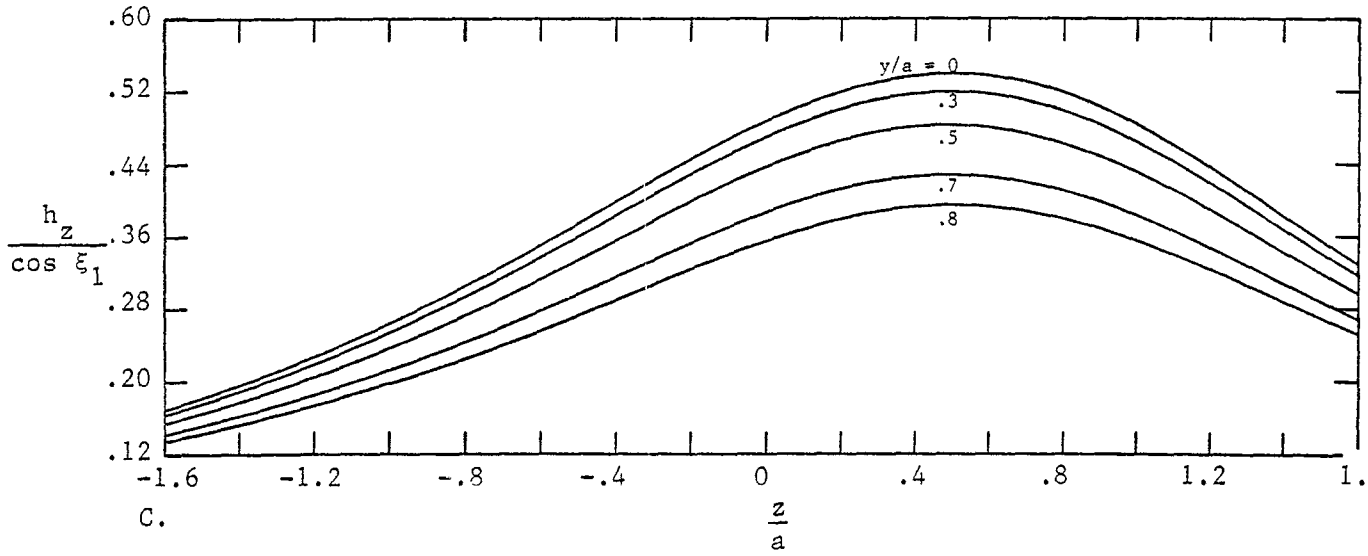

Figure 45. Magnetic Field Components as a Function of z: $\frac{2\xi_1}{\pi} = .7$; $\frac{x}{a} = -1$.

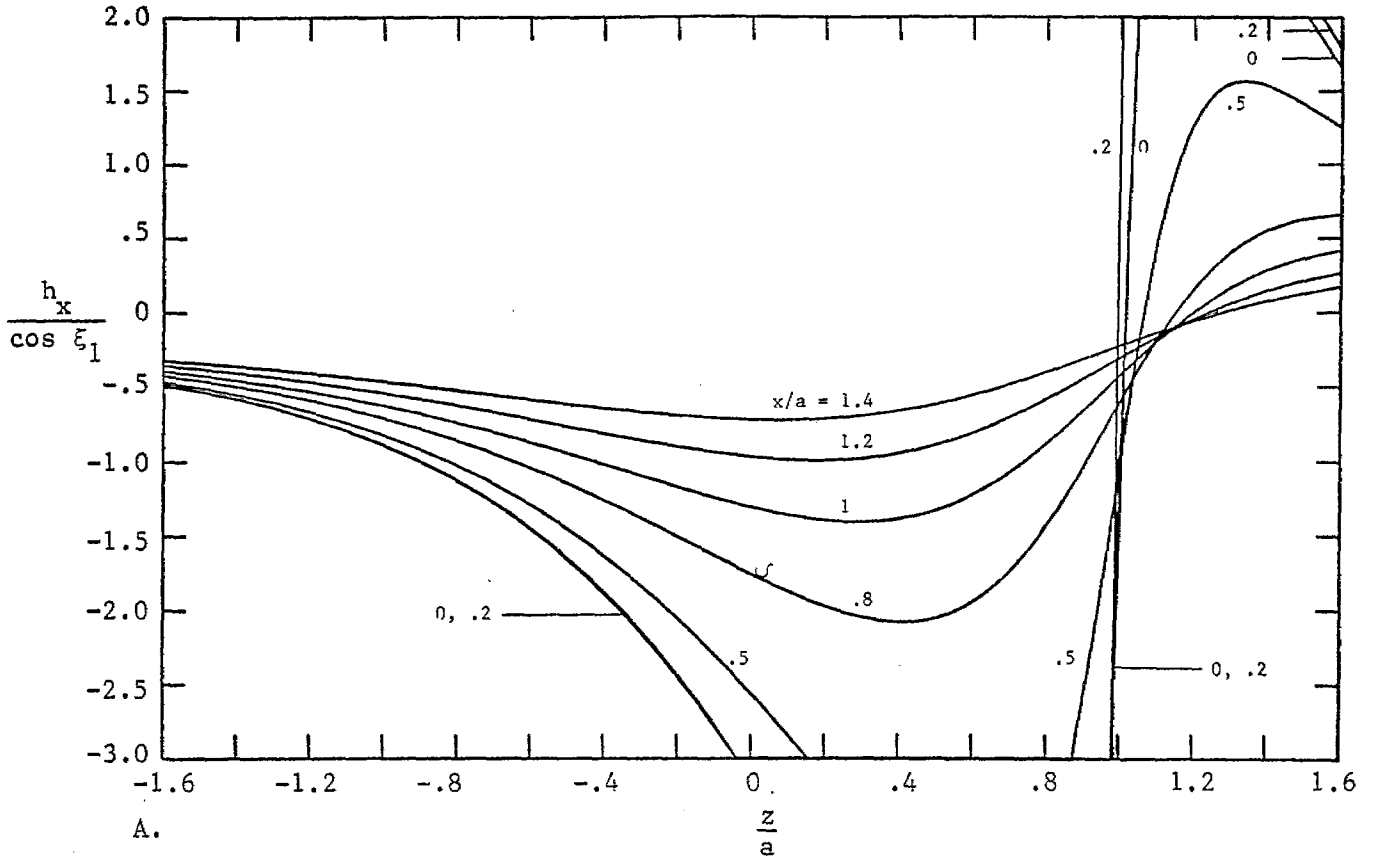

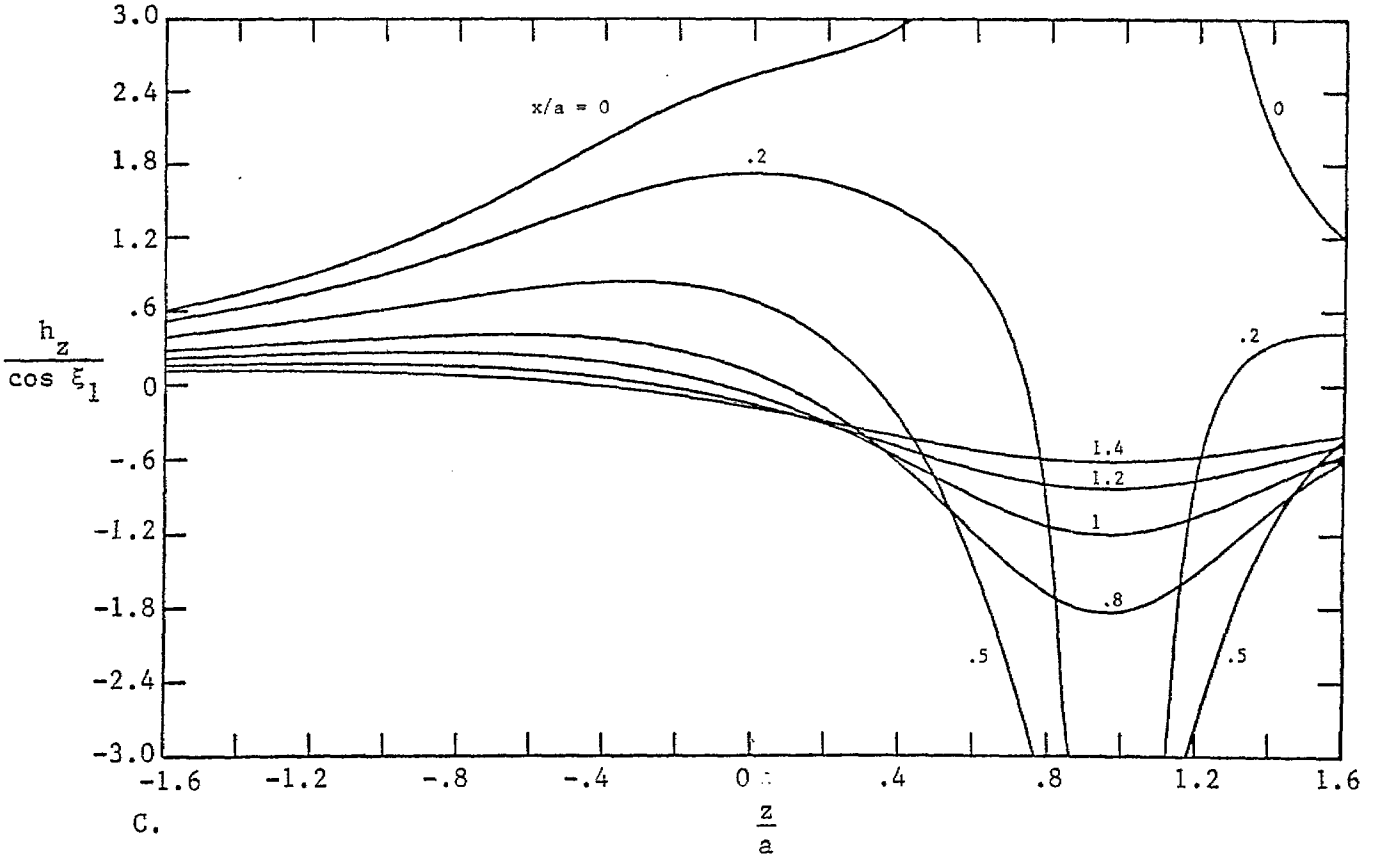

Figure 46. Magnetic Field Components as a Function of z; $\frac{2\xi_1}{\pi} = .9$; $\frac{y}{a} = 0$.

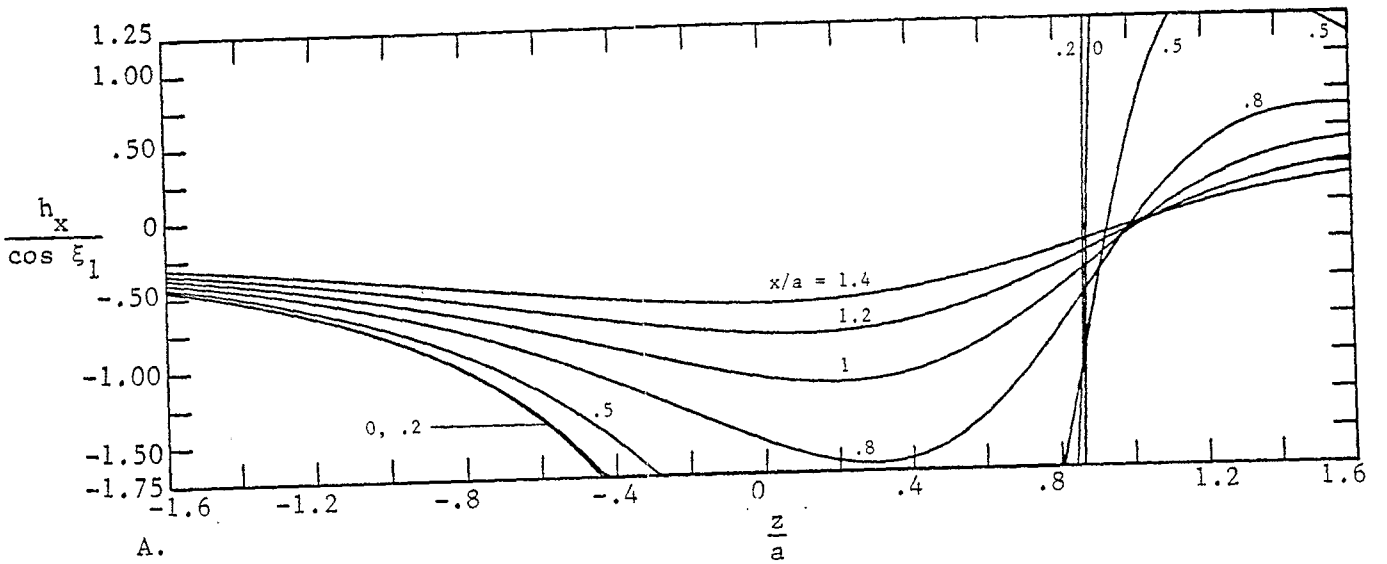

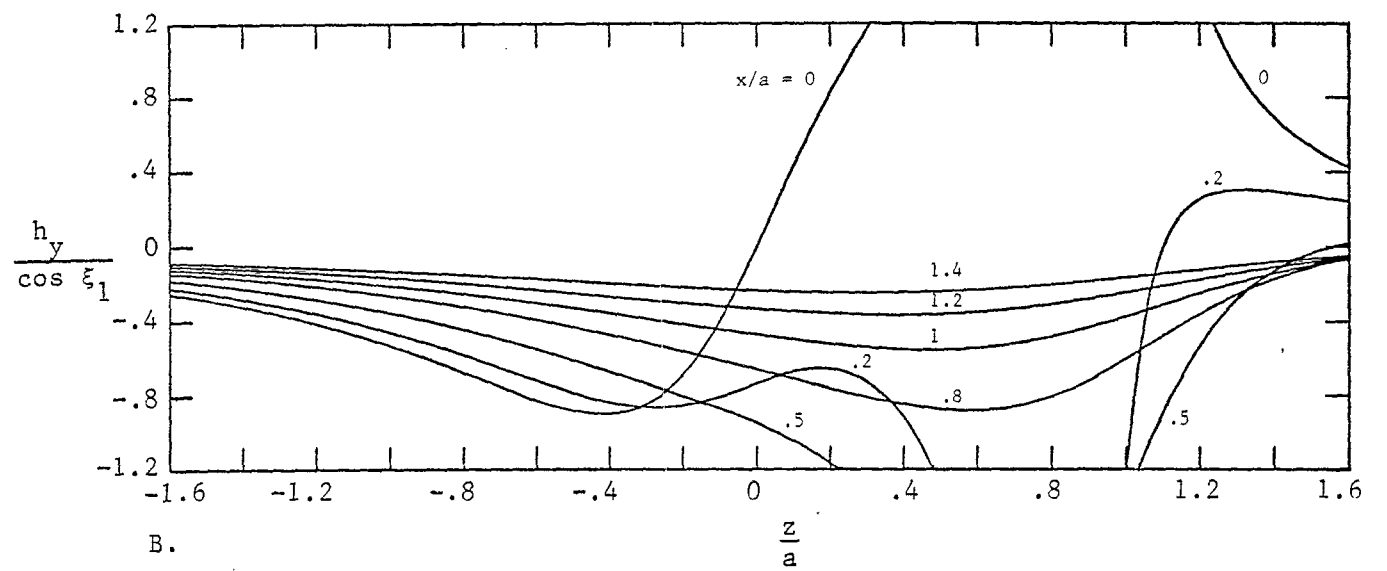

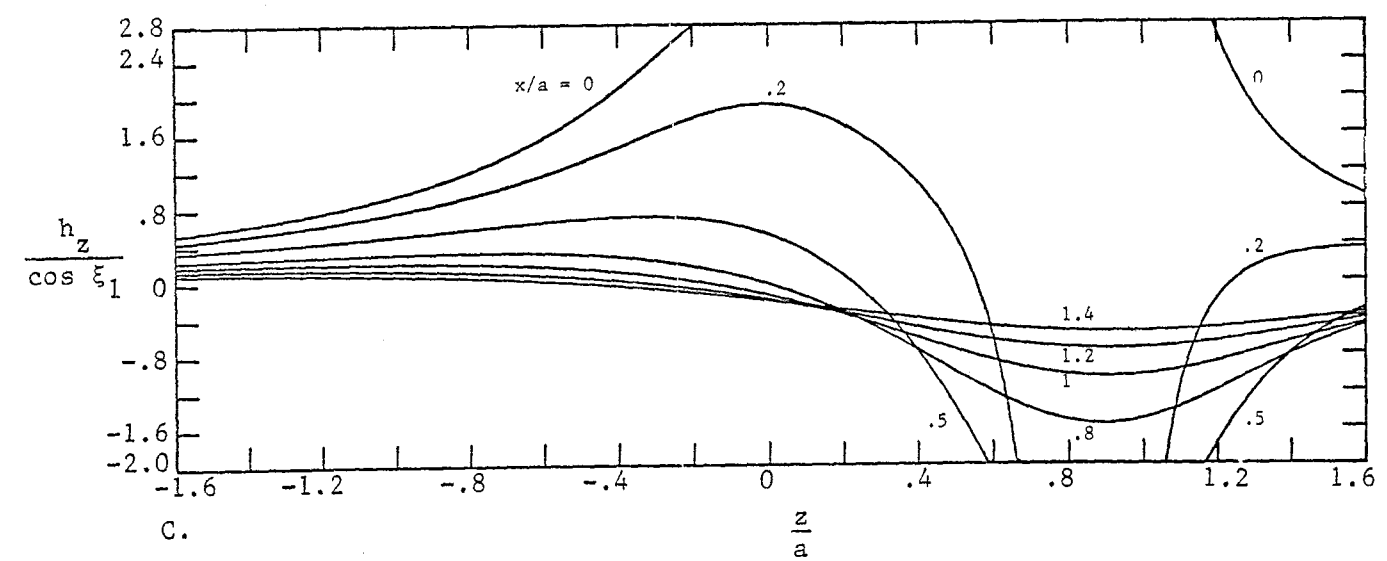

Figure 47. Magnetic Field Components as a Function of z: $\frac{2\xi_1}{\pi} = .9$; $\frac{y}{a} = .5$.

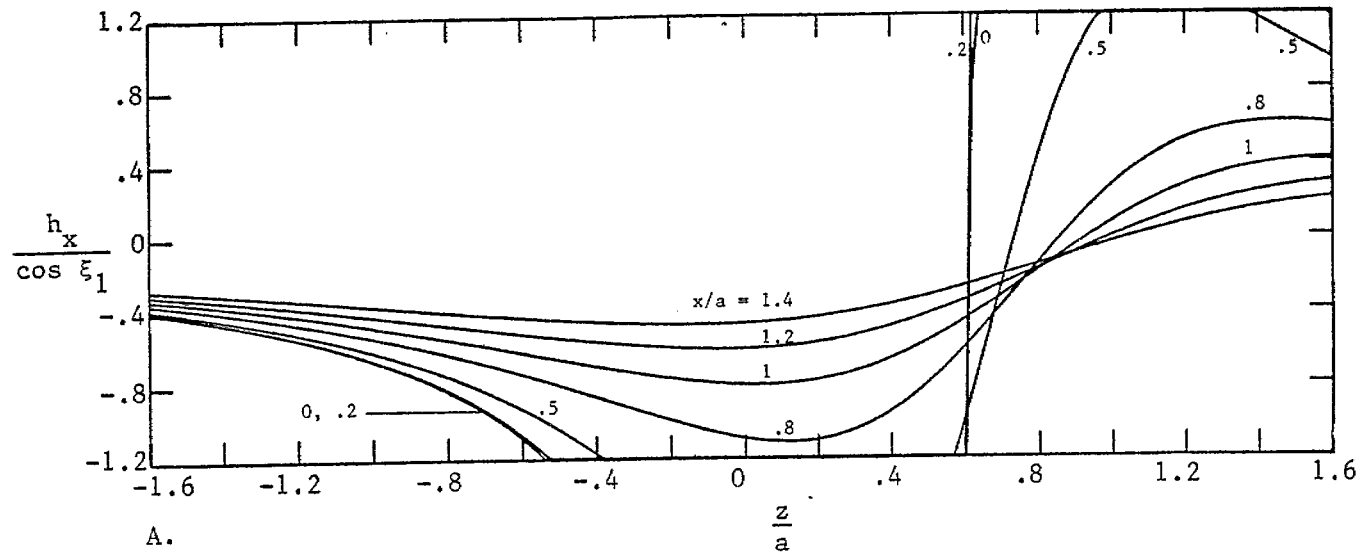

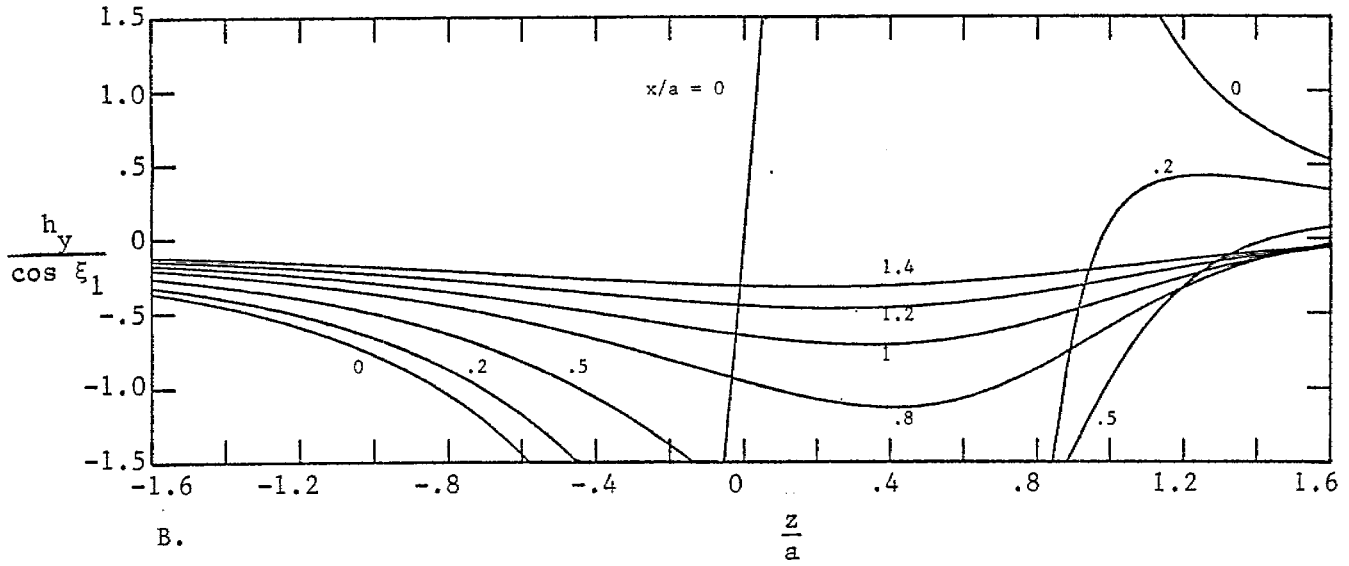

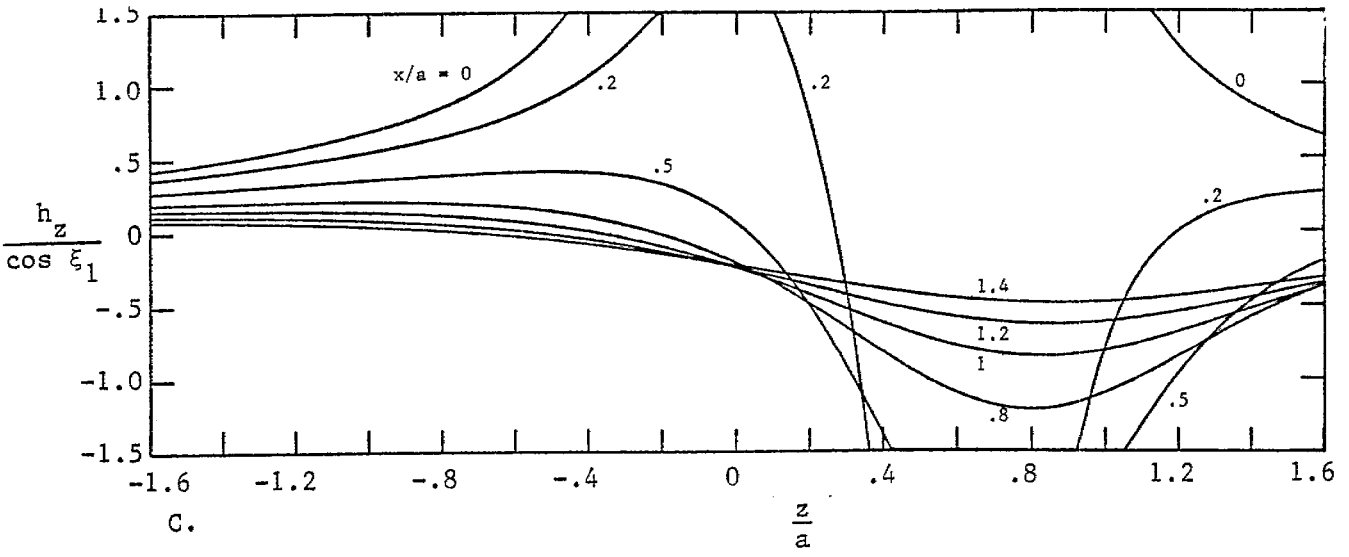

Figure 48. Magnetic Field Components as a Function of z: $\frac{2\xi_1}{\pi} = .9$; $\frac{y}{a} = .8$.

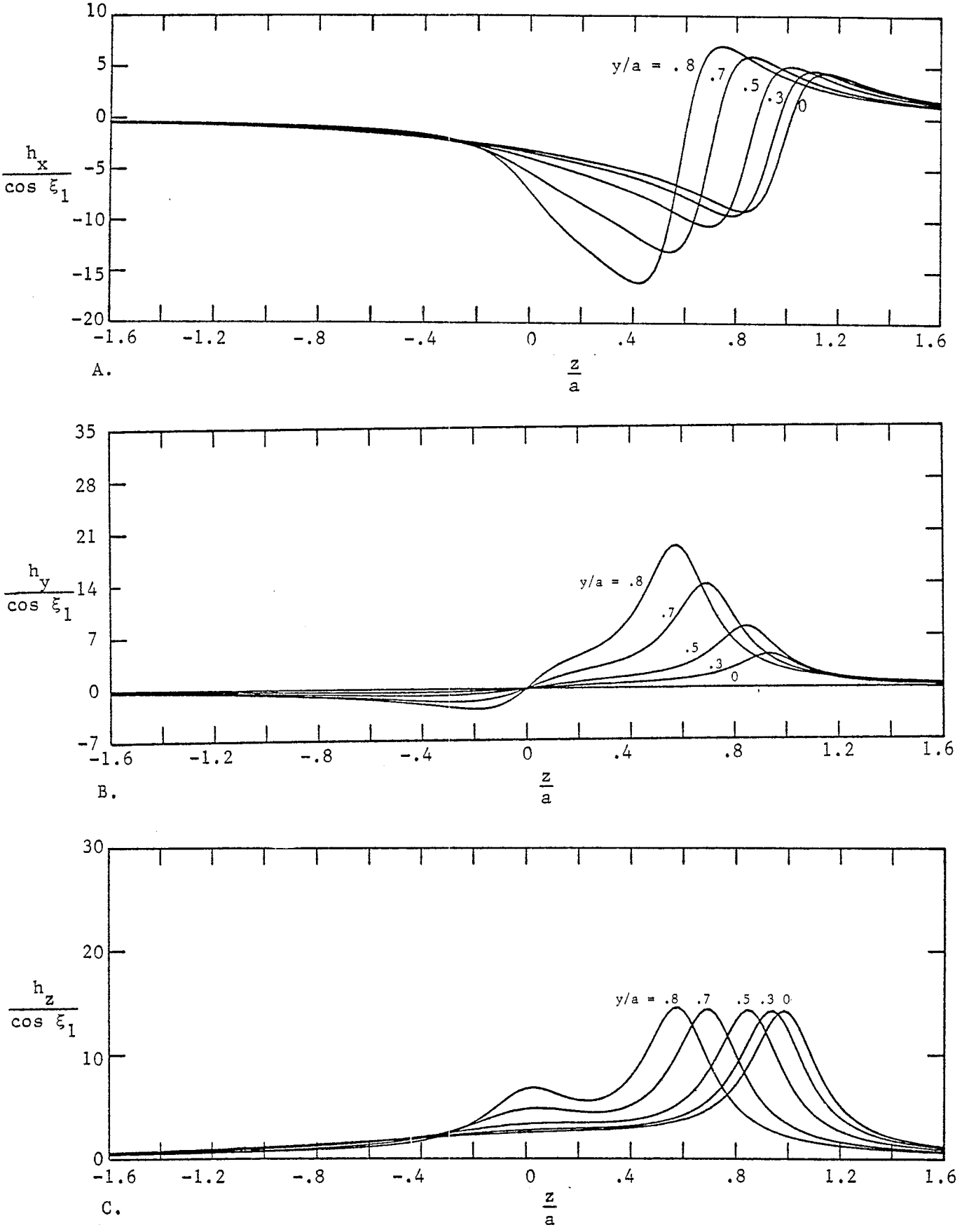

Figure 49. Magnetic Field Components as a Function of z: $\frac{2\xi_1}{\pi} = .9$; $\frac{x}{a} = 0$.

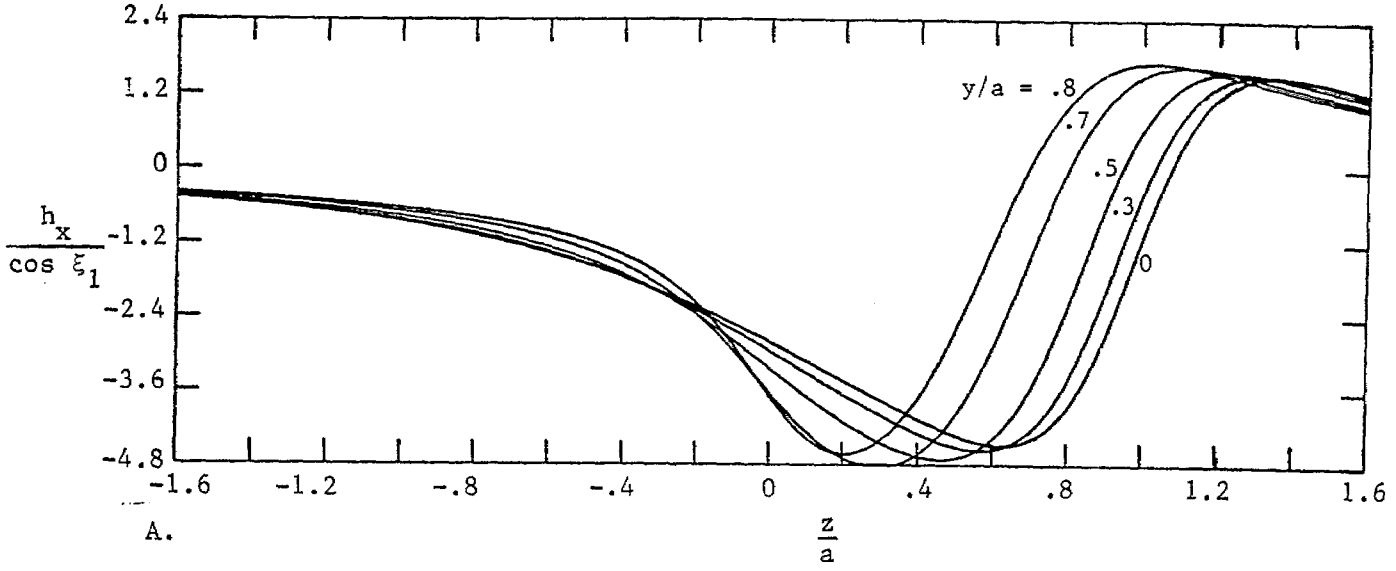

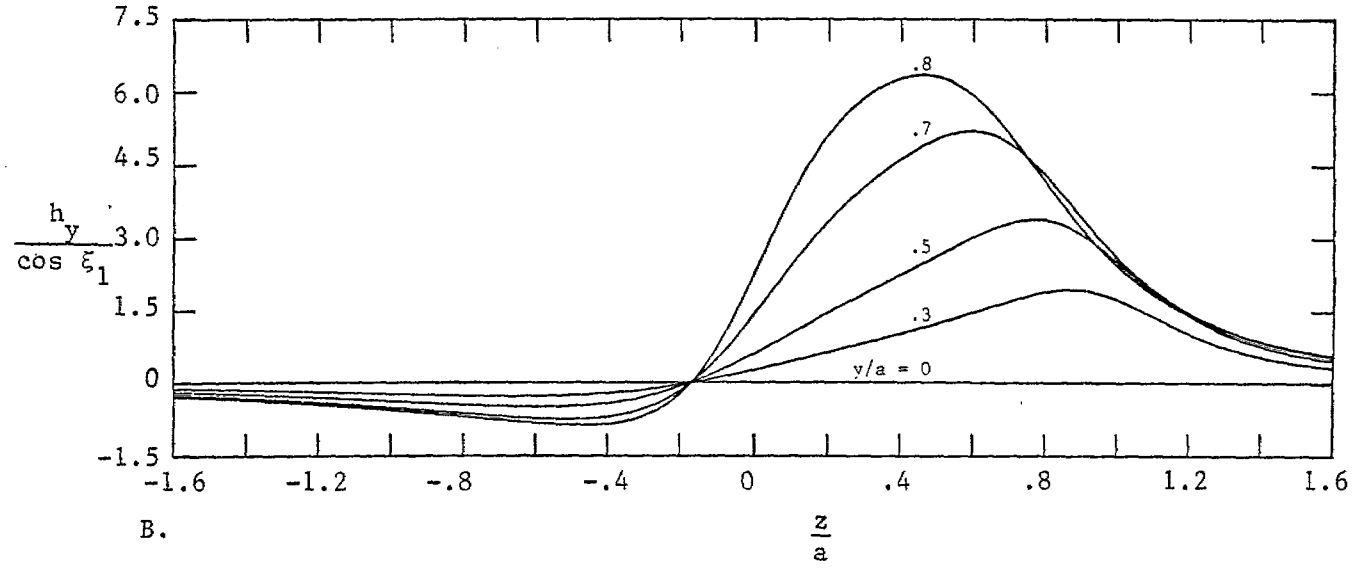

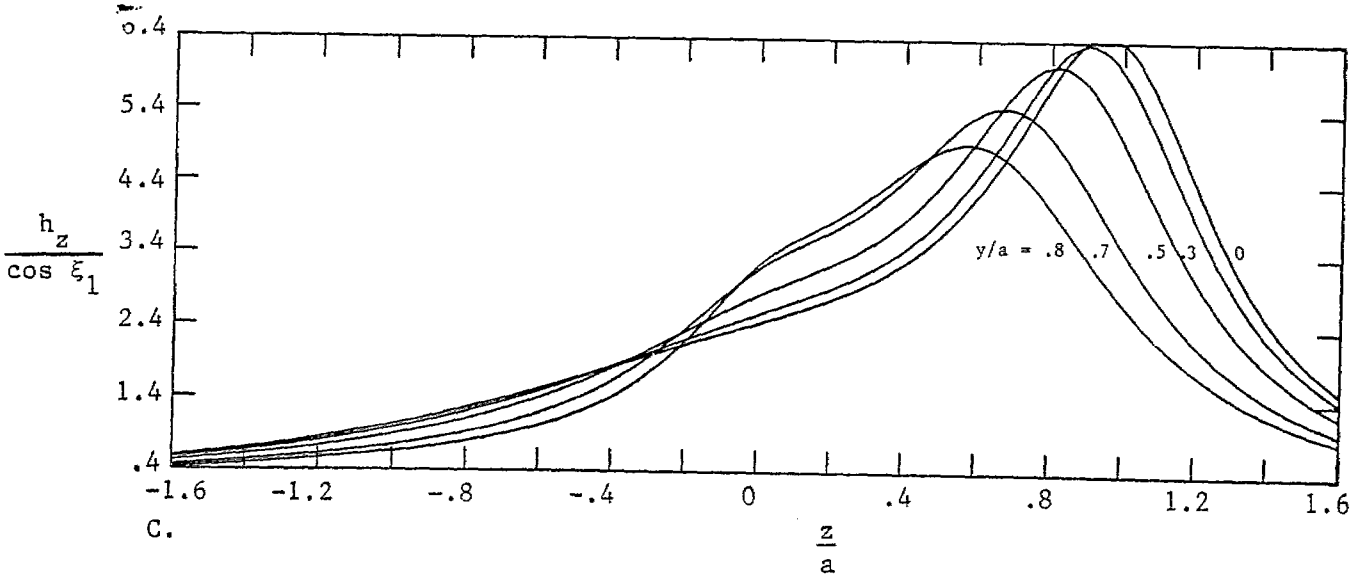

Figure 50. Magnetic Field Components as a Function of z; $\frac{2\xi_1}{\pi} = .9$; $\frac{x}{a} = -.2$.

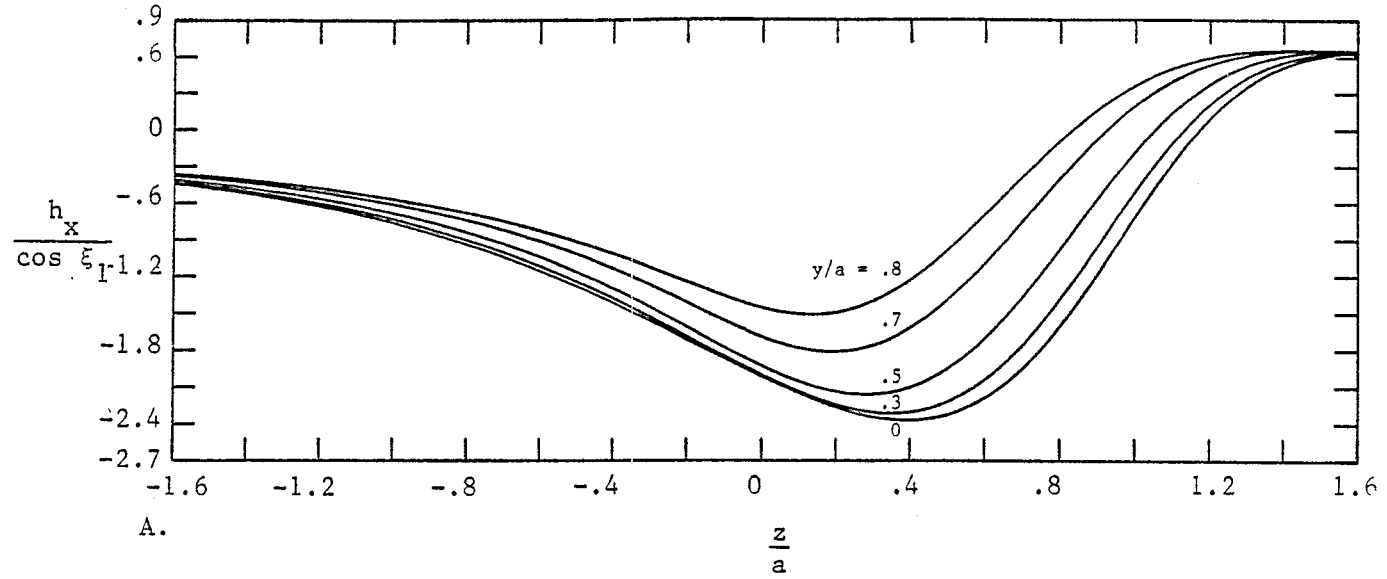

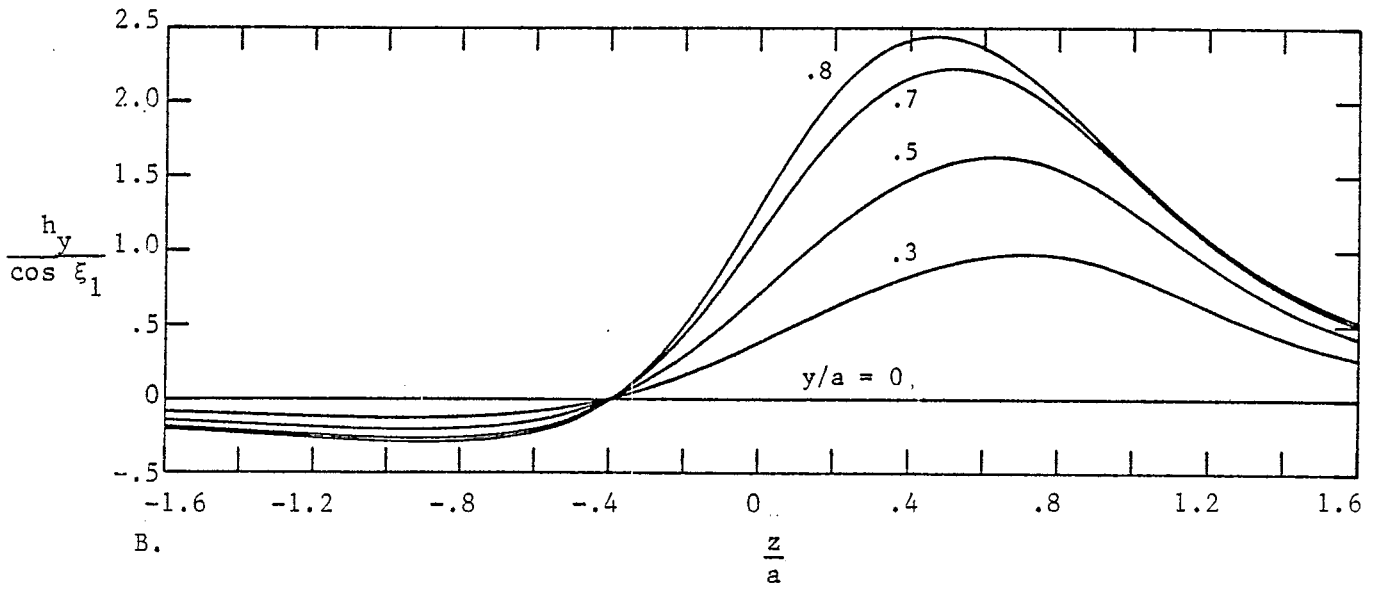

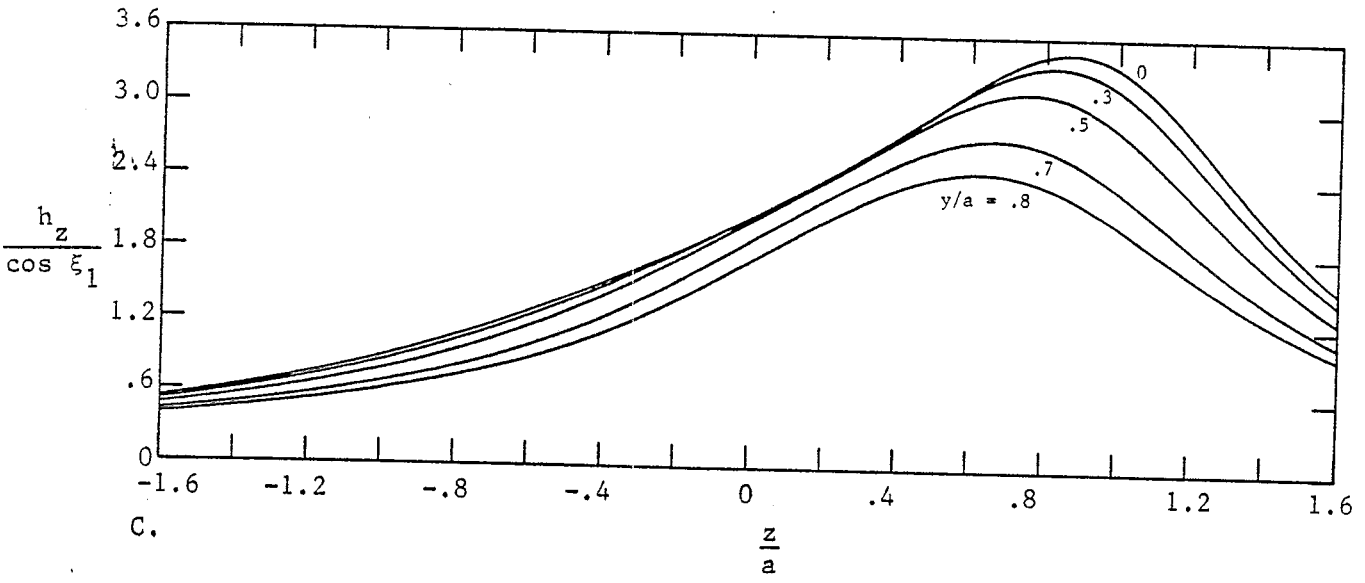

Figure 51. Magnetic Field Components as a Function of z: $\frac{2\xi_1}{\pi} = .9$; $\frac{x}{a} = -.5$.

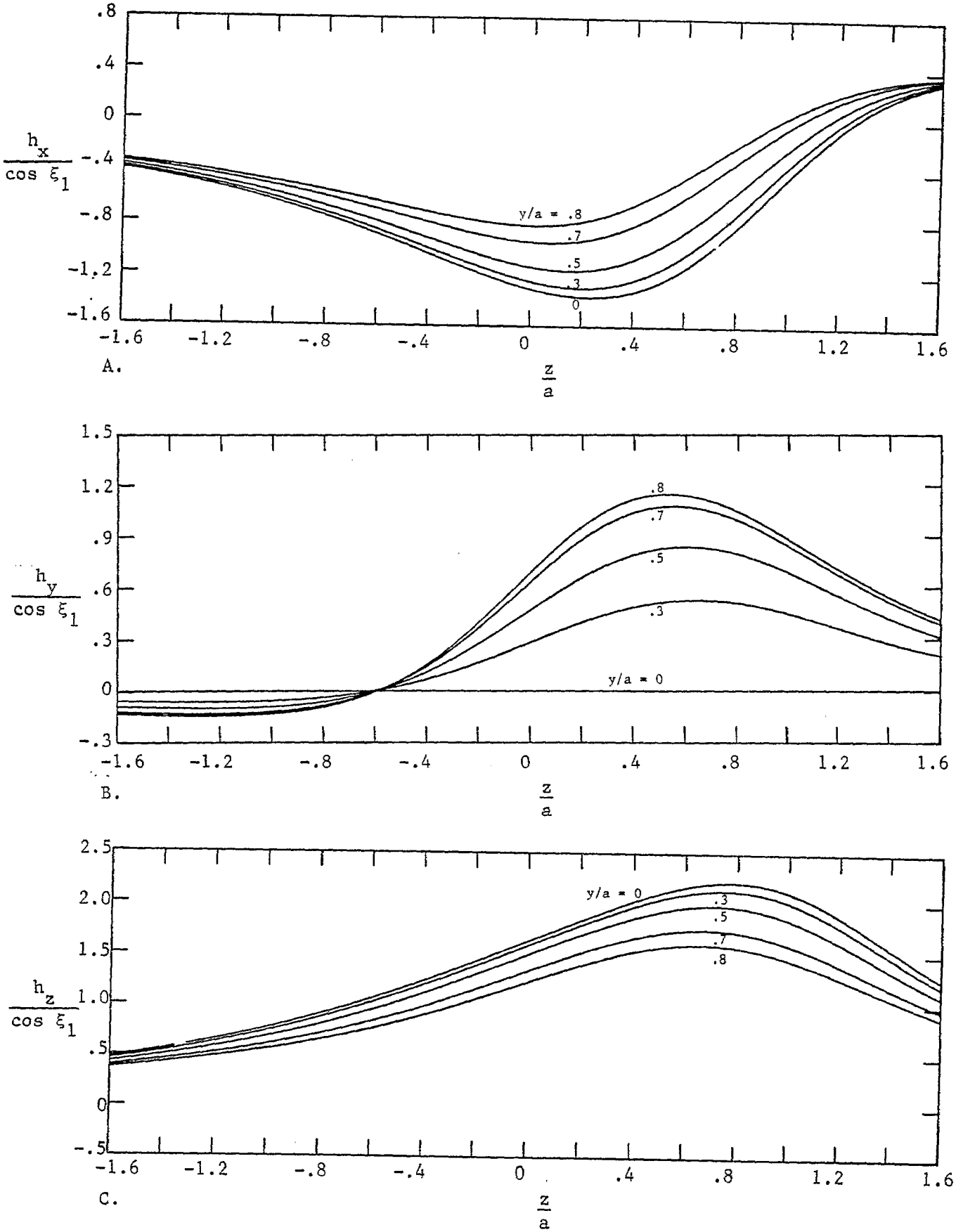

Figure 52. Magnetic Field Components as a Function of z: $\frac{2\xi_1}{\pi} = .9$; $\frac{x}{a} = -.8$.

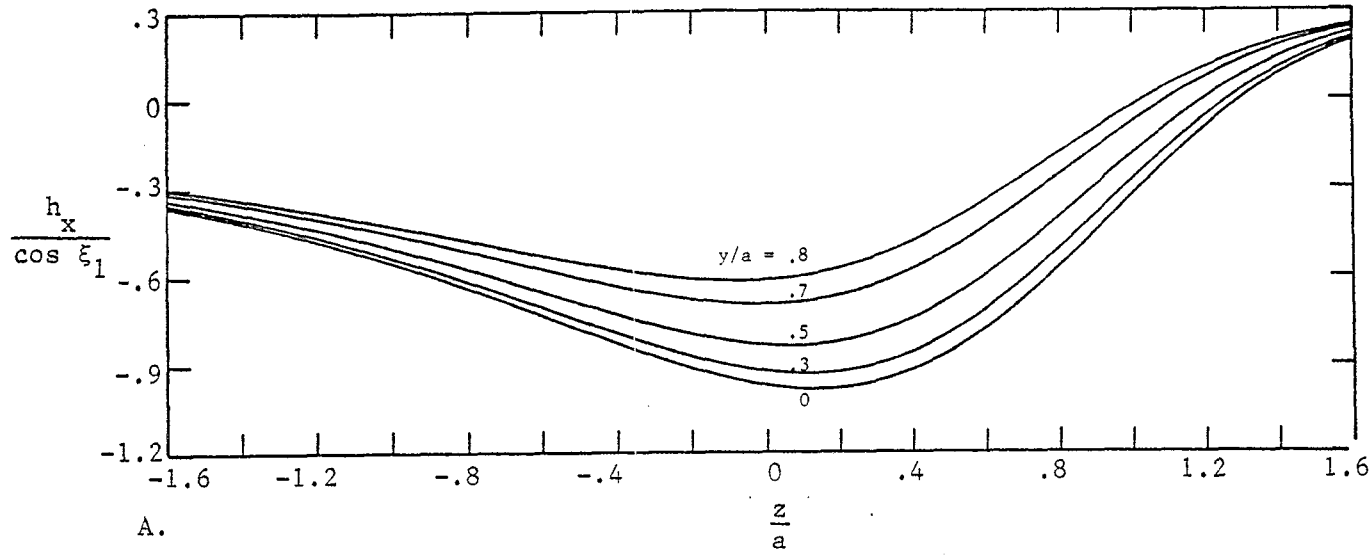

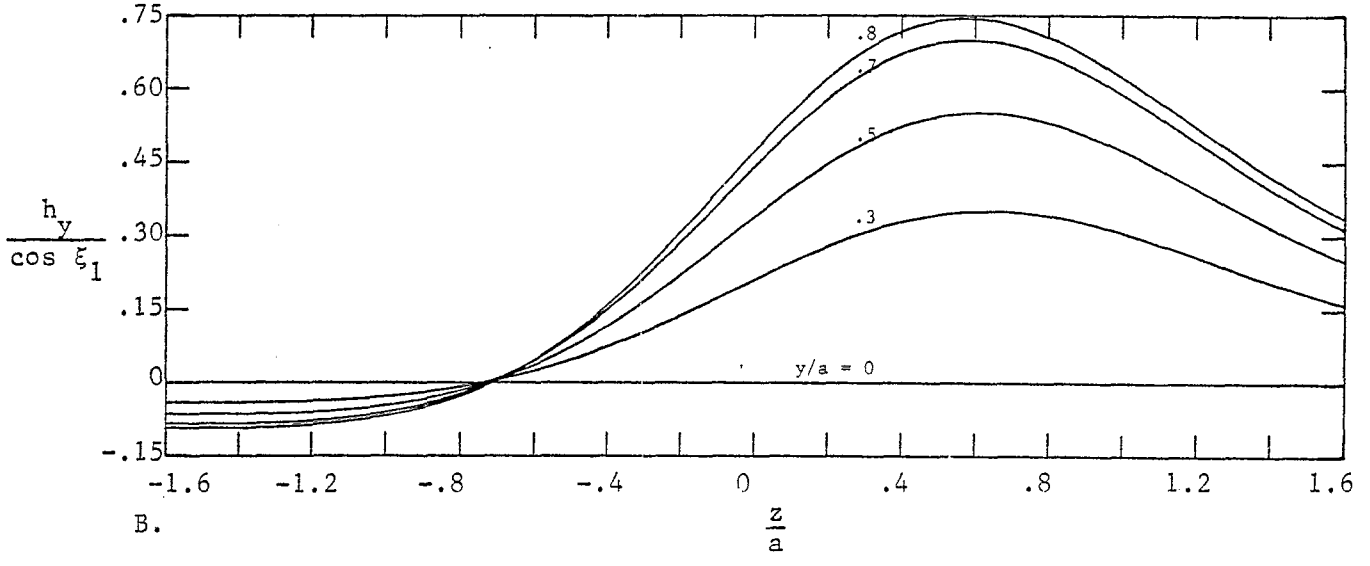

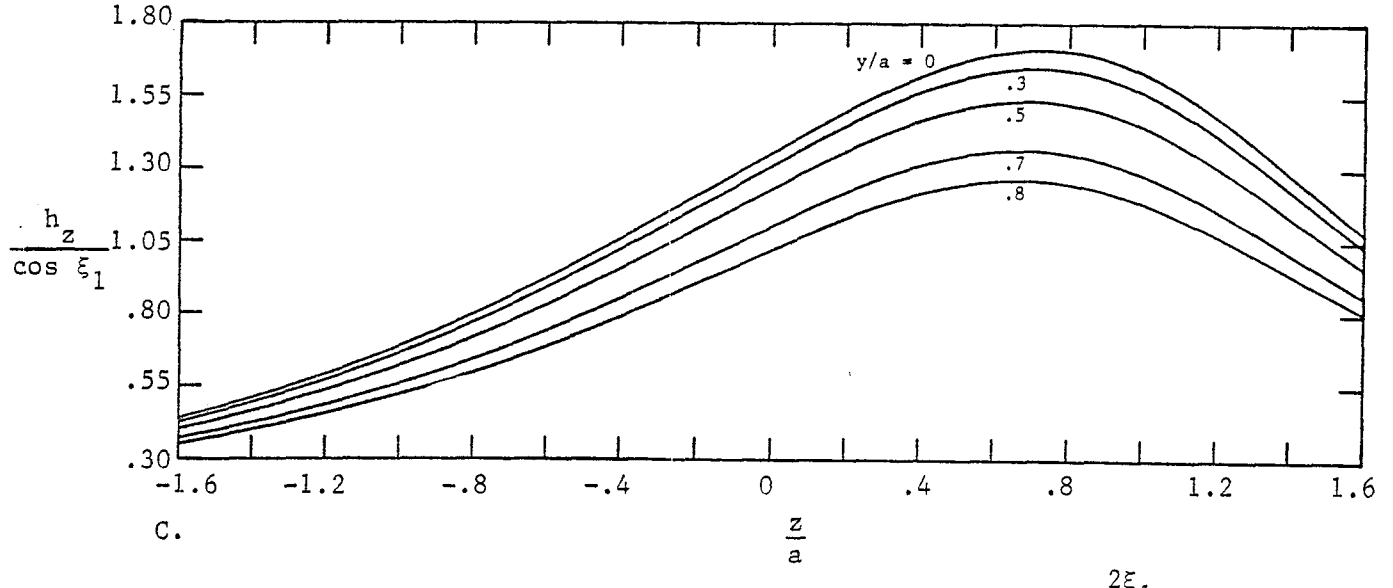

Figure 53. Magnetic Field Components as a Function of z: $\frac{2\xi_1}{\pi} = .9$; $\frac{x}{a} = -1.$

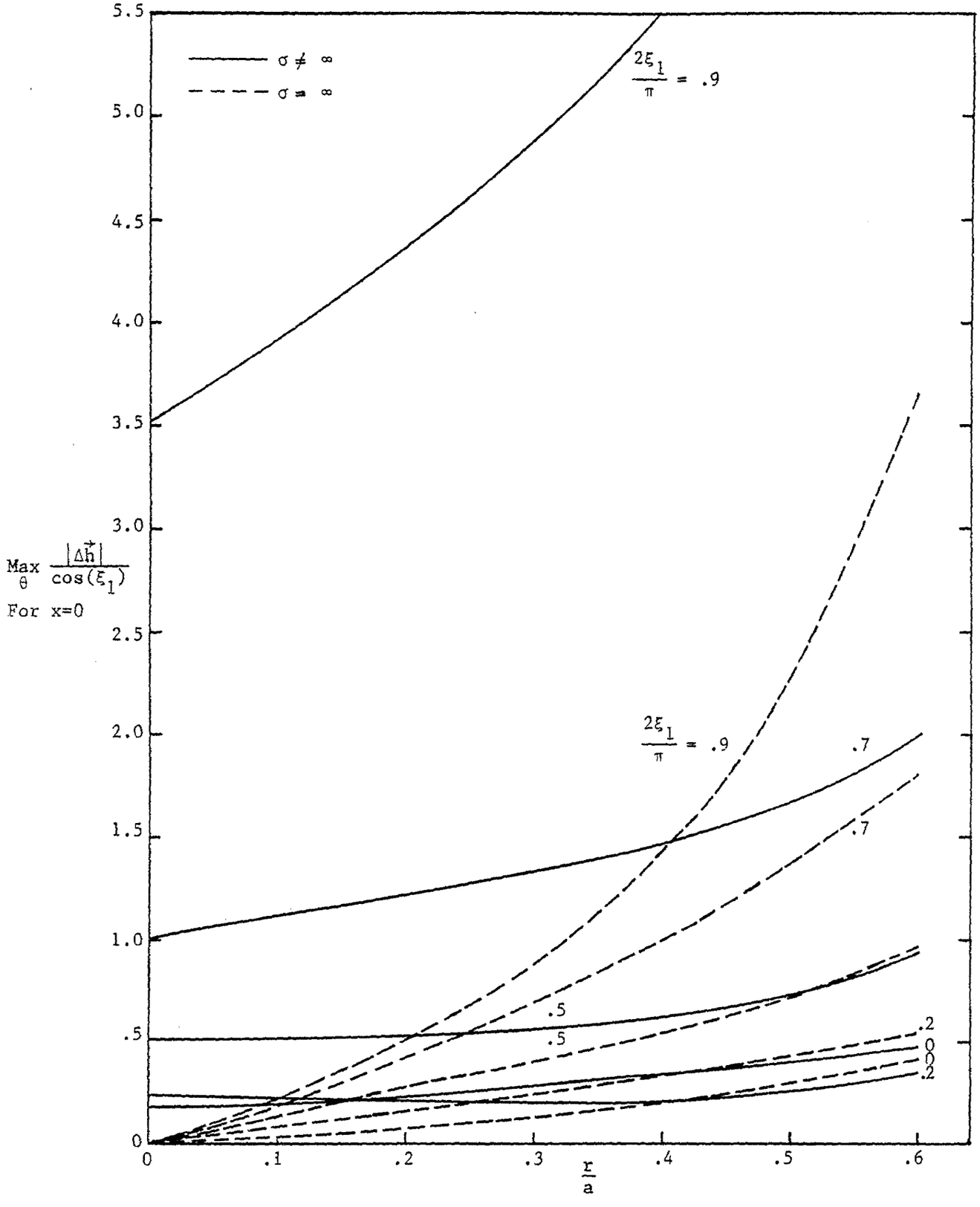

Figure 54. Maximum $\frac{|\Delta\vec{h}|}{\cos(\xi_1)}$ on the perimeter of a circle on the ground surface of radius r centered at the origin: $\frac{x}{a} = 0$.

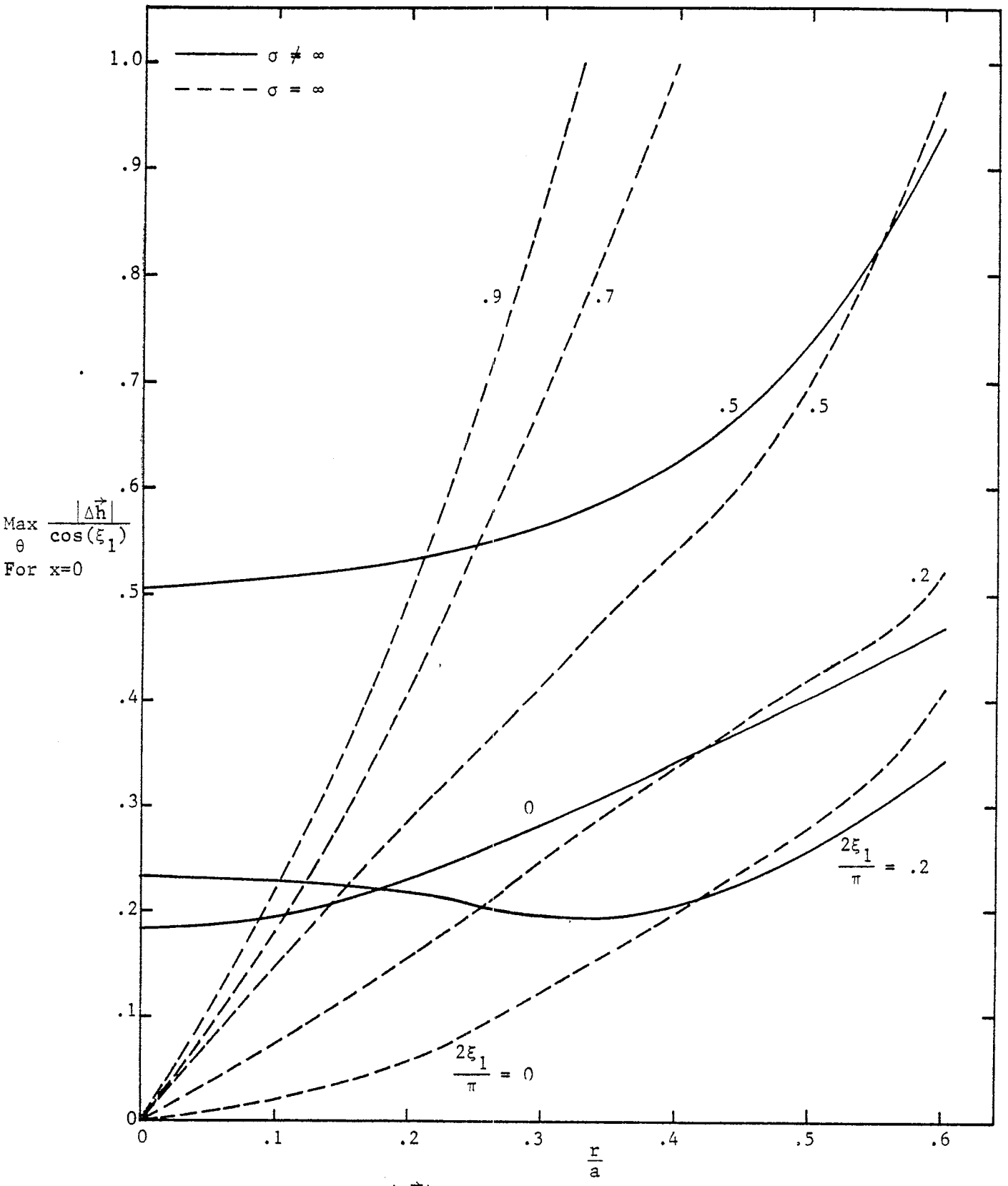

Figure 55. Maximum $\frac{|\vec{\Delta h}|}{\cos(\xi_1)}$ on the perimeter of a circle on the ground surface of radius r centered at the origin: $\frac{x}{a} = 0$ (scale of Figure 54 expanded).

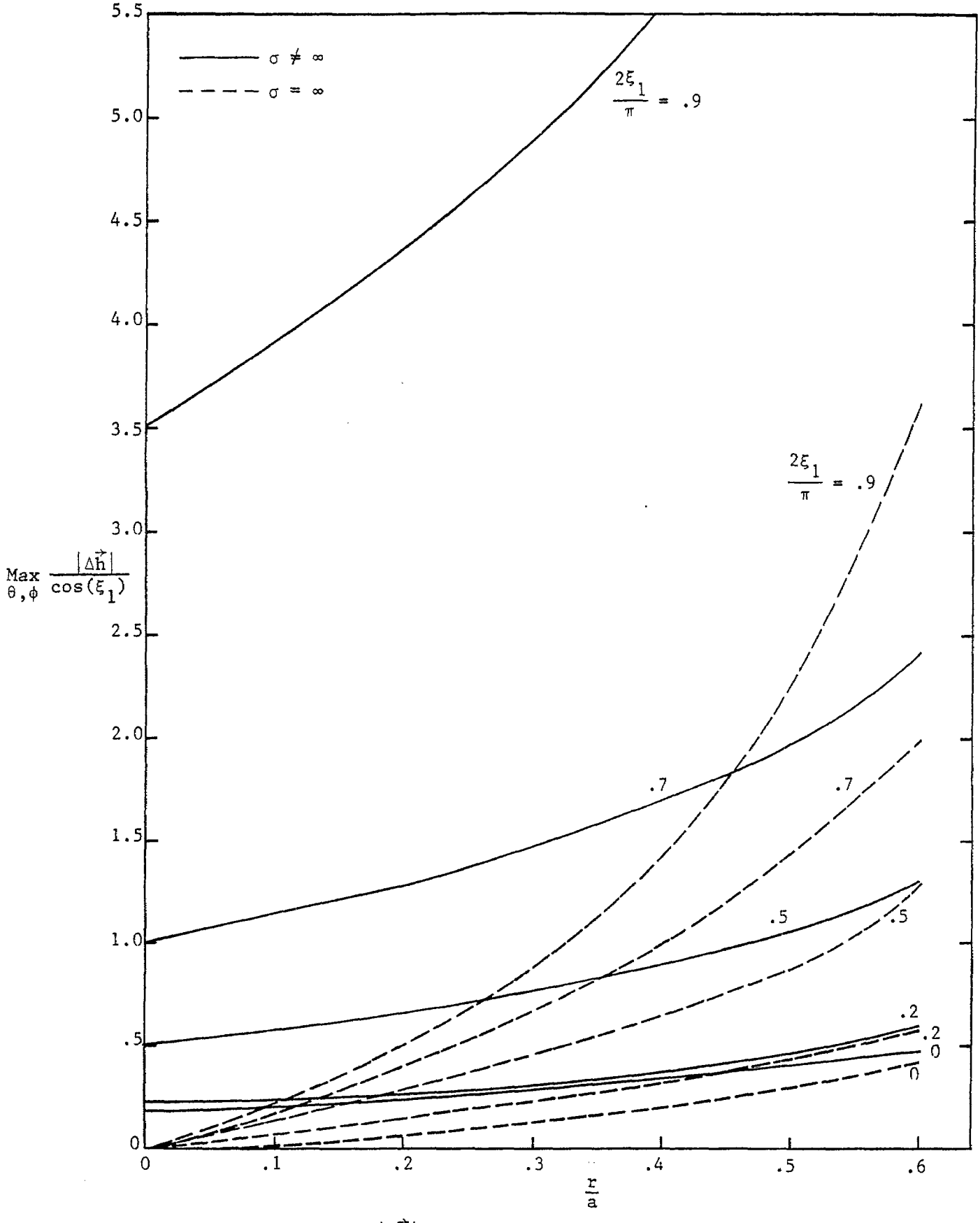

Figure 56. Maximum $\frac{|\vec{\Delta h}|}{\cos(\xi_1)}$ on the surface of a hemisphere or radius r centered at the origin.

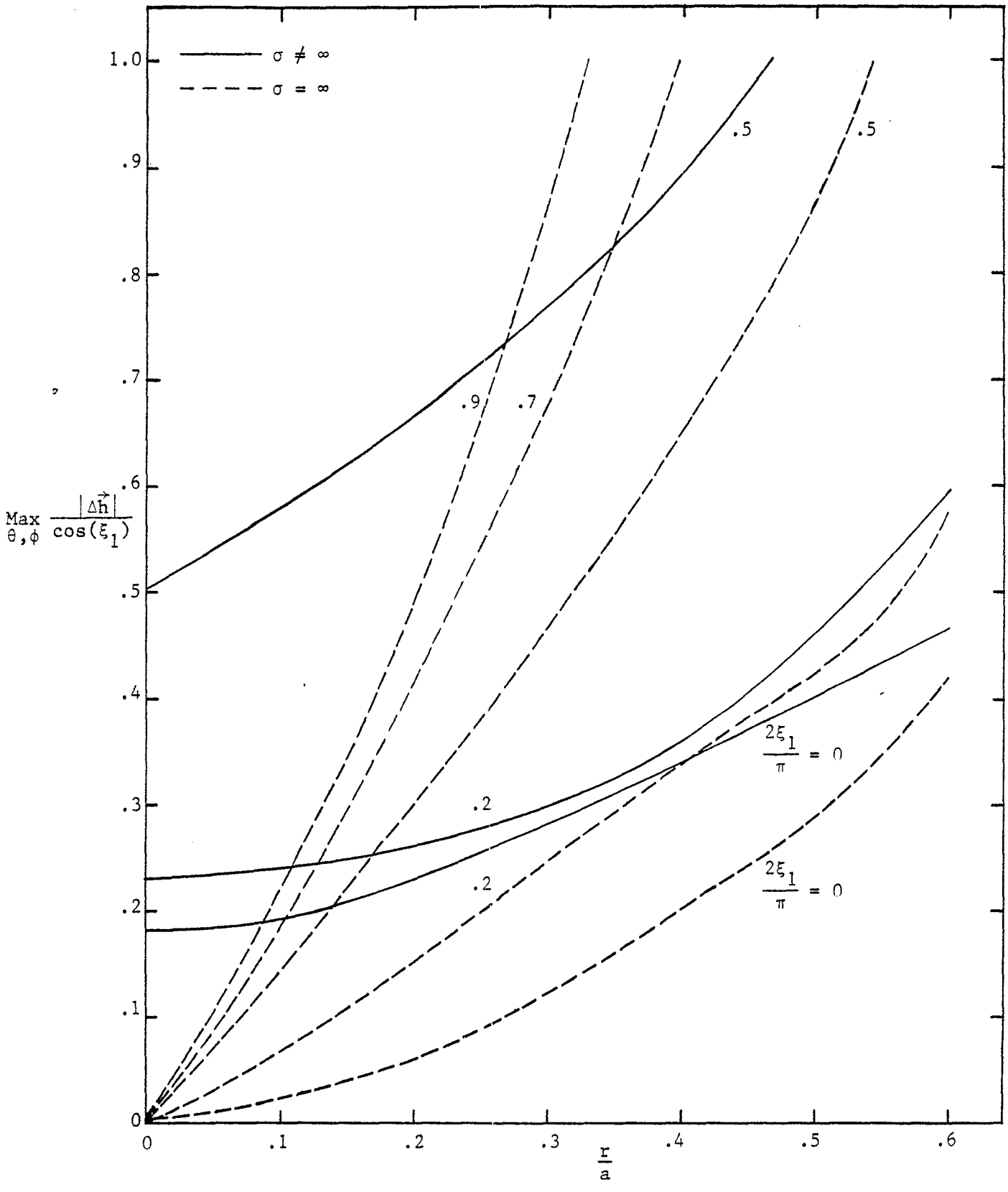

Figure 57. Maximum $\frac{|\Delta\vec{h}|}{\cos(\xi_1)}$ on the surface of a hemisphere of radius r centered at the origin (scale of Figure 56 expanded).

Acknowledgement

We thank Mr. R. W. Sassman for his invaluable assistance which enabled the computer plotting of our results. We also thank Dr. C. E. Baum, Dr. R. W. Latham, and Dr. K. S. H. Lee for their helpful comments.

References

1. Capt. Carl E. Baum, "Low-Frequency Magnetic Field Distribution for a Simulator with the Geometry of a Half Toroid Joined to the Surface of a Medium with Infinite Conductivity," Sensor and Simulation Note 112, 1 July 1970.
2. A. D. Varvatsis and M. I. Sancer, "Low-Frequency Magnetic Field Interaction of a Half Toroid Simulator with a Perfectly Conducting Hemisphere," Sensor and Simulation Note 120, October 1970.